NTNU

Norwegian University of
Science and Technology

Balancing Energy Activation with Network Constraints

Jonas Bøe

Master of Energy and Environmental Engineering
Submission date: June 2017
Supervisor: Gerard Doorman, IEL
Co-supervisor: Martin Håberg, Statnett

Norwegian University of Science and Technology
Department of Electric Power Engineering

Acknowledgements

I would like to express my sincere gratitude to my supervisors Prof. Gerard Doorman and Ph. d. candidate Martin Håberg for valuable input, corrections and motivating feedback throughout the work with this thesis. Thank you for arranging a fascinating visit to Statnett operations central in February and a warm welcome at Statnett workshop in May. I look forward to our cooperation in the future.

I also owe a special thanks to Ingrid M. Andersen for important corrections and input in the making of this report.

Finally, I am thankful to my family and friends for support throughout the work on this thesis.

Abstract

ENTSO-E has established the framework for integration of European balancing markets in the EU regulation "Guideline on Energy Balancing" (GL-EB). Differences in balancing market design between European countries prevent the exchange of balancing energy and optimal use of resources. Integration of balancing markets is motivated by the EU targets on integration of renewable energy, enhance social welfare and reduce EU dependency on energy imports. Key ingredients necessary to facilitate balancing market integration is a set of standardized balancing energy products, referred to as Standard Products, and an optimisation algorithm that decide optimal use of balancing resources. The algorithm is also referred to as Activation optimisation Function (AOF).

A proposal for AOF has been developed in this thesis. A real-time dispatch, DCOPF, balancing energy activation model that takes network flows into consideration and schedules FCR, aFRR and mFRR to balance Nordic imbalances in Nordic synchronous system is formulated in XPRESS. A network representation of the Nordic transmission system is input to the model together with a common, fictional Nordic bid list consisting of mFRR Standard Products. Nordic system frequency is modelled by a simplified system frequency bias factor and FCR activation. Imbalance forecast errors are represented with a fictional forecast deviation scaling factor. 5 scenarios are used to investigate model behavior upon change in Standard Product and network characteristics.

It is observed that the scenario in which no balancing energy can be exchanged between the Nordic countries leads to highest balancing cost and consequently lowest social welfare. This is because an increased activation of FCR and aFRR on the expenditure of reduced use of cheaper mFRR activations and low imbalance netting. The Reference scenario with exchange of balancing energy between Nordic countries showed a reduction in balancing cost by 22 % and increase in netted imbalance volume by 18 % compared to the Low Integration scenario. It is concluded that a large portion of mFRR activations are done to prevent violation of transmission capacities since the merit order is more closely followed when all transmission capacities are set to long term thermal values, in comparison to when transmission capacities are determined by Net Transfer Capacities (NTCs).

Producer ability to deliver balancing bids with short Full Activation Time (FAT) and minimum duration of delivery period allow the model to balance more of system imbalance with mFRR which reduce balancing cost and increase social welfare. A 9 % reduction in balancing cost is observed when all mFRR bids have minimum duration of 5 minutes and 3 % increase in balancing cost when number of bids with long Full Activation Time (FAT) is increased in the No P5 scenario.

An important simplification is the FCR modelling and indirect pricing of frequency deviations through a fictional FCR price. Sensitivity analysis of FCR price shows an increase in aFRR activations with increased FCR price. Possibility of consecutive mFRR delivery periods without new Full Activation Time (FAT) is an important cause of low balancing cost in scenario with short minimum duration of mFRR bids.

Results demonstrate that sufficient transmission capacity between balancing areas is a key element in increasing imbalance netting and reducing inefficient resource usage. Results also demonstrate the value of flexible mFRR products, i.e. bids with short Full Activation Time (FAT) and short minimum duration of delivery period.

Sammendrag

ENTSO-E har etablert rammeverket for integrasjon av europeiske balansemarkeder i EU-reguleringen "Guideline on Energy Balancing" (GL-EB). Ulikheter i utforming av europeiske balansemarked hindrer utveklsing av balanseenergi og optimal bruk av ressurser. Integrering av europeiske balansemarkeder er motivert av EUs målsetning om økt produksjon fra fornybare kilder, styrket sosial velferd og minke avhengighet av kraftimport. Nøkkeingredienser i markedsintegreringen er et sett av Standard-Produkter som skal kunne utveksles mellom land, og en optimeringsalgoritme som skal bestemme optimal aktivering av balanseressurser for å regulere europeiske kraftubalanser. Denne optimeringsalgoritmen kalles også Activation Optimisation Function (AOF).

I denne oppgaven er det blitt utviklet en prototyp for AOF basert på DCOPF i det nordiske synkronsystemet. Optimeringsmodellen for aktivering av balanseenergi tar hensyn til kraftflyt i nettet og lager kostnadsoptimale aktiveringsplaner for primære, sekundære og tertiære reguleringsreserver for å regulere historiske nordiske kraftubalanser. En nettverksrepresentasjon av det nordiske kraftsystemet blir innmatet til modellen sammen med en felles nordisk budliste for regulerkraft og prognoser for fremtidige ubalanser. Den nordiske systemfrekvensen er modellert ved en simplifisert nordisk regulerstyrke og aktivering av primærreserver. Stokastiske avvik i ubalanseprognoser er representert ved en fiktiv skaleringsfaktor for prognoseavvik. Det har blitt utviklet 5 scenarioer for å undersøke modellens oppførsel ved endring i Standard Produkt-definisjoner og nettverkkarakteristikker.

Det er observert økt aktiveringskostnad i scenarioet der ingen balansekraft kan utveksles mellom Norge, Sverige og Finland. Dette følger av økt aktivering av dyre primær- og sekundærresserver når mer rimelige tertiærreserver er utilgjengelige på grunn av lav markedsintegrering. Når balanseenergi kan utveklses over landegrensene, reduseres aktiveringskostandene med 22 % og ubalansenettingen øker med 18 % for samme ubalanser og nettverk. Det konkluderes med at en stor andel mFRR-aktiveringer gjøres for å forhindre brudd på overføringsrestriksjoner mellom markedsområder ettersom modellen evner å følge budpris-rekkefølgen i større grad ved økt overføringskapasitet.

En produsents evne til å levere fleksible balanseprodukter gjør at mer ubalanse kan reguleres av mFRR og reduserer total ressursbruk og aktiveringskostnader. En 9 % reduksjon i aktiveringskostnader er observert når alle mFRR-bud har minimum leveringsvarighet på 5 minutter, og en 3 % økning i aktiveringskostander når antall bud med full aktiverings-tid (FAT) på 15 minutter økes.

En viktig forenkling er modelleringen av FCR og indirekte prising av frekvensavvik gjennom fiktiv FCR-pris. Sensitivitetsanalyser for FCR-pris viser at aFRR-aktiveringer øker i alle scenarioer for økt FCR-pris. Muligheten for sammenhengende mFRR-leveringsperioder uten initiering av FAT er viktig årsak til reduserte aktiveringskostader i scenario med kort minimumsvarighet.

Resultatene viser at tilstrekkelig overføringskapasitet mellom balanseområder er en nøkkelfaktor i å øke sosial velferd ved aktivering av balanseenergi og redusere ineffektiv ressursbruk. Verdien av produsentfleksibilitet blir også presentert ved favorisering av bud med kort FAT og minimumsvarighet på leveranse.

Contents

List of Tables

List of Figures

Chapter 1

Introduction

1.1 Introduction

EU regulation on electricity balancing, "Guideline on Energy Balancing" (GL-EB) [13], was approved by EU member states on March 16., 2017. GL-EB describes a detailed framework for integration of European balancing markets. Balancing market designs differ today between countries and the integration will be an important step on the path towards a single wholesale European electricity market. More efficient use of resources and balancing flexibility will support installation of intermittent sources as wind and solar power in the EU, as such an installation is accompanied by increased uncertainty in supply and balancing need. A closer cooperation between EU member states is also expected to increase social welfare, as the cheapest resources are available and requirement for stand-by reserves is reduced.

The Nordic countries were among the first in Europe to liberalize the power sector in the 1990s. A liberalized power sector implies that the amount of electricity that is produced and fed into the grid is solely determined by the demand of the consumers and customers. The commercial participants in the power sector have little interest in ensuring operational security of the power system. If there is an imbalance between the electricity fed into and extracted from the grid the system frequency will deviate from the nominal frequency in the synchronous system. The Nordic synchronous system and the European Continental system are two separate synchronous systems, which both have a nominal system frequency of 50 Hz. A synchronous area is an geographical area in which all generators rotate at equal speed, and a synchronous area may be connected to other synchronous areas through HVDC cables. A frequency deviation of only +- 0.5 Hz from the nominal frequency may cause damages to system components and in the worst case lead to system-wide blackouts. In November 2006 a power imbalance after a line outage in Northern Germany led to blackout in 15 million European households [30]. The disturbance lasted for approximately 2 hours before normal conditions were restored. Insufficient cooperation of Transmission System Operators (TSOs) was concluded to be one of two main causes, the other cause was operation close to operational limits [30]. Increasing electrification of industry and households requires a strong focus on maintaining security of supply when increasing amounts of electricity come from intermittent sources.

The balancing markets are institutions where the non-profit, typically governmental organiza-

tions trade electricity with market participators to ensure power balance. A TSO is responsible for maintaining the balance within its control area, which is typically a country. Depending on whether there is an oversupply (positive imbalance) or undersupply (negative imbalance) the TSO will either buy power (upward regulation) or sell power (downward regulation) based on balancing bids that are submitted by producers (or consumers) on the balancing market. The TSO will incure a payment from the party that was responsible for the power imbalance, and use this payment to buy balancing energy. The balancing control mechanism can be either automatic or manual, the manual involves TSO operator calling up the producer to activate a bid. Social welfare is enhanced when the manual balancing operations maintain system power balance at minimum activation cost and with minimum unnecessary use of resources.

When integrating balancing markets an operator will have a larger area to balance when activating manual reserves, making the selection of bids more complex. GL-EB propose for this purpose an algorithm for optimal activation and exchange of standardized balancing products, also referred to as Standard Products. Standard Products will adhere to predefined characteristics and proposals for Standard Products are made in [38]. The optimisation algorithm is referred to as the Activation optimisation Function (AOF) and has the objective of maximizing social welfare when maintaining the power balance between production and consumption in integrated, liberalized power markets. The AOF will compare balancing bids with different location, price, volume and Standard Product characteristics, then determine cost-optimal activation schedule of manual balancing energy based on available transmission capacities in the grid.

1.2 Problem Description

The main objective of this thesis is to develop a balancing energy activation optimisation model for the Nordic synchronous system that may serve as a prototype for the AOF. The model compares Standard Products on balancing energy based on the proposals made in [38] to balance historical Nordic imbalance data.

Previous work in [27] investigated the behavior of Standard Products in a balancing energy activation optimisation model. However, the effects of balancing activations in a physical network was not considered. The model developed in this thesis puts the product specific characteristics of mFRR bids into a physical context through the inclusion of a network representation of the Nordic transmission system. The main contribution of this thesis is therefore a qualitative investigation of Standard Product behaviour and balancing activations when the physical flows and transmission capacities are accounted for.

1.3 Scope

A balancing activation optimisation model has been developed as a Mixed Integer Linear Problem (MILP) in XPRESS software. The model is a real-time dispatch DC Optimal Power Flow (DCOPF) formulation in which network flows are calculated based on line reactance and bus voltages in a Nordic network representation. Balancing energy activation schedules are created based on a deterministic imbalance forecast with a scheduling horizon of 45 minutes. Historical Nordic

imbalance data has been extracted from first week of January, 2017. The imbalance data is defined at area level and has been geographically distributed to network buses with an imbalance mapping algorithm also developed in this project.

Primary, secondary and tertiary balancing control mechanisms are modelled. A set of Standard Products for exchange of tertiary balancing energy has been developed based on proposals in [27] and [38]. System frequency deviation estimate is calculated from an averaged and simplified Nordic frequency bias factor and primary reserves activation. A load/generation shedding functionality is also included to ensure convergence in all balancing situations.

The margin between power flows resulting from the Nordic day-ahead clearing and Nord Pool Net Transfer Capacities (NTCs) determine the transmission capacity for balancing activations on lines that cross borders between Nord Pool bidding area.

1.4 Report Outline

Descriptions of Nordic power markets and causes of system imbalances begins this report in Chapter 2, which thereafter continues with a description of frequency control mechanisms in the Nordic system. An introduction to main challenges and design variables in balancing market integration and theoretical background in DC load flow is presented. Chapter 2 ends with presentation of relevant previous work on balancing energy activation models.

Methodology Chapter 3 begins with a presentation of key concepts such as modelling of primary control and energy bid delivering profiles. After the concepts have been introduced, the notation and mathematical formulations follow. Chapter 3 continues with presentation of data inputs; historical imbalance data, network representation and fictional balancing energy market data. The Chapter ends with the presentation and description of scenarios.

All results are presented and commented in Chapter 4, starting with a discussion of simplifications and assumptions and how results are affected by these. Presentation and comments of results from each scenario then follow. Chapter 4 also includes a sensitivity analysis of FCR pricing and transmission capacities. Future work is also discussed.

Chapter 2

Background

2.1 Introduction

The electrical power system form the basis of our modern living. Societies are increasingly dependent on electrical energy and there are no indications that this dependency will decrease in the future. An electrical power system generally consist of three main parts; generation, transmission and distribution, all of which were operated by a single, centralized operator prior to the liberalisation of the power sector. TSO will activate ancillary services to ensure that system restrictions are not violated and that the power balance is maintained in a liberalized power market. Ancillary services comprise of balancing services and system services ranging from reactive power compensation to load/generation shedding.

This Chapter will initially give an overview of Nordic power markets, causes of power imbalances and provision of balancing services, before presenting theoretical background in balancing control mechanisms and load flow analysis.

2.2 Nordic Power Market and Imbalances

Nord Pool Spot is the Nordic exchange for trade of electricity in Norway, Sweden, Finland, Estonia, Denmark and Lithuania, and enable producers, retailers, traders and large-scale end-users to buy and sell electricity. Nord Pool is divided into bidding zones as depicted in Figure 2.1 to prevent bottlenecks in key transfer corridors. A bottleneck occurring on a border between two bidding zones means that no more power can be transferred across that border. Each bidding zone is associated with an area price. All bidding zones will have equal area price if no bottlenecks occur between any bidding zones, also referred to as the system price. Largest bottlenecks usually occur on the North-South borders since electricity with low marginal cost of production, especially hydro power, is located to the North of the industrial centers of Southern Sweden and Finland.

Note the difference between Nord Pool Spot areas and the Nordic synchronous area. The Nordic synchronous area share the same nominal frequency of 50 Hz, and is shown in green in Figure 2.1. HVDC cables connect the Nordic synchronous area to the Continental synchronous area from NO2, SE4 and FI. The nuclear phase-out in Germany and necessity of flexible and storable hydro power in Continental Europe with increasing RES penetration are factors that motivate further development

of HVDC links between Nordic and Continental system. Western Denmark is not part of the Nordic synchronous area although Western Denmark is.

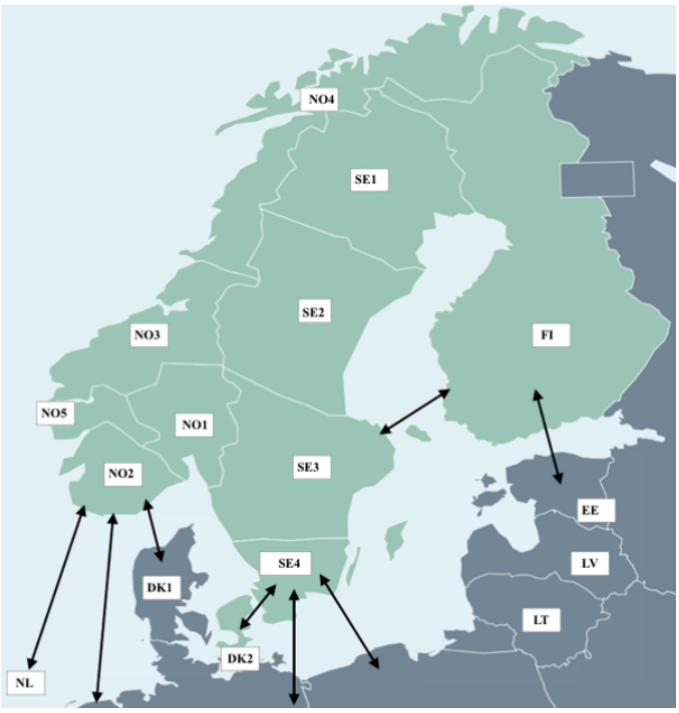

Figure 2.1: Nord Pool bidding areas, Nordic synchronous area and HVDC links.

2.2.1 Nordic Power Markets Overview and Participants

Transition from market phases to control phases on Nordic power markets is depicted in Figure 2.2. Long before hour of operation, financial forward and future markets opens and initiate the market phase. Strategic trading is done by market participants to protect against price risks, referred to as price hedging. This is also the phase where TSO will procure regulating reserves to be activated in real-time balancing.

One day before hour of operation the day-ahead spot market opens. Since this is a day-ahead market market participants trade energy to be delivered the following day. Day-ahead is integrated implying that a Finnish consumer can trade with a Norwegian producer. The spot market has gate-closure (market closing time) at 12:00 on the day before delivery.

Elbas is an intraday market where power can be traded up to one hour before operational hour. Elbas enables participants to adjust their posititions closer to real-time, which reduces balancing needs in the operational phase. Elbas opens two hours after the closing of day-ahead at 12:00 and Norway joined the Elbas market in 2008.

Each TSO is sent quarterly schedules by Balance Responsible Parties (BRPs) in the evening before operational hour. BRPs are market entities that are responsible for maintaining a balanced positions and can be utilities that buy and sell electrical power to consumers. A balanced position means an equilibrium between production, consumption and trade with other BRPs. BRPs are

allowed to adjust their schedules up to 45 minutes before operational hour. There are two main types of system imbalances that occur due to BRP imbalance, structural imbalances and stochastic imbalances.

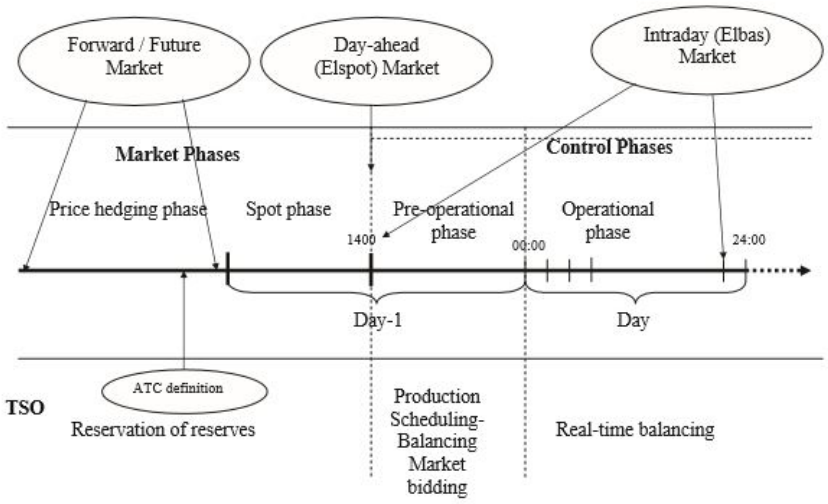

Figure 2.2: Market and control phases in Nordic power trading, from [17, page 29].

2.2.2 Structural imbalances

Structural imbalances occur due to the low resolution of production schedules. For instance, production schedules may be determined at an hourly basis, while the demand is always continuously changing. Demand at beginning of an hour when the generation schedule is determined may differ significantly from the demand at the end of the hour. This is depicted in Figure 2.3, where the demand increases linearly from 0 MW to 100 MW. This may resemble a demand increase in morning hours although real demand is non-linear. The generation schedules with hourly resolution are shown in blue, and the mismatch between generation and consumption indicates power imbalances at the beginning (oversupply) and end (undersupply) of the hour. When increasing the schedule resolution to 30 minutes, shown in the black line, the power imbalances at hour shifts are reduced by half. Greatest structural imbalances occur at hour shifts in periods when demand changes most rapidly. Figure 2.4 depicts historical structural imbalances on the evening of January 3. 2017 in the Swedish bidding area SE3, which is located in the South of Sweden. Large structural imbalances begin to occur around 19:00 and last until midnight. Structural imbalances are handled by production scheduling which redistributes supply schedules more evenly around hour shifts [42].

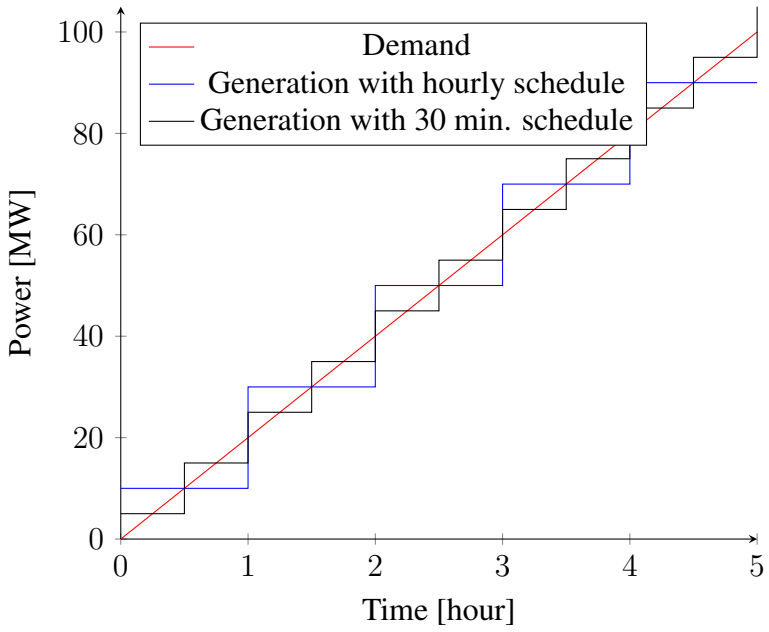

Figure 2.3: Structural imbalance at hourly generation dispatch schedule

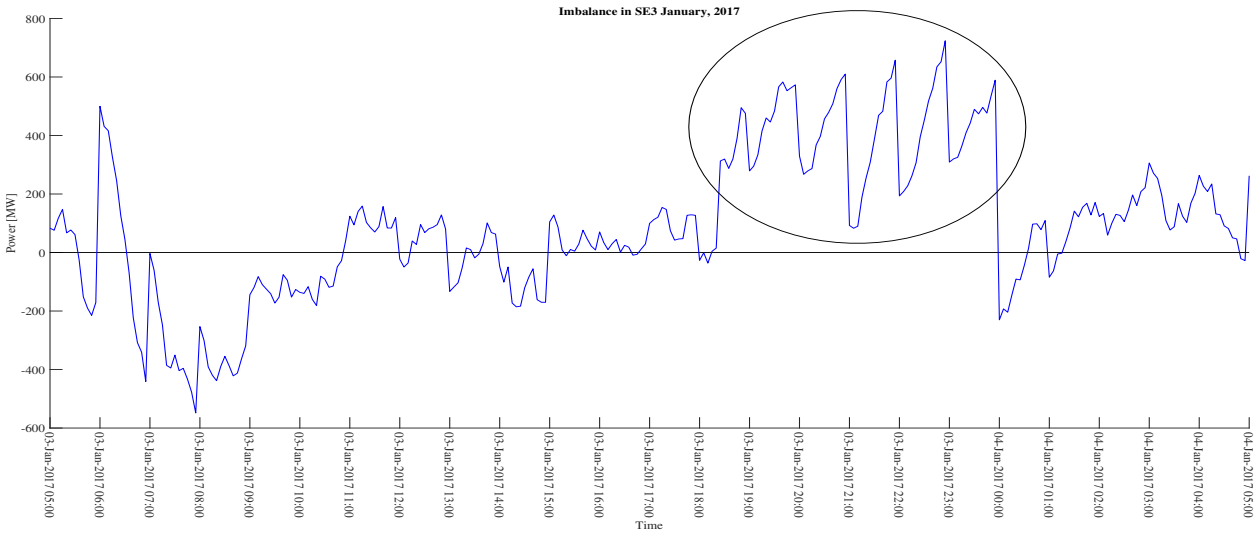

Figure 2.4: Structural imbalances in Southern Sweden in January 2017

2.2.3 Stochastic Imbalances

Stochastic imbalances occur due to the number of uncertainties and stochastic parameters that may disturb the power system. Loss of generation, system failure and line outages are examples of events that may cause stochastic imbalances. These imbalances do not occur because of market conditions but due to a natural uncertainty.

A special form of stochastic imbalances occur when the difficulty of accurately predicting the future lead to forecasting errors. Forecasting errors are deviations between production/consumption forecasts and production/consumption that actually occurred. In thermal or hydro power plants it is relatively easy to regulate the production and deliver accurate production forecasts, given sufficient water in reservoir or fuels in stocks. For intermittent power sources such as wind and solar power it is more difficult since the production rely on weather forecast. A future power system with large-scale installation of wind and solar power may therefore face larger forecasting errors [1], [31].

2.2.4 Provision of Balancing Services

A common balancing market where balancing energy is shared and exchanged between countries has been developed in the Nordic region. The purpose of balancing markets is to ”provde a framework for guarateeing system security a minimum socio-economic costs” according to [17, page 16], and this framework is constructed on three main pillars according to [45]; balancing service provision, balance responsibility and balance settlement. The participants in energy balancing are named after their function in energy balancing: Balance Service Provider (BSP), Balance Responsible Party (BRP) and Transmission System Operator (TSO). The TSO is responsible for the secure operation of the high voltage grid and will operate ancillary services to protect consumers from frequency deviation and black-outs. TSO is a non-commercial and typically governmental organization. The TSO will settle the balancing cost with BRPs to financially clear the balancing operation. BSPs are producers that can offer supply of electrical power into the grid. The BSP will bid their capacity into the balancing reserve market and be activated in real-time operation by the TSO. When there is a deficit of power in the grid, the TSO will activate upward regulation from BSPs to prevent a negative frequency deviation based on the price and location of the bid. As previously mentioned will each BRP send TSO their position; their production minus consumption and trade with other BRPs. The sum of BRPs imbalances will therefore equal the system imbalance. If the BRP is not in balance, BRP as the financially responsible entity will either sell (long position) or buy (short position) power of the TSO through the imbalance settlement. This is an incentive for BRPs to have balanced portfolios. The relation between the three entities is depicted in Figure 2.5, which underlines that BSPs are paid indirectly from BRPs through the imbalance settlement.

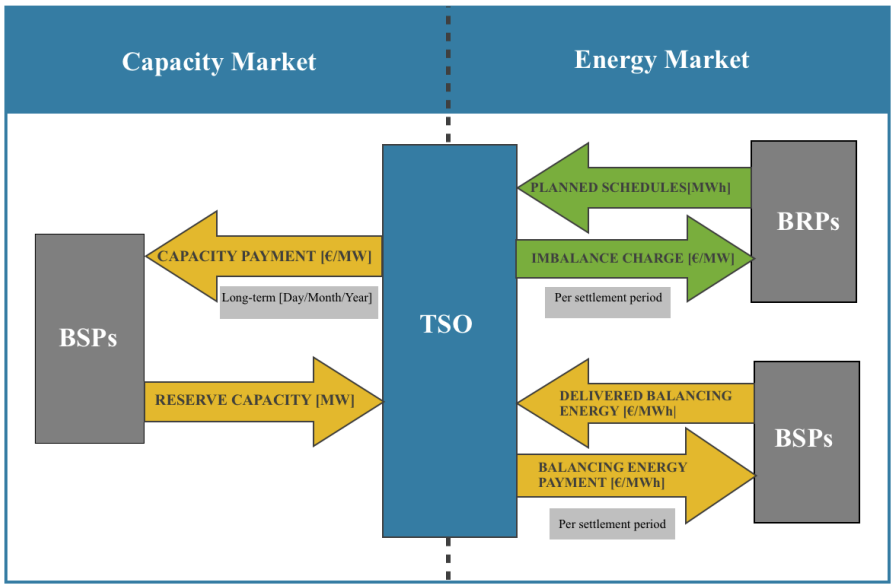

Figure 2.5: Relation between the capacity and energy balancing markets from [17, page 18]

Direction of payment between TSO, BRP and BSP is defined in Tables 2.1 and 2.2, as defined in the GL-EB [13, page 50]. GL-EB states that "TSO shall set up rules to calculate the imbalance price, which can be positive, zero or negative, as defined in Table 2.2". Positive balancing energy in 2.1 means that BSP is increasing generation to balancing a power deficit, and a positive imbalance in 2.2 means a system power surplus.

	Balancing energy price positive	Balancing energy price negative
Positive balancing energy	Payment from TSO to BSP	Payment from BSP to TSO
Negative balancing energy	Payment from BSP to TSO	Payment from TSO to BSP

Table 2.1: Direction of payment for mFRR, from [13, page 50].

	Imbalance price positive	Imbalance price negative
Positive imbalance	Payment from TSO to BRP	Payment from BRP to TSO
Negative imbalance	Payment from BRP to TSO	Payment from TSO to BRP

Table 2.2: Direction of payment between TSO and BRP, from [13, page 55].

Balancing service provision consist of two phases; procurement phase and employment phase. The purpose of the procurement phase is to ensure sufficient balancing reserves available to TSO for regulating system imbalances. This reserve is procured through a capacity market in which BSPs bid their capacity and the TSO pay the BSPs to have reserve capacities available for activation. Reserve Capacity agreements are normally long-term contracts between BSP and TSO. In the employment phase TSO activates balancing energy from the previously procured balancing capacity to handle real-time power imbalances. The balancing energy is activated based on BSP bids

in the energy market, and restrictions in the transmission network. Sufficient bids in the energy market is ensured by mandatory bidding for the BSPs that were activated in the procurement phase [43]. Each of the two phases of providing balancing services is handled at separate markets.

All Nordic balancing energy bids are placed on a common merit order list which the TSOs will activate from. However, each Nordic country has a different system to ensure that there is procured reserve capacity for balancing. In Norway, Norwegian bids on reserve capacity are bid into the Reserves Option Market (RKOM), which was established by Statnett in 2001. Bids in the RKOM can have time resolution of a week or a season. Statnett will buy the cheapest bids on reserve capacity in RKOM and all BSPs will be paid the price of the highest accepted offer. The BSPs that have their bid purchased by Statnett are obligated to bid their reserved regulation capacity in the energy market, and such is sufficient balancing energy ensured. The bids delivered by BSPs in balancing market are separated in upward and downward bids. In a upward regulating bid the BSP asks to be paid for a certain amount of increased production or reduced consumption. A bid on downward regulation states how much the BSP will pay to reduce production or increase consumption [20]. Bid prices are not known when the balancing reserve is procured in the capacity market; i.e. when procuring reserves, the price of keeping a reserve available is known, but the price of activating the reserve is not [49, page 293]. A BSP is incentivised to bid in the reserve capacity market by the possible net income, as formulated in equation 2.1 from [49, page 294];

$$\begin{aligned}\text{Net Income From Reserve Market} = {} & \text{Capacity} \cdot \text{Reserve Option price} \\ & - \text{Operating cost of keeping reserves available for generation} \\ & + \text{Expected revenue from possible activation in Balancing Market}\end{aligned} \tag{2.1}$$

Denmark has adopted the options market for regulation reserves, while Sweden and Finland procure regulation reserves through bilateral contracts [25, page 28].

2.3 Handling of Power Imbalances: Frequency Deviations and Control Mechanisms

It was previously stated that a power imbalance in a power system will cause a frequency deviation from the nominal value, which is undesirable from operations perspective. Three different control mechanisms are available for maintaining and restoring a frequency deviation following a disturbance; primary, secondary and tertiary control. They are named after their order in the balancing activation sequence presented in Figure 2.6, which is initiated by a frequency deviation in the orange graph. Shortly afterwards, primary reserve is activated, followed by secondary and tertiary reserves. Subsequently, frequency deviations are reduced and system power balance is restored. Working principles of each control mechanism are presented in greater detail in the following subsections.

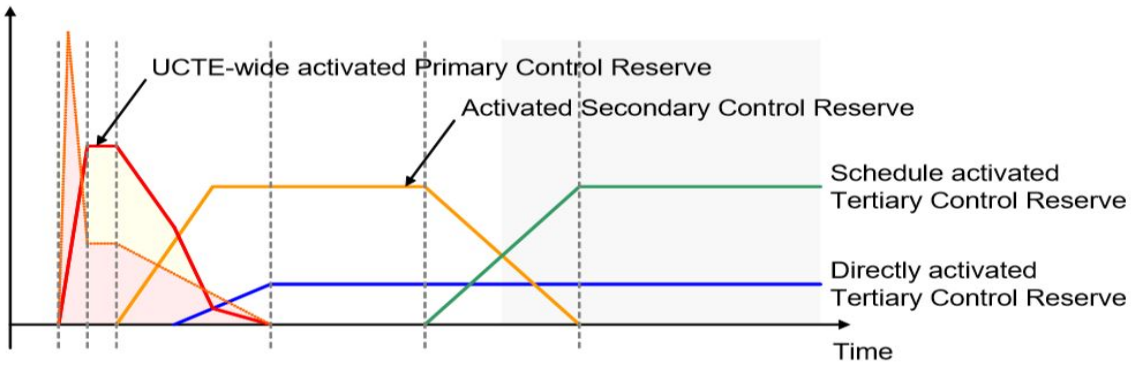

Figure 2.6: Balancing reserves activation sequence from ENTSO-E Operation Handbook [9, page 3].

2.3.1 Primary Control

Primary control is the first control mechanism activated after a disturbance, with purpose of containing the frequency deviation. Primary reserves are referred to as Frequency Containment Reserves (FCR) in the ENTSO-E classification. FCR activation is automatic and decentralized and a joint action of all TSOs in the synchronous area.

Primary control is based on automatic regulation of turbine governors through speed sensitive controllers [27, page 9]. Stable turbine operation means that electrical output power matches mechanical input power [2, page 31]. If rotational speed of turbine was to increase due to e.g. a frequency deviation in the network, mechanical input power to turbine must be decreased to restore equilibrium between electrical output of generator and mechanical input to turbine. Assuming a linear relationship between position of turbine valves and mechanical output power of the turbine, the ideal turbine characteristic is formulated in equation 2.2 [2, page 33].

$$\frac{\Delta\omega}{\omega_n} = -\rho\frac{\Delta P_i}{P_n}, \tag{2.2}$$

Equation 2.2 states the relation between change in rotational speed, $\Delta\omega$, and mechanical power output of unit i, ΔP_i, where ρ is referred to as the speed-droop coefficient, an adjustable parameter in the turbine controller. The rotational speed of the turbine is proportional to electrical frequency of the generator and equation 2.2 can be rewritten to equation 2.3 for generator i [2, page 367]. K_i is referred to as the effective gain of the governing system [2, page 33].

$$\frac{\Delta P_i}{P_{ni}} = -\frac{1}{\rho_i}\frac{\Delta f}{f_n} = -K_i\frac{\Delta f}{f_n} \tag{2.3}$$

Generation characteristics of all turbines in a large system are superimposed to obtain system generation characteristic c.f. equation 2.4, where ΔP_T represents the total mechanical power generated by all N_g generators:

$$\Delta P_T = \sum_{i=1}^{N_G}\Delta P_i = -\Delta f\sum_{i=1}^{N_G}\frac{K_i P_{ni}}{f_n} \tag{2.4}$$

.

Having system generation equal to system load, $\sum_{i=1}^{N_G} P_i = P_L$, and dividing equation 2.4 by system load P_L, the system generation characteristic can be formulated as equation 2.5.

$$\frac{\Delta P_T}{P_L} = -K_T \frac{\Delta f}{f_n}, \tag{2.5}$$

where K_T is calculated based on system load P_L

$$K_T = \frac{\sum_{i=1}^{N_G} K_i P_{ni}}{P_L} = \frac{1}{\rho_T}. \tag{2.6}$$

A prerequisite for primary control mechanism is that turbine is operating away from its maximum capacity when the rotational speed drops. If it was operating at its maximum capacity no increase in power output as described by equation 2.2 would be possible. The difference between the actual load and the power rating of the generator is referred to as spinning reserve and generating units delivering primary reserve are thus in part load operation.

Similar frequency dependence can be formulated for the system load ΔP_L as stated in equation 2.7.

$$\frac{\Delta P_L}{P_L} = K_L \frac{\Delta f}{f_n} \tag{2.7}$$

However, load sensitivity on frequency is much lower than for generation: K_L is typically between 0.5 and 3 while $K_T \approx 20$ [2, page 339]. Note opposing signs in equations 2.5 and 2.7 as the load increases for a positive frequency deviation.

The system equilibrium point is defined by equation 2.8 where the generation and load characteristics equal system demand ΔP_{demand} [2, page 339]. $K_f = K_T + K_L$ is referred to as system stiffness.

$$\Delta P_{demand} = \Delta P_T - \Delta P_L = -K_f P_L \frac{\Delta f}{f_n}, \tag{2.8}$$

Equation 2.8 states that a transition between equilibrium points following a change in system demand is sum of increased/decreased generation and decreased/increased load. Figure 2.7 depicts a transition from equilibrium point 1 to 2 where an increased demand ΔP_{demand} leads to decreased system frequency [2, page 339]. The new equilibrium in point 2 is established by an increased generation of ΔP_T and reduced load ΔP_L. Difference between nominal frequency and frequency at the new equilibrium is called the quasi-steady-state frequency deviation [17, page 20].

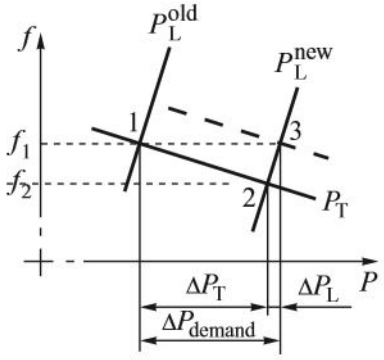

Figure 2.7: Transition between equilibrium points following a system demand increase, from [2, page 339].

The frequency bias factor for unit i, λ_i, is given in [MW/Hz] and calculated by equation 2.9. This factor relates change of power output from generator i following a frequency deviation Δf, closely related to the droop coefficient ρ.

$$\lambda_i = \frac{\Delta P_i}{\Delta f} = -\frac{1}{\rho_i}\frac{P_{ni}}{f_n} \tag{2.9}$$

Total frequency bias in a system λ is equal to the aggregate bias of all generating units N_G,

$$\lambda = \sum_{i}^{N_G} \lambda_i = -K_T \frac{P_L}{f_n}, \tag{2.10}$$

when neglecting the frequency sensitivity of demand in equation 2.7. System frequency bias λ describes amount of primary control that is activated for a given load and frequency deviation. Frequency bias in actual power systems is non-linear around nominal frequency, but averaged bias $\lambda = 5000$ MW/Hz in the Nordic synchronous system this project it is used an , similar to [27]. This simplification is further discussed in Section 4.2.1.

In the Continental synchronous area the maximum permissible quasi-steady-state deviation is $\pm$ 200 mHz [9, page 4] and 3000 MW primary control reserve is procured based on the reference incident. A reference incident is defined in [9] as "maximum instantaneous power deviation between generation and demand by the sudden loss of generation capacity or load-shedding/loss of load to be handled by Primary Control starting from undisturbed operation". Each control area within the synchronous area is obligated to contribute to total primary reserve based on contribution factors c_i. Contribution factors for each control area are calculated from the control area contribution in energy production as a share of total production in synchronous area [9, page 10].

Nordic FCR is divided into "Frequency Controlled Normal Operation Reserve" (FCR-N) and "Frequency Controlled Disturbance Reserve" (FCR-D). FCR-N is activated automatically at $\Delta f = \pm 0.1$ Hz with a reserve capacity of at least 600 MW at 50 Hz [10]. FCR-N is distributed based on annual consumption of each subsystem in the Nordic as presented in Figure 2.8a. FCR-N is a symmetrical reserve, meaning that it offers both upward and downward regulation.

FCR-D is only activated in upward regulation to prevent a frequency drop below 49.5 Hz. Distribution of FCR-D within the interconnected Nordic system is based on dimensional fault of each subsystem as presented in Figure 2.8b.

	Annual consumption 2013 (TWh)	Frequency controlled normal operation reserve (MW)
Eastern Denmark	13.7	22
Finland	85.2	138
Norway	130.0	210
Sweden	142.5	230
Synchronous system	371.4	600

(a) Distribution of FCR-N

	Dimensioning faults (MW)	Frequency controlled disturbance reserve (MW)	Frequency controlled disturbance reserve (%)
Denmark	600	176.5	14.7
Finland	880	258.8	21.6
Norway	1,200	352.9	29.4
Sweden	1,400	411.8	34.3
Total		**1,200**	**100.0**

(b) Distribution of FCR-D

Figure 2.8: 2013 distribution of FCR-N and FCR-D in the Nordic synchronous system from [10].

Since FCR is dimensioned to handle an outage of a large element, system security may be compromised if multiple elements fail simultaneously. Primary reserves therefore need to be freed as soon as possible to handle new imbalances, and this is done by secondary and tertiary control.

2.3.2 Secondary Control

As described in the previous Section, primary control alone is not sufficient to restore a deviating frequency back to nominal value. Frequency restoration is the purpose of secondary control and secondary reserves are also referred to as Frequency Restoration Reserves (FRR), further divided into manual FRR (mFRR) and automatic FRR (aFRR). However, only aFRR is considered secondary control and mFRR is a part of tertiary control described in the next Section.

Secondary control is operated in parallel with primary control and is based on automatic regulation of generator reference points. To ensure that imbalances are handled in the same area they originated aFRR is activated based on a Area Control Error (ACE) signal. ACE is calculated as sum of the tie line power deviations (power control error) ΔP_{tie} and frequency deviation (frequency control error) in each area Δf, c.f. equation 2.11.

$$ACE = -\Delta P_{tie} - \lambda_R \Delta f \tag{2.11}$$

Tie line power flows are flows that connect areas by crossing area borders, and aFRR activation by ACE implies that each area regulator is responsible for its own area power balance and maintaining the planned net exchange with its neighbouring areas. Area frequency bias factor λ_R is obtained from stiffness K_f and FCR participation in area. Use of ACE is presented in the diagram in Figure 2.9 where the ACE signal is integrated in a PI regulator and distributed on all generating units based on participation factors, changing their each generator operating reference to zero the ACE.

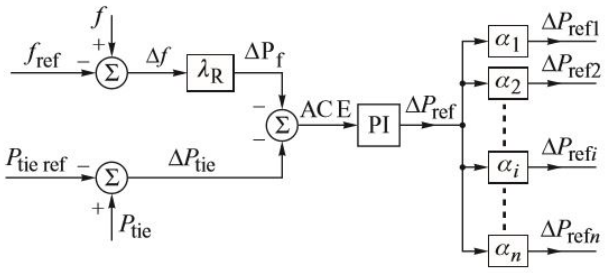

Figure 2.9: Diagram of ACE usage in a central area regulator, from [2, page 343]

The processes in Figure 2.9 underlines the slightly increased response time for secondary control compared to primary, with a maximum response time of 15 minutes in the Continental grid (response time here means total time required to zero ACE). Actual response time is normally shorter; 5-10 minutes on the Continent and 2-3 minutes in the Nordic system [27, page 11].

Secondary control was introduced in the Nordic system in 2013 and present work is done to develop a common market for aFRR between the Nordic member states [33]. Functioning of Nordic aFRR differs from Continental aFRR in that Nordic aFRR only handles frequency deviations, not tie line power flows [40]. Modelled aFRR in this project will therefore not consider tie line power flows.

2.3.3 Tertiary Control

Tertiary control is activated to free secondary reserves and restore frequency deviation upon persisting imbalances. Tertiary control may also be used to free transmission capacities to relieve bottlenecks, and consist of mFRR and Replacement Reserves (RR). Tertiary reserves have longest response time of all balancing reserves with a response time between 10 and 15 minutes. Manual reserves in the Nordic system are also called Fast Active Disturbance Reserve (FADR), while RR is not in use in the Nordic system.

Activation of mFRR is done manually by the TSO through a bid list. Producers can bid their reserve capacity to the TSO, with the obligation of providing real time balancing energy. In the Nordic system the balancing energy activation market is harmonized, meaning that all TSOs share a common merit order list for balancing energy. Procurement of mFRR capacity is done on a national level, c.f. Section **??**. TSO is obligated to reserve mFRR capacity equal to the control area dimensional fault through the Nordic System Operation Agreement [11] and Statnett procures 1700 MW, which is 500 MW more than dimensional fault.

2.3.4 Summary of Balancing Control Mechanisms

Relations and purpose of different control mechanisms are depicted in Figure 2.10.

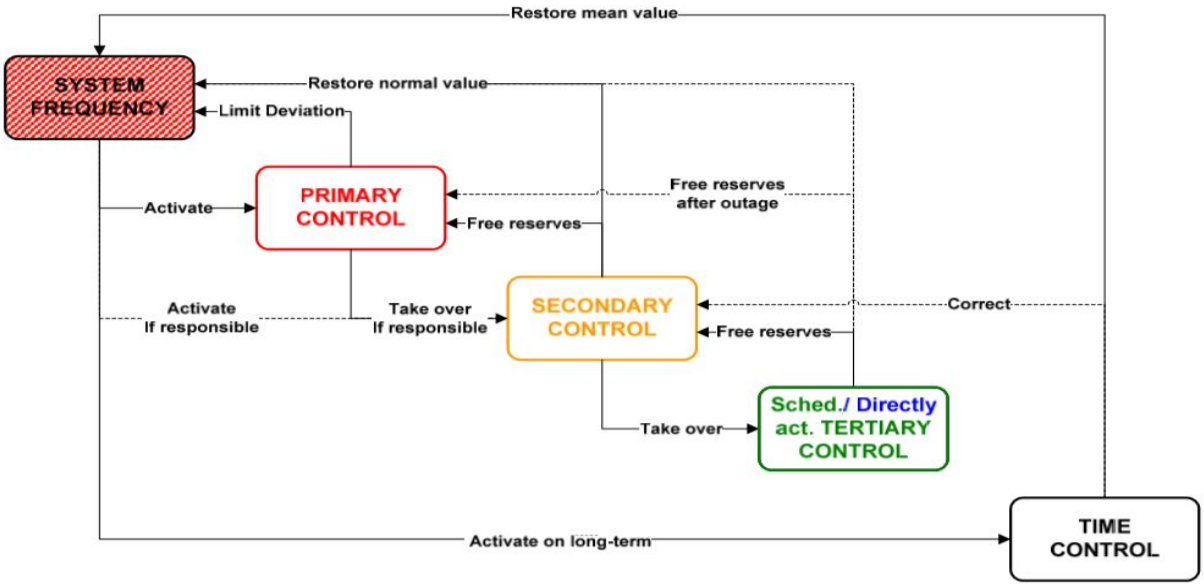

Figure 2.10: Overview of reserves functions from ENTSO-E Operation Handbook [9, page 2].

2.4 Integration of European Balancing Markets

To facilitate an integration of European balancing markets key functions and market mechanisms must be standardized and harmonized between EU member states. As of today, balancing philosophies, pricing mechanisms and imbalance settlement processes differ significantly between countries [51]. [45] presents the differences in balancing responsibility and imbalance settlement between the Dutch, German and Nordic balancing market, where the Program Time Unit (PTU), scope of balancing responsibility and main imbalance pricing mechanism are found to be design variables that contribute most to market design differences. PTU is the time interval between delivery of BRP schedules and hence the time period the BRP is responsible for its imbalances.

In [6] key design variables for multi control area balancing markets are presented and reviewed in Figure 2.11. Market design proposals are constructed by combining design variables, and the performance of each market design is measured from a set of weighted performance criteria. It is concluded that the market design with a common merit order list for balancing energy has highest score. The model developed in this project uses a common Nordic bid list of mFRR and aFRR balancing energy. A common merit order list for exchange of balancing energy is also a specified requirement in GL-EB [13].

Design variable	Values the variable can take
Type of exchanged balancing energy	• Secondary control • Tertiary control • Secondary and tertiary reserves
Definition of balancing regions	• Control areas correspond to balancing areas (separate balancing areas) • Two or more control areas are grouped into balancing regions
Market arrangements for balancing energy exchange	• None • Imbalance netting • BSP-TSO trading • Additional voluntary pool • Common merit order list
Market arrangements for reserve capacity exchange	• None • BSP-TSO trading • Additional voluntary pool • Common merit order list
Reservation of cross border capacity for balancing	• None • Independent of reserve capacity markets • Coordinated with reserve capacity markets

Figure 2.11: Design variables for a multi control balancing market, presented in [6]

Note that the design variables are separated with respect to reserve capacity and balancing energy, and that the design variable for cross-border balancing is only defined with regard to reserve capacity. Reservation of cross-border capacity for balancing purposes is a controversial issue as it may interfere with day-ahead and reduce the overall market outcome. In ENTSO-E position paper on cross-border balancing [12] it is stated that ”reservation of transfer capacity should only be carried out if social welfare can be demonstrated”. The optimal cross-border capacity reservation is depicted in Figure 2.12 as the intersection between marginal value of cross-border capacity in day-ahead market and balancing market (named ”AS” short for ancillary services in figure). An increase in transmission capacity in both markets would decrease social welfare. In [23] it is concluded that approximately 30 % of interconnection capacity between Norway and the Netherlands should be reserved for reserve capacity procurement, and between 5 % and 26 % on the links between Nordic system and Germany.

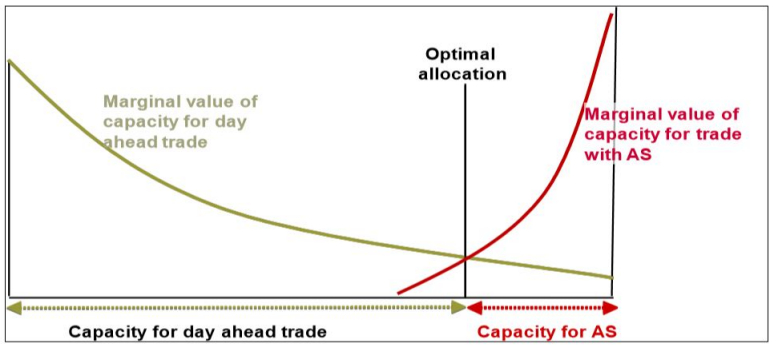

Figure 2.12: Optimal reservation of cross-border transmission capacity between day-ahead and balancing market, obtained from [12, page 9]

2.4.1 Standard Products

According to [13], all TSOs have to define a set of Standard Products to be available for TSO for energy balancing as part of the European balancing markets integration. Standardization of energy balancing bids means that exchange of balancing energy is possible between TSOs that before used different and incomparable products. A Standard Product is a set of predefined characteristics that a balancing bid must adhere to. Such characteristics may be full activation time (time between activation and full delivery), minimum or maximum duration and activation mode. The Standard Products will be defined for manual and automatic products but in this project only Standard products for mFRR has been used. Table 2.3 present the Standard products that have been formulated in this project, which represent a subset of proposed Standard products in [38].

Product type	**P1**	**P2**	**P3**	**P5**
Preparation period	5 minutes			0 minutes
Ramping period	10 minutes			5 minutes
Full Activation Time	15 minutes			5 minutes
Minimum volume	5 MW			
Maximum volume	9999 MW			
Minimum duration of delivery period	5 minutes	10 minutes	15 minutes	5 minutes
Maximum duration of delivery period	30 minutes	30 minutes	30 minutes	30 minutes
Divisible	Defined by BSP/bid list			

Table 2.3: Specifications for Standard Products used in model.

Only 5 different Standard products have been used in this project. GL-EB [13, page 34] specifies that TSO needs should be covered with a limited number of Standard Products to reduce market fragmentation between products.

Full Activation Time (FAT) is the total time between activation of a bid and full delivery, or the sum of preparation time (a) and ramping time (b) in Figure 2.13a. The delivery period begins at time-step h. FAT is normally constrained by type of power plant that is delivering the bid. A

hydro power plant will be able to deliver bids with a shorter FAT than a thermal power plant, where ramping duration may be longer. Not only ramping duration is of importance, the amount of energy delivered during ramping must also be considered by the TSO. For products with long FAT a considerable amount of energy may be delivered during ramping. Figure 2.13b show some of the different ramping profiles that may occur. A Time To Restore Frequency (TTRF) is defined as the target time for the TSO to restore frequency following an event. A TTRF of 15 minutes is the target in Europe [38, page 12]. This implies that some bids must have an FAT below 15 minutes, shown by the green graphs in Figure 2.13b. The 5 minute and 10 minute mFRR ramping profiles that have been formulated in this project are presented in Section 3.1.3. Hence, the BSPs may select a ramping profile to follow. In real-life operation this would be meaningful to the TSO as it is easier to match requested and delivered energy. However, if the BSP is only paid for requested energy and not delivered energy, it would be reasonable for BSP to minimize ramping power if possible, i.e. the lowermost ramping profile in Figure 2.13b. With installation of flexible storage technologies (batteries, pumped hydro, flywheel etc.) and fast demand response, one may speculate that delivered ramping volume in future power systems may decrease.

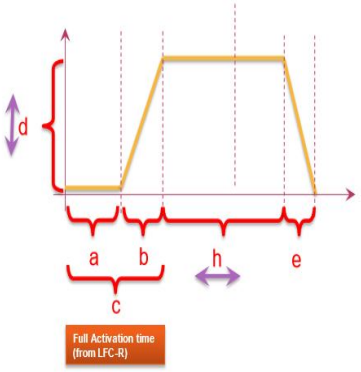

(a) Full Activation Time (FAT), from [38, page 9]

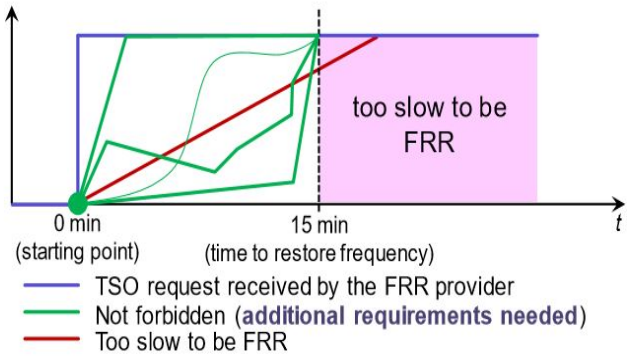

(b) Ramping profiles, from [38, page 12]

Figure 2.13

2.4.2 Activation Optimisation Function (AOF)

The motivation behind an AOF is to ensure optimal balancing energy activation and exchange of balancing energy between control areas in integrated balancing operation. AOF is thereby an optimisation algorithm able to compare balancing bids with different locations, prices, volumes and Standard Product characteristics to schedule balancing activations. AOF must be non-discriminatory, and commonly agreed upon and developed by the relevant TSOs. Main steps in AOF functioning is presented in [14, page 22] accordingly:

> The steps involved in the activation of Balancing Energy are as follows:
>
> 1. The Requesting TSOs send their requirements to the Activation Optimisation Function.

2. After the Balancing Energy Gate Closure Time, the Activation Optimisation Function calculates the most efficient activation taking the following into account:
   (a) Common Merit Order List containing all Balancing Energy bids
   (b) Available Cross Zonal Capacity either available after Intraday or reserved previously
   (c) Network stability constraints
   (d) Balancing requirements of the TSOs
   (e) Imbalance Netting potential
3. Activation Optimisation Function sends the individual activation amounts (as a correction signal) to each responsible TSO (connecting TSO)
4. The Connecting TSO activates the successful Balancing Energy Bids (via phone call or automatically by activation system such as a MOL-Server or local controller).
5. Balancing Energy is exchanged through commercial schedules or virtual tie-lines.
6. Balancing Energy is settled between the providers and the TSOs involved.

2.5 Power Flow Analysis, DC Load Flow and DC Optimal Power Flow

A power flow analysis is carried out to determine the power flows in a network. The power flow depends on voltage magnitude, voltage angle, line reactance and resistance and power injections/withdrawal at every bus. In general terms it may be stated that power flow calculations determine the electrical state of the system [2, page 122]. Voltage magnitudes and angles are also called state variables, and are used to determine other system parameters such as transmission losses and voltage drops.

Buses in a network are characterized in a power flow analysis according to Table 2.4, where P and Q are active and rective injections, $|V|$ is voltage magnitude and δ is voltage angle. A bus connected to a synchronous generator (generator bus) is able to control and maintain a constant active power output and voltage magnitude by regulation of terminal voltage through Automatic Voltage Control (AVC) which regulates the DC field current and hence magnetic flux within the rotor [3, page 216]. Active power output is regulated by the turbine governor adjusting turbine valves.

Negative injections are specified for load buses, also referred to as PQ-buses, leaving voltage magnitude and angle to be computed. The slack node serves as angle-reference for all other nodes in the network, and a voltage angle of zero degrees is specified for this bus. Voltage magnitude is also specified, leaving active and reactive injections to be determined. If there is mismatch between power injected at generator buses and power consumed at load buses e.g. due to transmission losses, this will correspond to power injection at the slack bus.

	Known	Find
Load bus (PQ-bus)	P,Q	$\|V\|$,δ
Generator bus (PV-bus)	P,$\|V\|$	Q,δ
Slack bus	$\|V\|$,δ	P,Q

Table 2.4: Different bus types in power flow analysis

2.5.1 DC Network Equations

In the optimisation model presented in Section 3, equations for calculating power flows resulting from balancing energy injections are presented. AC network equations will not be presented here, but can be reviewed in power system literature [2, page 113]. Most importantly, AC network equations formulate the non-linear relationship between active and reactive power injections and nodal voltage magnitudes, and state variables are normally calculated in the iterative Newton-Rhapson computation technique. AC equations can be linearised to avoid this time-consuming calculation method, resulting in a DC load flow. Linearisation of AC network equations enable them to be formulated as linear constraints in an MILP optimisation problem as formulated in Section 3, leading to an extensive use of DC load flow assumptions in market clearing formulations and economic dispatch models. When deriving DC network equations, the following assumptions are made [5]:

1. Equal nodal voltage magnitude of 1 pu at every node in network (flat voltage profile).
2. Line conductance is negligible compared to line susceptance.
3. Small voltage angle differences between nodes.

A consequence of the second assumption is the absence of active transmission losses. This underlines the fact that a DC load flow does not equivalent a load flow for a DC network. In the latter case line resistance would lead to transmission losses, while transmission losses are neglected in a DC load flow. Equation 2.12 gives active power flows between bus i and j as function of voltage angle difference between the buses and line reactance, resulting in the nodal active power balance in equation 2.13 [5].

$$P_{ij} = \frac{(\delta_i - \delta_j)}{X_{ij}} \tag{2.12}$$

$$P_i = \sum_{j=1, j\neq i}^{Buses} |Y_{i,j}| \cdot (\delta_i - \delta_j) \tag{2.13}$$

Where:

- P_i: Active power injected in node i
- $Y_{i,j}$: Admittance matrix
- $P_{i,j}$: Active power flow from node i to node j.

- $X_{i,j}$: Susceptance of line connecting node i and j.
- $\delta_i - \delta_j$: Voltage angle difference between node i and j.

The nodal energy balance in equation 2.13 formulates the relation between power injection and line reactance on power flows in the network, implying that a nodal injection will cause larger flows on lines with small reactance than on lines with larger reactance, which again means that the power will not necessarily flow in the intuitive direct path between two nodes. Instead, it may take long de-routes or loops. Figure 2.14 depicts loop flows from a 1000 MW trade transferred from Northern France to Italy where 38 % of the power flows directly in contracted path.

Although power flows are ultimately determined by the Kirchoff laws measures are available to TSO to control power flow. Examples are series compensators, quadrature booster transformers and FACTS (controlling the power flow through voltage angle control), and functioning of these devices may be further studied in [2, page 119].

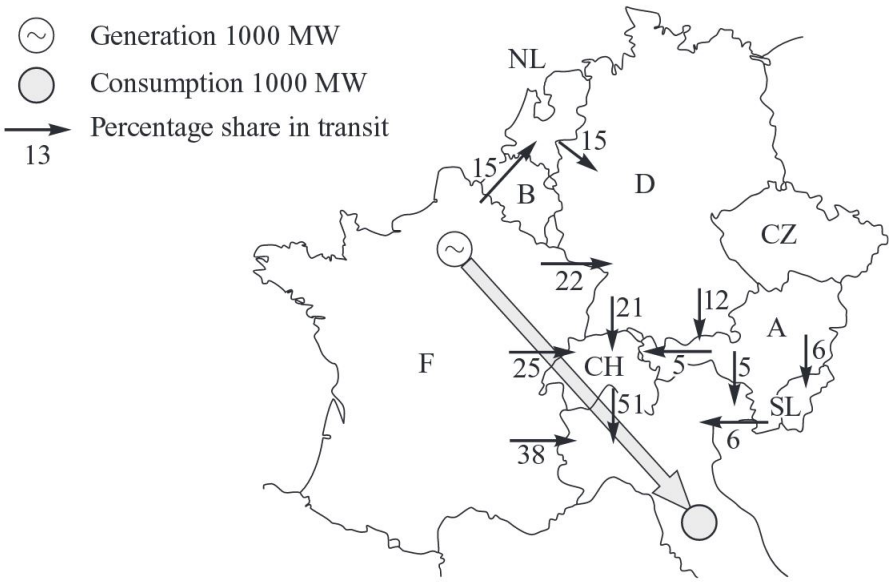

Figure 2.14: Loop flows from a 1000 MW trade between northern France and Italy, from [2, page 121] (originally published in Haubrich and Fritz, 1999).

Loop flow effects pose a challenge for system operators that are responsible for system security in liberalized power markets, in the sense of determining available transfer capacity between market areas. Two approaches for determining the transfer capacities are flow-based and Net Transfer Capacity (NTC) approach. In a flow-based approach, line flow sensitivity coefficients from nodal injections, referred to as Power Transmission Distribution Factors (PTDFs), are used to locate loop flows. A flow-based approach will therefore include effects on individual power flows from nodal injections. In an NTC approach, the loop flow effect is addressed by a security margin on the power flow between areas. Hence, NTC approach gives the exchange capacity between neighbouring market areas neglecting actual flow path. This implies that TSO do not know exactly what path the power will take between seller and buyer since nodal injections from a trade are not transformed

into physical network flows. That may lead to inefficient utilization of the transmission network as large security margins may be used on lines with small risk of being overloaded and reduce positions available on the market compared to a flow-based approach, reducing overall market efficiency [8]. [50] concludes that a flow-based formulation will increase the network efficiency (better utilization of physical transmission capacities), and thereby lead to higher economic welfare in the modelled Central Western European region. [24] show that the average balancing cost is approximately 20 % higher for the NTC approach for an integrated case study on the IEEE 30-bus system due to different generator unit commitments. Although possibly increasing market efficiency, a flow-based approach would require increased computational effort compared to an NTC approach.

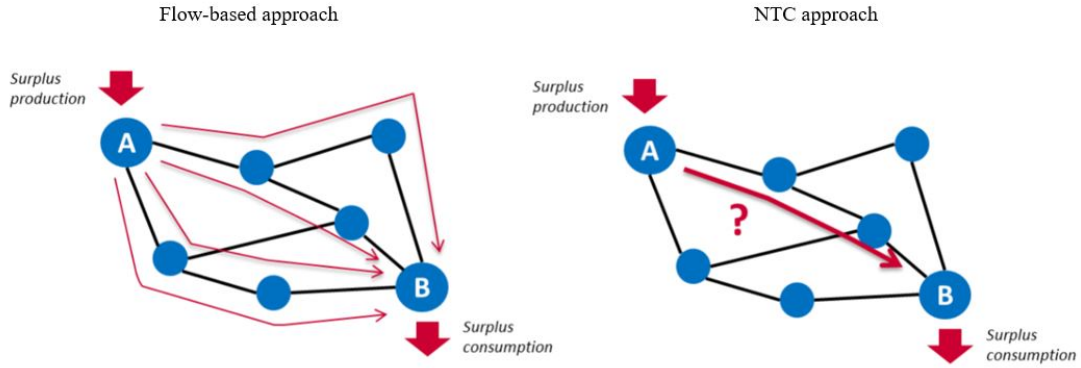

Figure 2.15: A flow-based approach accounts for the physical flows in the network, from [8].

The EU Guideline on Capacity Allocation and Congestion Management (CACM) [22] specifies the flow-based approach for cross-border transfer capacity calculation. The NTC approach is currently in use in the Nordic system, although the evaluation of possibly introducing flow-based market coupling in the Nordic system has been started [8], [7].

2.5.2 DC Optimal Power Flow (DCOPF)

The purpose of a DC Optimal Power Flow (DCOPF) is to determine optimal dispatch of generators to cover a load, constrained by the DC load flow equations in 2.13. Producers have different marginal costs of production and a DCOPF will calculate the mix of generators that needs to be active for reducing the cost of the consumers. A simple DCOPF problem can be formulated as the optimisation problem in equations 2.14-2.17.

$$\min \quad Cost = \sum_{g \in Gens.} P_g \cdot C_g \tag{2.14}$$

S.t.

$$\mathbf{A}_{g,i} \cdot P_g = L_i + \sum_{j=1, j\neq i}^{Buses} \frac{(\delta_i - \delta_j)}{x_{i,j}} \qquad \forall \quad i,j \in Buses, \quad g \in Gens \tag{2.15}$$

$$\underline{P_g} \leq P_g \leq \overline{P_g} \qquad \forall \quad g \in Gens \tag{2.16}$$

$$\underline{P_{i,j}} \leq \frac{(\delta_i - \delta_j)}{x_{i,j}} \leq \overline{P_{i,j}} \qquad \forall \quad i,j \in Buses | i \neq j \tag{2.17}$$

$$P_g \geq 0 \qquad \forall \quad g \in Gens \tag{2.18}$$

Equation 2.14 is the objective function of minimizing total generation cost given as the product of generation, P_g, and marginal cost of production, C_g. Equation 2.15 states that the generation at bus i, must equal the load L_i and total net flow out of the node, similar to equation 2.13. The binary connection matrix $\mathbf{A}_{g,i}$ connects generator g to bus i. The equality sign in equation 2.15 expresses a hard constraint on bus energy balance. If there is insufficient generation capacity to cover the load, no solution can be found that satisfies equation 2.15 and the optimisation problem is infeasible. To prevent infeasible solutions, the nodal energy balance constraint can be made soft by formulating an inequality constraint and incure a penalty cost on deviations from 0. Energy balance is incentivized if the penalty cost level is greater marginal cost of production C_g. This technique forms the basis of the energy balance soft constraint concept presented in Section 3.1.4, where net energy imbalance at bus i is interpreted as required activation of load/generation shedding for energy balance restoration. Load/generation shedding is a functionality in real-life system operation to maintain system security [41]. The generator capacity and transmission line capacity are constrained by equation 2.16 and 2.17, respectively.

The above DCOPF represents a simple formulation to match supply and demand while considering grid constraints and loop flows. More complex formulations based on DCOPF can be written to account for security margins, referred to as a Security Constrained Optimal Power Flow OPF (SCOPF). Such a formulation can be found in [32], where socioeconomic tradeoff between system security, represented by voltage stability margins, and social welfare in market clearing is optimized.

2.6 Relevant Previous Work

In [27], a Mixed Integer Linear Programming (MILP) optimisation problem is formulated to model balancing energy activation. A set of mFRR Standard Products based on proposals in [**?**] is defined. Effects of Standard Product definitions on balancing energy activation cost and model behaviour is investigated. An important conclusion is that imposing constraints that reduce product flexibility lead to higher activation costs. Product specific constraints that are presented in Section 3.2.3 are based on equations presented in [27]. The model presented in [27] does not include a network representation or delivered energy during bid activation (ramping power). Ramping constraints for mFRR products with 15 FAT are presented in [28] and form the basis of ramping constraints formulated in this model. The main contribution of the work in this thesis is the inclusion of physical network effects and a network representation.

TERRE project presented in [26] is a proposed platform for exchange of Replacement Reserves (RR) in the European Continental system (UCTE). TERRE project is a pilot initiative with 8 European TSOs participating. None of the participating TSOs are Nordic, as RR is not in use in the Nordic system. The goal of TERRE project is "to establish and operate a platform capable of gathering all the offers for Replacement Reserves from TSO's local balancing markets and to provide an optimized allocation of RR to cover the TSOs imbalance needs" [26, page 9], in compliance with GL-EB [13]. TERRE proposes an algorithm for RR exchange between TSOs that uses an Available Transfer Capacity (ATC) optimisation model with minimization of cross-border flows in the objective function. An ATC formulation assumes that power flows are in their contracted path, c.f. Section 2.5.1 and will not consider actual network flows. TERRE also uses a block bid formulation neglecting ramping energy delivered between activation and scheduled delivery. These are necessary simplifications that improve computational effort for the large and complexly meshed Continental synchronous system.

[19] describes a model for an integrated Northern European balancing market, using a flow based approach. For the case where HVDC interconnectors between the Nordic and CE system can be used for balancing purposes a reduction of 31 % of reserve activation is observed compared to non-integrated case. In addition, the results show that 30 % of total required upward regulating reserve in the continental system is procured in the Nordic system due to the large capacities of flexible and cheap hydro-power.

In [24] a DCOPF based balancing energy market model compares balancing cost of a flow-based and NTC approach on a modified IEEE 30-bus test system. For the case where balancing energy is exchanged between zones it is shown that about half of the imbalance energy is netted, with the NTC approach leading to highest balancing cost. The use of Power Transmission Distribution Factors is a distinction from the formulation in this project, all the while the physical flows from nodal injections are accounted for in both formulations.

[20] proposes an incremental DCOPF formulation for dispatch of regulation resources including transmission losses. Transmission losses are calculated in an iterative procedure based on the flows in an initial DCOPF, adding these losses to transmission lines from the DCOPF and then use the losses in the new dispatch solution. This forms an alternative to a ACOPF where the iterative DCOPF procedure is faster [36], [29].

[18] presents a two-step approach for modelling integration of Northern European balancing markets; first settling the day-ahead and procuring the required regulation reserve, then activating balancing energy in real-time dispatch with the day-ahead clearing results constraining exchange capacities. A DCOPF is used both in the day-ahead and balancing market modelling. Three different cases are defined, specifying different levels of integration between control areas. It is demonstrated reduced cost for both reserve procurement and balancing for the Northern European area in case with highest level of market integration, where a significant decrease in balancing cost is caused by imbalance netting. Imbalance netting is the cancelling of opposing imbalances without balancing activations. Most of the procured balancing reserve is located in Norway in the full integration case due to cheap hydro power, leading to a net export from the Nordic system to the Continent, most from NO1 to NL.

Chapter 3

Methodology

3.1 Introduction

In this Chapter the optimisation problem is presented together with relevant data inputs and description of scenarios. The Chapter begins with presentation of key concepts; pricing of aFRR and frequency deviations, geographical distribution of imbalances, pricing of load/generation shedding and mFRR energy delivery profiles. Mathematical formulations of all constraints are then presented, followed by description of input data.

The model is formulated as a Mixed Integer Linear Programming (MILP) problem with linear and binary constraints. Some of the constraints originates from previous work in [27, 28, 17, 24], and therefore follow same notation to a large extent. The model is formulated in XPRESS and is run and initialized using the MATLAB-XPRESS interface, documented in [21].

The model has a scheduling horizon of 45 minutes and time-resolution of 5 minutes. A trade-off between algorithm run-time and advantage of long term planning must be considered when deciding on scheduling horizon. A long scheduling horizon would take more time to compute, too short horizon means that activations are made based on close-to-operational conditions. This is a problem when the bids are required to remain active for a long period of time, and a model with a long scheduling horizon would be better able to plan activation of such bids.

A rolling horizon simulation procedure using an incremental real-time dispatch similar to the implementation in [28] is used. Rolling horizon formulation is used to simulate one day of balancing operation in this thesis although longer analysis periods are also possible. The procedure is based on continuously updating imbalance forecast and bid activation history. Balancing activations may be sunk decisions considering the activation history and time-coupling through minimum duration periods; a bid can not be deactivated or changed if it was activated 5 minutes ago and is required to remain active for minimum 15 minutes. Rolling horizon procedure is presented in Figure 3.1.

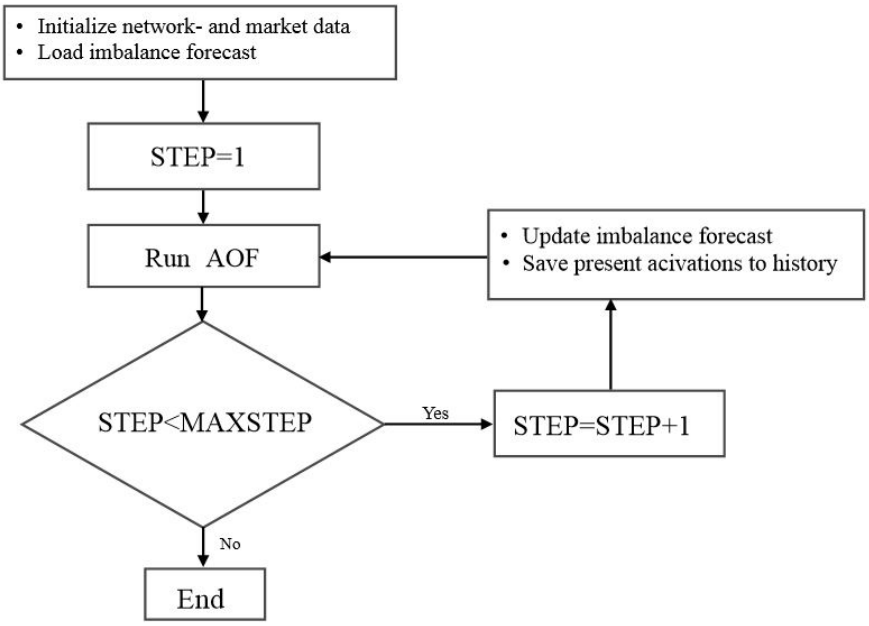

Figure 3.1: Flowchart of rolling horizon simulation procedure.

3.1.1 Pricing and Geographical Distribution of aFRR

It is assumed that aFRR is bid to the balancing market similarly as mFRR. A common Nordic aFRR energy activation market is currently being developed [33], and the aFRR pricing used in this project therefore is a temporary approach. Price of upward and downward regulating aFRR bids is set to 55 €/MWh as a modelling measure to ensure that aFRR is only activated when mFRR capacity is exhausted. Because aFRR is assumed to have a shorter response time than the time-resolution of 5 minutes used in the model, no ramping constraints for aFRR activation is formulated. For the same reason the modelled aFRR neither has a minimum duration period or any other temporal couplings.

The aFRR capacity is distributed according to Figure 3.2. Each area has some aFRR capacity, and SE3 is the area with the largest aFRR capacity of 50 MW. The presented aFRR distribution originates from a proposal in [34]. The total aFRR capacity in the system equals 300 MW in each regulating direction. The aFRR bids for upward and downward regulation are presented in Tables 3.6 and 3.7.

The aFRR in the Nordic system operates differently from Continental aFRR where the input signal to the aFRR controller is ACE. In the Nordic system, aFRR is activated from a frequency signal, meaning that a Nordic aFRR will not be used to restore scheduled tie line flows.

Figure 3.2: aFRR distribution in model.

3.1.2 Modelling Frequency Deviation Penalty Cost as a Fictional FCR Price

The model will not regulate imbalances if there is no incentive to do so. A frequency deviation will arise if there is a mismatch between imbalance power and activated balancing power, ergo will a frequency deviation imply FCR activation. The relation between activated FCR and frequency deviation is described in equation 2.9 on Page 17, where the activated FCR multiplied with the frequency bias factor, λ, gives system frequency deviation.

A fictitious price has been set to the activation of FCR to give the model an incentive to reduce frequency deviations. The fictitious FCR price operates as a soft constraint on system frequency deviations. Note that this is a modelling measure to reduce frequency deviations and does not represent real life balancing, where FCR energy is not priced but automatically activated by droop settings as described in Section 2.3.1.

Indirect pricing of frequency deviations through a fictitious FCR price means that a reasonable FCR price must be used to prevent balancing the system using FCR, although the social cost of frequency deviations is not known. A too low price on FCR may favour having FCR reserves active instead of maintaining system energy balancing by mFRR and aFRR. The objective of the algorithm presented in Figure 3.3 is to find the FCR price that leads to fewer than 10 000 minutes at frequency deviations exceeding $\pm$ 0.1 Hz per year, which is the standard on frequency quality in the Nordic system [15].

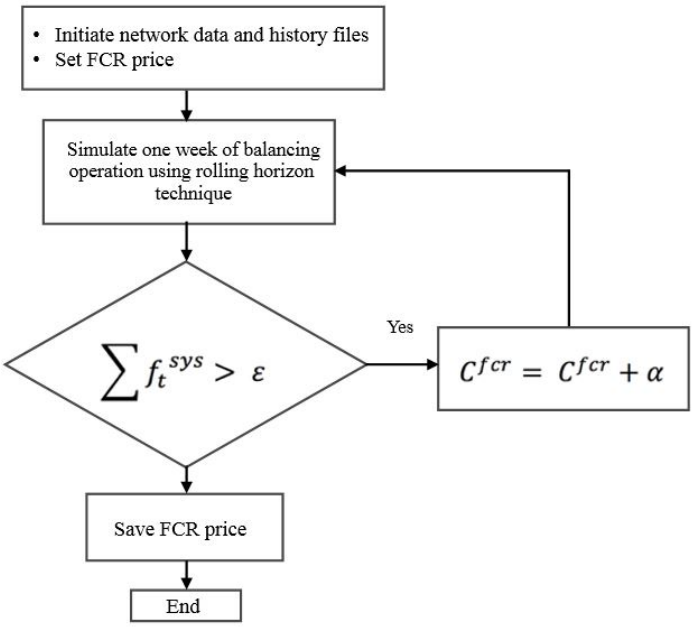

Figure 3.3: Flowchart of algorithm for FCR-pricing

The frequency quality requirement is defined for a year but is scaled to one week when the FCR price is determined in this project. This is because only one week of historical imbalance data is available, specifically the first week of January 2017, from January 2. to January 9. Scaling the yearly frequency requirement to one week equals about 190 minutes on frequency deviations outside $\pm$ 0.1 Hz, or 38 time-steps when a 5 minute time-resolution is used. Thus, $\epsilon = 38$ is set as the frequency quality target. An incremental value on FCR price between simulations of $\alpha = 10$ has been used. Table 3.1 shows that an FCR price of C^{fcr}=40 €/MWh leads to 32 time-steps with unsatisfactory frequency deviation, and this FCR price is used in all scenarios presented in Section 3.4.

Which FCR price that leads to a satisfactory frequency quality is dependent on balancing capacity of mFRR and aFRR, network structure and imbalances. For instance, if the model is able to cancel all opposing imbalances without balancing activations, the frequency quality standard will be met with a low FCR price. A cost of 40 €/MWh for frequency deviations would therefore not necessarily guarantee satisfactory frequency quality for a different analysis period or different bid lists.

FCR-price [€/MWh]	Number of time-steps outside frequency band ± 0.1 Hz
0	1437
10	63
20	45
30	44
40	32

Table 3.1: Results from FCR pricing algorithm

3.1.3 mFRR Ramping and Delivery Profiles

Upon activation of a bid the entire activated amount of energy will not be delivered immediately. Initially, some preparation time for BSP to prepare the bid must be expected. Then, the BSP will start delivering the energy, but following a ramp profile, meaning that the delivered energy increases until the activated volume is reached. A ramp profile will depend on the technology that is delivering the bid; a hydro plant will have a shorter ramping period than a thermal power plant.

Ramping profiles will normally not follow a smooth, linear curve, and may differ substantially between producers. A focus area in the harmonization of balancing products is whether it should be specified ramping profiles that producers are obligated to deliver, if any profile could be followed as long as the correct activation volume is reached within a defined time limit or if an equivalent delivered power is determined by also included the energy delivered during ramping [38]. In either case, the energy delivered during ramping may contribute to a large share of the total bid energy and should therefore be included in the formulation.

Full Activation Time (FAT) is the sum of the preparation period and ramping period. Two different ramping profiles according to the profiles in Figure 3.4 have been developed. Ramping profile for 15 minutes FAT is based on the constraints in [28]. The 15 minute FAT ramping profile is depicted to the left in Figure 3.4 and marked in blue. In this example the delivery set-point is 40 MW but this volume is not delivered until after completion of 3 time-steps (15 minutes) of preparation and ramping. Figure 3.4 presents a profile with FAT=5 minutes to the right. Ramping begins immediately after activation. In reality, a preparation period will precede the ramping period, but because the preparation period is less than the time resolution of 5 minutes when FAT=5 minutes, no preparation period is formulated. Ramping begins immediately with half of the activated power of 40 MW, and the bid remains active for 15 minutes. No ramping is formulated for aFRR bids, as these are assumed to have shorter activation time.

The mFRR bids are constrained to a flat profile for a minimum duration equal to the minimum duration period after FAT is completed. If the model wants to change delivery set-point after the initial FAT and before having to deactivate at maximum duration, the power-level can be changed without having to go through another FAT. This is a simplification further discussed in Section 4.2.5.

Mathematical formulations of ramping profile constraints will be described later in the Chapter but the approach is introduced here. For each mFRR bid b there is one decision variable $y^R_{b,t}$ which is the ramping power that is delivered from mFRR bid b at time t. The ramping variable will deliver ramping power according to the variable $y^S_{b,t}$, which is referred to as the delivery set-point variable.

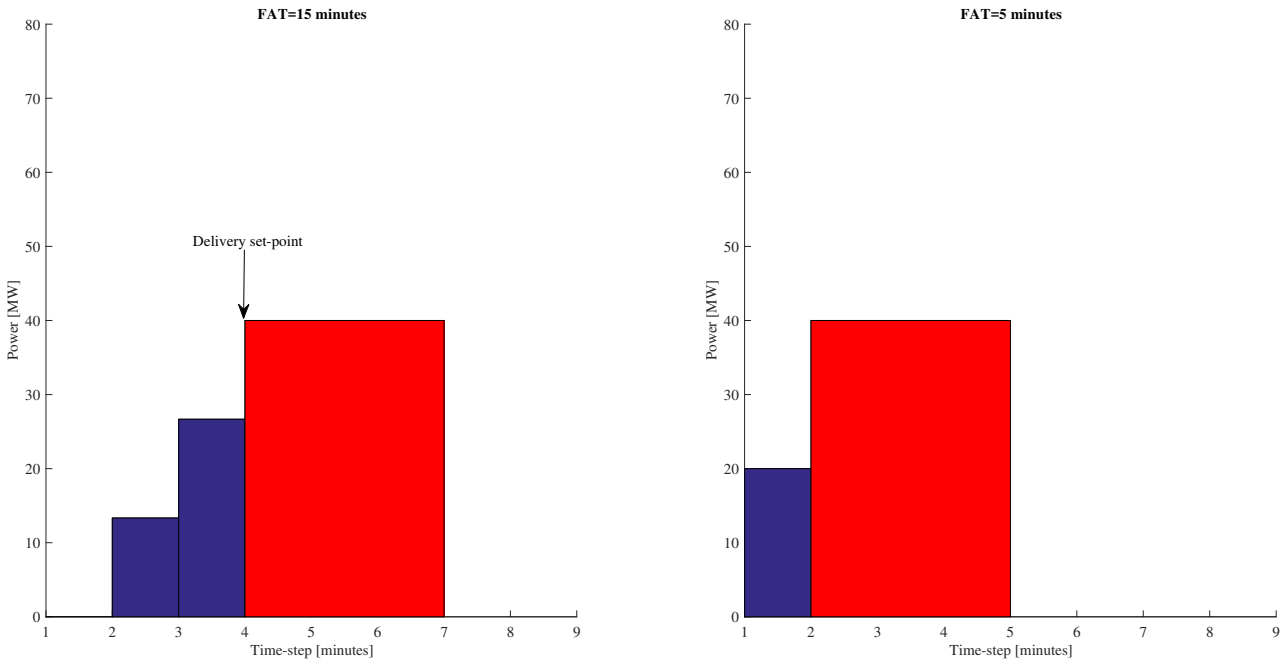

Figure 3.4: mFRR bid profiles with different Full Activation Time (FAT)

The set-point variable is expressed as the share of bid capacity. For instance, in leftmost graph in Figure 3.4, $y^S_{1,4} = 0.5$ if volume of bid 1 is 80 MW. The ramping power in prior time-step, $y^R_{b,t-1}$, is 2/3 of the set-point variable, while $y^R_{b,t-2}$ is 1/3 of the set-point variable value. For bids with 5 minute FAT the set-point variable is defined equally to the 15 minute FAT products. However, ramping power is set to 1/2 of the set-point variable, giving the rightmost ramping profile.

3.1.4 Modelling of Load/Generation Shedding as Soft Constraint on Nodal Energy Balance

In real system operation TSO has the possibility of disconnecting loads or generators to protect lines and equipment from overloads or excessive frequency deviations [11, page 8]. A load/generation shedding functionality has been implemented in the model by imposing a soft constraint on the energy balance in each bus as presented in equation 3.5 in Section 3.2.2 and simplified in equation 3.1 for bus i in time t.

$$dev_{i,t} = mFRR_{i,t} + aFRR_{i,t} + FCR_{i,t} + (flow_{in,i,t} - flow_{out,i,t}) + imbalance_{i,t} \tag{3.1}$$

The shedding variable $dev_{i,t}$ will have a non-zero value if the imbalance $w_{i,t}$ is not regulated by FCR, aFRR, mFRR or imbalance netting at bus i in time-step t. If $dev_{i,t}$ <0, it is interpreted as the volume of shedded load, and opposite can $dev_{i,t}$ >0 be interpreted as volume of shedded generation. Load/generation shedding is not meant to be activated frequently but will serve as a last resort for ensuring convergence in challenging balancing situations.

A piecewise-linear cost function is formulated for load/generation shedding, as depicted in Figure 3.5. A piecewise-linear cost curve is used to prevent large effects on total balancing cost when small volume below 1 MW is shed. For less than 1 MW shedding, a cost of p_1=10.000 €/MWh will be incured on the optimisation problem. When volume exceeds 1 MW shedding will cost p_2 =100.000 €/MWh. These are fictional modelling costs. A high cost has been used to ensure that it is only activated as a last resort when the model can not handle the imbalances by other means.

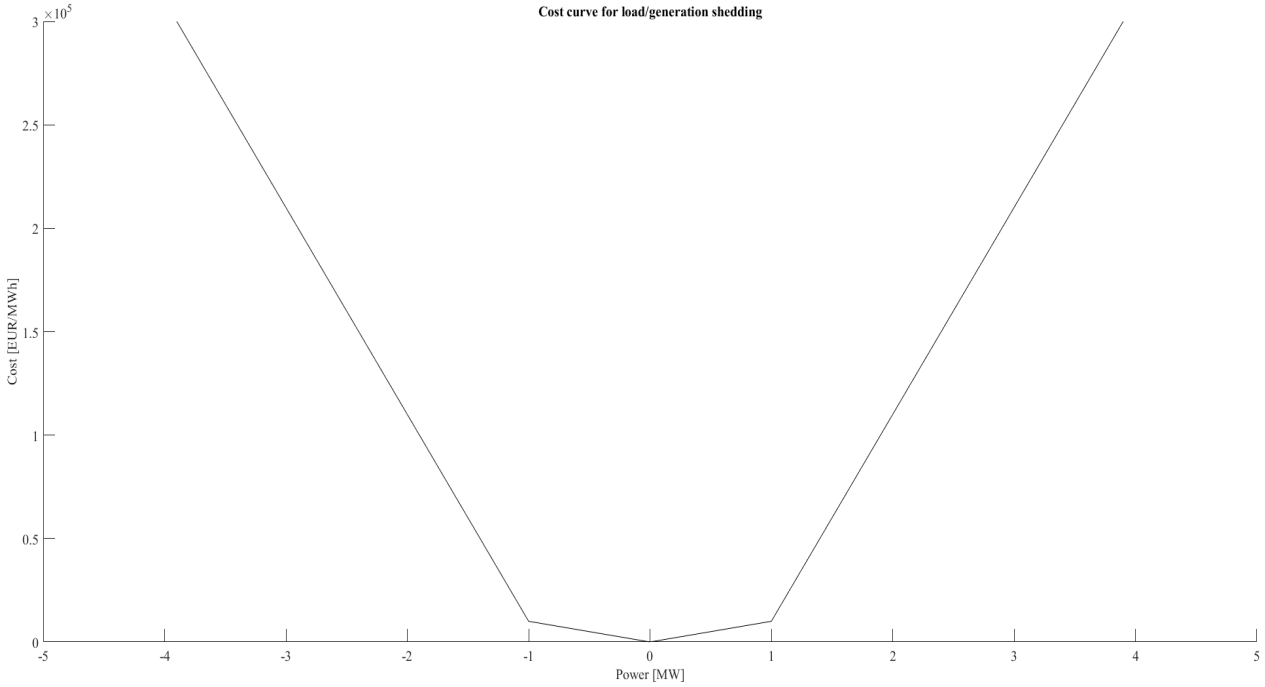

Figure 3.5: Piecewise-linear cost function for load/generation shedding

3.1.5 Representation of Imbalance Forecasting Errors by Fictional Deviation Factor k

This subsection will describe the methodology for representing deviations between forecasted imbalance and the actual imbalance. As previously mentioned, the model will develop activation schedules based on imbalance forecasts up to 45 minutes ahead of time. Real life experiences suggest that imbalance forecasts may deviate significantly from the imbalance that will actually occur, and that forcast uncertainty may increase when predicting far into the future. An imbalance forecast could be generated based on historical imbalance forecasts but due to lack of these a method for representing deviations in forecast using a fictional error scaling factor k has been developed.

Bus imbalances are drawn from a normal probability distribution with a mean equal to the actual imbalance in bus i $w_{i,t}^{actual}$ and standard deviation proportional to the amount of time-steps into the future the forecast is predicting. Equation 3.2 describes this procedure where function $f(\mu, \sigma)$ is the normal probability density function. The forecasting error scaling factor k, multiplied with the time-step, will determine the standard deviation. k is a fictional parameter to set the level of

inaccuracy in the forecasting. Thus, a small k will give a sharp probability distribution around the actual imbalance, while a large k will give a flatter distribution and a less accurate forecast.

$$w_{i,t} = f(w_{i,t}^{actual}, kt) \qquad \forall \quad t \in T, i \in Buses \tag{3.2}$$

Two different forecast representations with k=1 and k=4 are depicted in Figure 3.6.

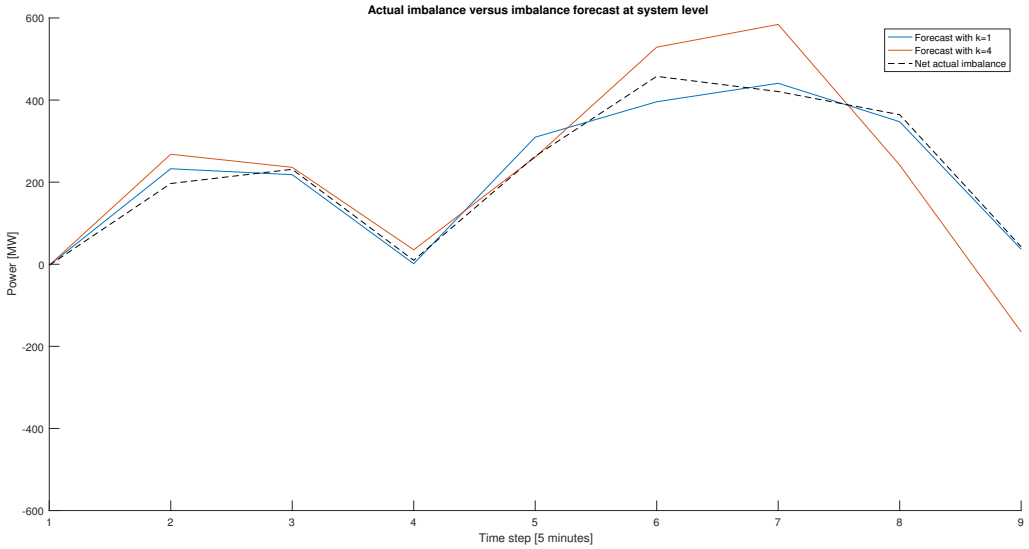

Figure 3.6: Imbalance forecasts with different forecast error scaling factor k.

It is difficult to acquire actual forecasting inaccuracies, and this forecasting formulation distances the model from real life balancing operation. For instance, it can be assumed that the forecasting accuracy is based on several local factors and not distributed equally at every bus.

A forecast error factor k is used to study the effect of forecasting inaccuracy on balancing costs, and the objective is not to present a methodology for generation of imbalance forecasts. Forecasts could be generated by looking at multiple historical imbalances and use these to say something useful about future imbalances. That would mean a start in the other end. Perfect knowledge about future imbalances is a prerequisite for presented formulation with k, will for therefore be unrealistic for real-life operation.

3.1.6 Setting Transfer Capacities between Areas based on Nord Pool Day-Ahead Clearing

To prevent unrealistically large transfer capacities between market areas and to more closely represent actual balancing operations in the Nordic system, it has been extracted historical Nord Pool data from first week on January 2017. The data include power flows resulting from day-ahead clearing and NTCs between all bidding areas. To set the cross-border transmission capacity on each line according to NTC, the constraint in equation 3.3 is formulated, which is also presented in equation 3.8 on Page 45:

$$P^d_{i,j,t} + P_{i,j,t} \leq \frac{NTC_{s,t}}{\sum Lines_s}, \qquad \forall s \in Border, t \in T \tag{3.3}$$

Equation 3.3 states that the flow from day-ahead and balancing activations, $P^d_{i,j,t} + P_{i,j,t}$, must not exceed the NTC of border s, divided by the number of lines crossing the border, $\sum Lines_s$. An example is shown between areas SE1 and SE2 in Figure 3.7. There is defined an NTC in each direction, and three transmission lines cross area boundary, $\sum Lines_s$=3. This gives the capacities on each line in separate directions as shown to the right in Figure 3.7 based on NTCs on the left. Lines that do not cross any area boundaries have thermal capacity. Power flows from Nord Pool day-ahead is distributed on cross-border lines in similar manner.

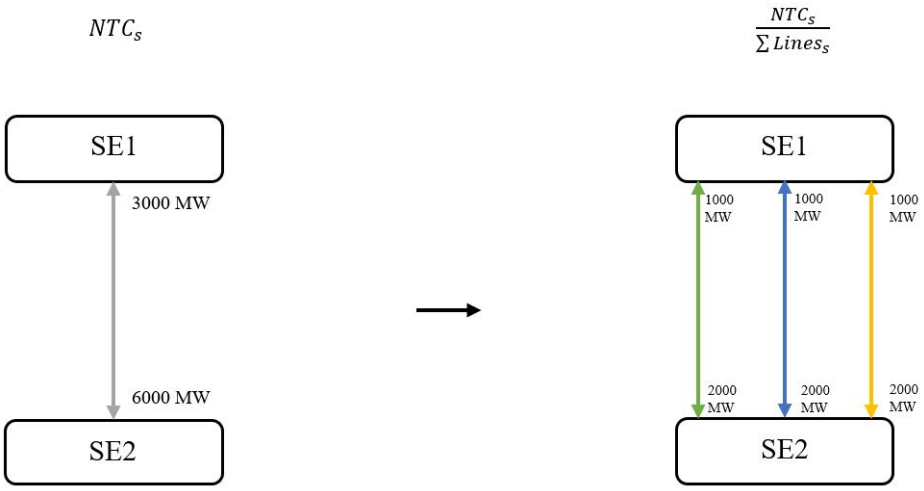

Figure 3.7: Setting cross-border capacities for each transmission line based on Nord Pool NTCs.

This is a simplified formulation to ensure that cross border flows do not exceed NTCs. An improved formulation would be to constrain the sum of flows on the three lines in each direction, e.g. allowing a flow of 3000 MW towards SE1 on the green line if blue and yellow line transfer to SE2. Such a formulation would possibly lead to improved utilization of transmission capacity and is presented as further work in Section 4.6.

Figure 3.8 presents the sum of day-ahead flows on lines that cross area boundary s, $\sum_{i,j \in s} P^d_{i,j,t}$, and NTC for each area border on January 2. 00:00 to 01:00. The NTCs and day-ahead flows are updated hourly from Nord Pool market data in [39]. Consequently, there is an bottleneck between NO1 and NO3, between NO4 and SE1 and between NO4 and SE2 after day-ahead for this specific hour. The capacity between SE2 and FI is zero because this border does not exist in Nord Pool data, but do exist in the network representation. As a result, the line connecting SE2 and FI will not participate in balancing at any hour in the analysis period.

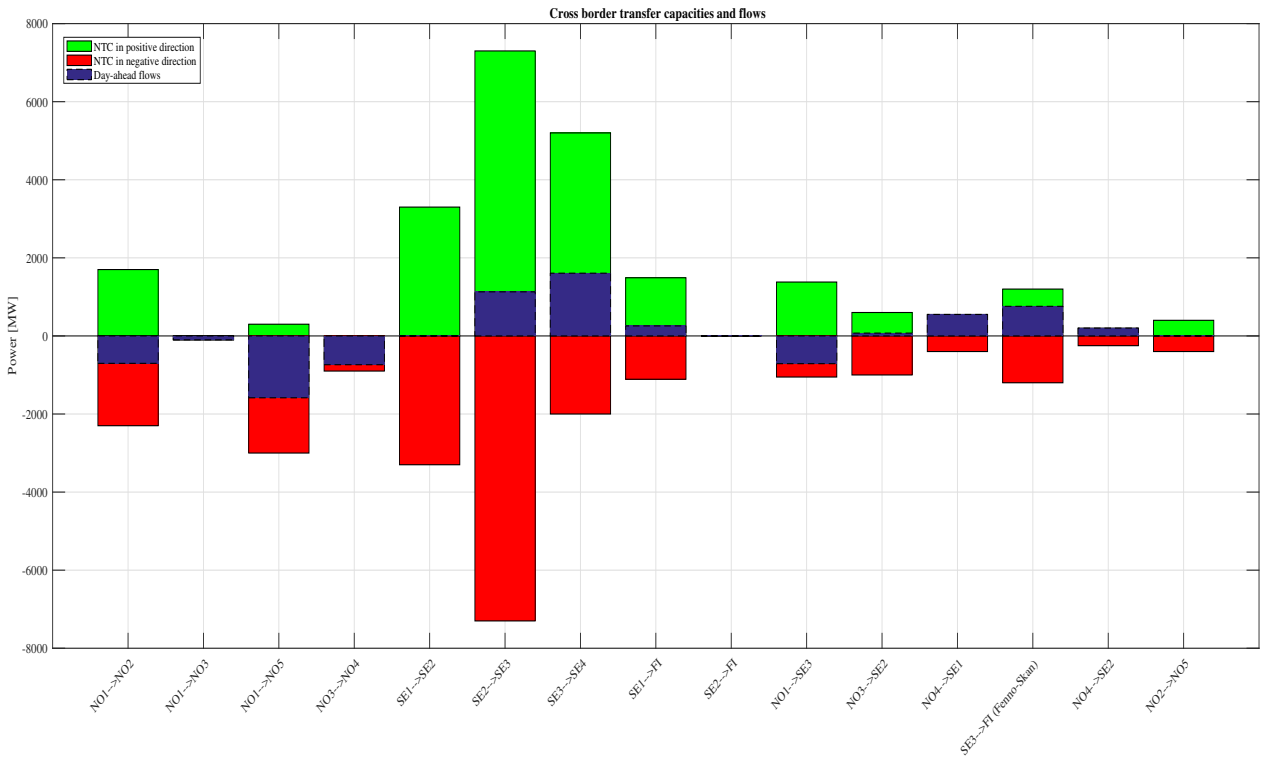

Figure 3.8: Example of cross border transmission capacities (NTC) and day-ahead clearing flows in model on January 2. from 00:00 to 01:00, obtained from Nord Pool market data.

Remaining cross-border capacity for energy balancing after day-ahead is depicted in Figure 3.9.

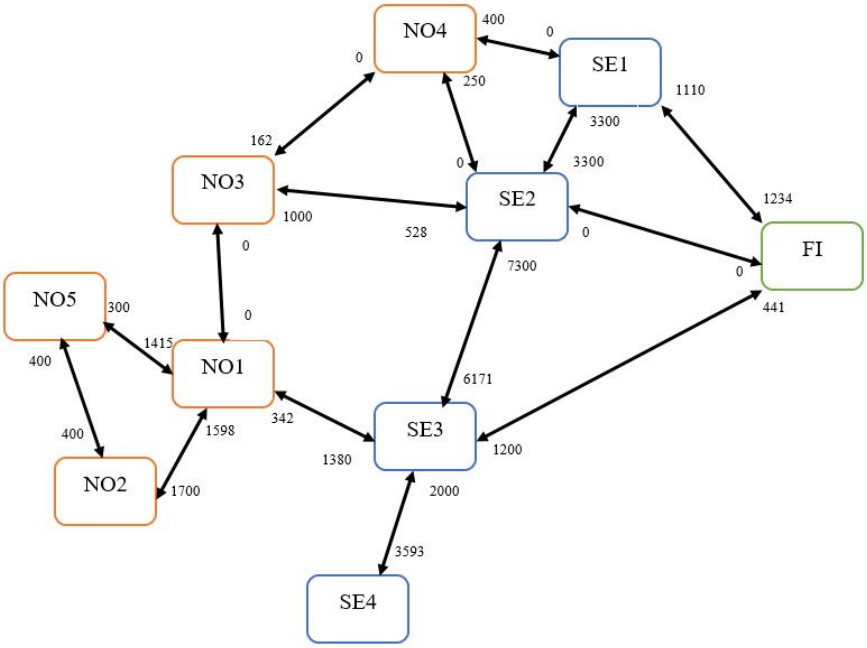

Figure 3.9: Remaining cross-border capacities after day-ahead clearing, January 2. 2017 00:00 to 01:00.

Notation

Variables

$\delta_{i,t}$ voltage angle at bus i in time-step t in radians

$dev^{ok}_{i,t}$ generation shedding at bus i in time-step t in piece k of piecewise-linear load/generation shedding cost curve in [MW]

$dev^{uk}_{i,t}$ volume of load shedding at bus i in time-step t in piece k of the piecewise-linear load/generation shedding cost curve in [MW]

$dev_{i,t}$ activated load/generation shedding at bus i in time-step t in [MW]

f^{sys}_t system frequency in time-step t

$P_{i,j,t}$ power flow from bus i to j in time-step t in MW

$u_{b,t}$ binary commitment variable of mFRR bid b in time t

$v_{b,t}$ binary initiation status of mFRR bid b in time-step t

$x^{\downarrow}_{b,t}$ activated downward aFRR volume from bid b in time-step t [MW]

$x^{\uparrow}_{b,t}$ activated upward aFRR volume from bid b in time-step t in MW

$y^{\downarrow}_{b,t}$ activated downward volume from mFRR bid b in time-step t in MW

$y^{\uparrow}_{b,t}$ activated upward volume from mFRR bid b in time-step t in MW

$y^{S}_{b,t}$ set-point variable for ramping power of bid b in time-step t [MW]

$y^{R\downarrow}_{b,t}$ ramping power of downward mFRR bid b in time-step t [MW]

$y^{R\uparrow}_{b,t}$ ramping power of upward mFRR bid b in time-step t [MW]

$z^{\downarrow}_{i,t}$ activated downward FCR volume at bus i in time-step t MW

$z^{\uparrow}_{i,t}$ activated upward FCR volume at bus i in time-step t in MW

Parameters

λ frequency bias factor in Nordic system: 5000 MW/Hz

$\overline{DP_b}$ maximum duration of bid b

$\overline{P}_{i,j}^{hvdc}$ maximum transmission capacity on HVDC cable from bus i to j

$\overline{P}_{i,j}$ maximum (long-term thermal) transmisson capacity on line connecting bus i and j

$\overline{R}_{i,j}^{hvdc}$ maximum ramping volume on HVDC cable of 600 MW/h

$\overline{x}_b$ maximum activation volume of aFRR bid b in MW

$\overline{y}_b$ maximum activation volume of mFRR bid b in MW

$\overline{z}$ maximum activation volume of FCR in system in MW

$\mathbf{L}_{i,j}$ connection matrix connecting line to bus

$\underline{DP}_b$ minimum duration of delivery period of bid b

$\underline{x}_b$ minimum activation volume of aFRR bid b in MW

$\underline{y}_b$ minimum activation volume of mFRR bid b in MW

$b_{i,j}$ susceptance of line connecting bus i and j

C_b^{afrr} price of aFRR bid b in €/MWh

C^{fcr} fictional FCR price in €/MWh

C_b^{mfrr} price of mFRR bid b in €/MWh

f_n nominal frequency in Nordic grid of 50 Hz

LT length of time-step of 5 minutes

$P_{i,j,t}^d$ flow on line from bus i to j from day-ahead dispatch in time-step t

p^{spot} spot price in €/MWh

$p_{1,2}$ cost for each step in piecewise-linear cost curve for load shedding (Figure 3.5) in €/MWh

T_{start} first time-step in scheduling horizon

$w_{i,t}$ imbalance at bus i in time-step t MW

$\mathbf{A}_{b,i}$ binary matrix connecting bid b to bus i

Sets and Indices

$Areas$ set of areas in network

b bid

B_d set of downward regulating balancing bids

B_u set of upward regulating balancing bids

$Buses^{hvdc}$ set of buses connected to HVDC link

$Buses^{non-nordic}$ set of all buses that are not in the Nordic synchronous grid

$Buses^{nordic}$ set of buses in the Nordic synchronous grid

d day-ahead dispatch

i, j buses in the network

k steps in piecewise-linear cost curve for load/generation shedding

$Lines$ set of all lines (HVDC and AC) in network

$Lines^{ac}$ set of all AC transmission lines

$Lines^{hvdc}$ set of all HVDC cables

T set of time-steps in scheduling horizon

t time-step

$\mathrm{B}_{u}^{DP_b=1}$, $B_{d}^{DP_b=1}$ set of upward and downward regulating bids with 5 minutes minimum duration of delivery period

$\mathrm{B}_{u}^{DP_b>1}$, $B_{d}^{DP_b>1}$ set of upward and downward regulating bids with larger than 5 minutes minimum duration of delivery period

3.2 Model Formulation

3.2.1 Objective function

The objective function is presented in equation 3.4. Objective of the optimisation problem is to maximize social welfare through minimization of balancing costs. The model will minimize activation costs for entire scheduling horizon of 45 minutes. Total balancing cost is the sum of mFRR, aFRR, FCR and load/generation shedding activation costs.

Activation cost for an upward regulating mFRR bid is the product of bid price C_b^{mfrr} and upward activation volume $y_{b,t}^{\uparrow}$ for bid b in time-step t. For a downward activation the mFRR activation cost is the product of downward activation volume $y_{b,t}^{\downarrow}$ and difference between spot price and bid price, $p^{spot} - c_b^{mfrr}$. Activation cost of aFRR is similarly the product of bid price C_b^{afrr} and aFRR activation volume in each direction. The aFRR price is set to a fixed price of 55 €/MWh for all bids, c.f. Sections 3.1.1 and 4.2.2. The total system FCR capacity is assumed available at every bus and FCR-price C^{fcr} is homogeneous in entire Nordic system. These are modelling simplifications that reduce model realism since only a small portion of total FCR could be assumed available at every bus in real-life, c.f. discussion in Section 4.2.1. Load/generation shedding cost is given by the final term in 3.4 as the product of penalty level p_k and shedded volume at bus i. Total shedding volume is expressed as the sum of shedding volume in each piece of piecewise-linear cost curve $dev_{i,t}^{o,1}$ and $dev_{i,t}^{o,2}$, where o specifies an upward shedding direction/generation shedding and u downward shedding/load shedding.

$$\begin{aligned}\min \quad \text{TotalCost} = \frac{LT}{60} \cdot \sum_{t \in T} \Big(\sum_{b \in B_u} (C_b^{mfrr} \cdot (y_{b,t}^{\uparrow} + y_{b,t}^{R,\uparrow})) + \sum_{b \in B_d} ((C_b^{mfrr} - p^{spot}) \cdot (y_{b,t}^{\downarrow} + y_{b,t}^{R,\downarrow})) \\ + \sum_{b \in B_u, B_d} (C_b^{afrr} \cdot x_{b,t}^{\uparrow} + C_b^{afrr} \cdot x_{b,t}^{\downarrow}) + \sum_{i \in Buses} (C^{fcr} \cdot (z_{i,t}^{\uparrow} + z_{i,t}^{\downarrow})) \\ + \sum_{i \in Buses} (p_1 \cdot (dev_{i,t}^{o,1} + dev_{i,t}^{u,1}) + p_2 \cdot (dev_{i,t}^{o,2} + dev_{i,t}^{u,2}))\end{aligned} \tag{3.4}$$

3.2.2 Bus Energy Balance and Network Specific Constraints

There are formulated different energy balance constraints for buses that are located in the Nordic synchronous grid versus buses that are not. Equation 3.5 presents the energy balance for Nordic buses, while equation 3.6 for buses connected to synchronous system via HVDC links and thus located outside the Nordic synchronous system.

Equations 3.5 and 3.6 specify balance between activated balancing energy, net power flows into bus and imbalance at bus i. In this formulation a positive imbalance at bus i in time t, $w_{i,t}$, means a long position and will be balanced by downward regulating activations. Binary matrix $\mathbf{A}_{b,i}$ nonzero coefficient if bid b is located in bus i, and matrix $\mathbf{L}_{i,j}$ has coefficient 1 for line connecting buses i and j if the line direction is positively defined into bus j. If line is positively defined out of bus the coefficient is -1, otherwise zero.

$$dev_{i,t} = \mathbf{L} \cdot \sum_{j \in Buses, j \neq i} -P_{i,j,t} + \sum_{b \in B_u} \mathbf{A}_{b,i} \cdot (y^{\uparrow}_{b,t} + y^{R,\uparrow}_{b,t} + x^{\uparrow}_{b,t}) - \sum_{b \in B_d} \mathbf{A}_{b,i} \cdot (y^{\downarrow}_{b,t} + y^{R,\downarrow}_{b,t} + x^{\downarrow}_{b,t}) + w_{i,t} + z^{\uparrow}_{i,t} - z^{\downarrow}_{i,t}, \qquad \forall \quad i \in Buses^{nordic}, \quad t \in T \tag{3.5}$$

$$0 = \mathbf{L} \cdot \sum_{j \in Buses, j \neq i} -P_{i,j,t} + \sum_{b \in B_u} \mathbf{A}_{b,i} \cdot (y^{\uparrow}_{b,t} + y^{R,\uparrow}_{b,t} + x^{\uparrow}_{b,t}) - \sum_{b \in B_d} \mathbf{A}_{b,i} \cdot (y^{\downarrow}_{b,t} + y^{R,\downarrow}_{b,t} + x^{\downarrow}_{b,t}) + w_{i,t}, \quad \forall \quad i \in Buses^{non-nordic}, \quad t \in T \tag{3.6}$$

A net non-zero value of right side of equation 3.5 implies that the model is not able to regulate the imbalance by activation of reserves or netting (cancelling of opposing imbalances), leading to activation of load/generation shedding. i.e. a non-zero value of shedding variable $dev_{i,t}$ at bus i.

The imbalance term, $w_{i,t}$ in equation 3.6 can be set to positive or negative values at buses outside the Nordic system to simulate an import or export situation, respectively. If no bids are located in bus i outside Nordic synchronous area, equation 3.6 will ensure that the the imbalance power $w_{i,t}$ is imported ($w_{i,t} > 0$) or exported ($w_{i,t} < 0$) out of the Nordic system. This may be used to simulate import or export scenarios.

It should be noted that no FCR is available at buses that are not in the Nordic synchronous system. This is because these buses are part of a different synchronous system and connected to Nordic system via HVDC cables and will therefore not share same frequency deviation. Also, no aFRR or mFRR bids are located outside the Nordic system since exchange of balancing energy across synchronous systems is out of the scope of this project.

The power flow on each transmission line in network is given by equation 3.7 for AC lines, under DC load flow assumptions. Power flow $P_{i,j,t}$ is determined by the line susceptance $b_{i,j}$ connecting bus i and j and voltage angle difference between sending and receiving bus. The line can be made unavailable by setting line susceptance to zero.

$$P_{i,j,t} = b_{i,j} \cdot (\delta_{i,t} - \delta_{j,t}), \qquad \forall i, j \in Lines^{ac}, t \in T \tag{3.7}$$

Available transmission capacity for exchange of balancing services play a crucial role in determining balancing costs and required procurement of balancing reserves. Transmission capacity on tie-lines between balancing areas are defined by NTC values that set available transmission capacity lower than the thermal capacity to account for contingencies and congestion management [17, page 87]. Sum of power flows that cross an area-border s are constrained by the margin between day-ahead dispatch, $P^{d}_{i,j,t}$, and NTCs between areas in the Nordic synchronous system according to equation 3.8, c.f. Section 3.1.6.

$$P^{d}_{i,j,t} + P_{i,j,t} \leq \frac{NTC_{s,t}}{\sum Lines_s}, \qquad \forall \quad s \in Borders, t \in T \tag{3.8}$$

If the line does not cross any area borders, or it is crossing borders to another synchronous system, its capacity is set to the thermal capacity of the line, according to equation 3.9. Thus,

transmission capacity of HVDC links that connect the Continental and Nordic synchronous grid and Finland and Sweden (Fenno-Skan) are set to thermal capacity, in accordance with [16, page 8].

$$-\overline{P_{i,j}} \leq P_{i,j,t} \leq \overline{P_{i,j}} \qquad \forall \quad i,j \in Lines, t \in T \tag{3.9}$$

There are formulated constraints on how much the power flowing on HVDC links are allowed to change in equation 3.10. The HVDC ramping parameter $\overline{R}_{i,j}^{hvdc}$ specifies the maximum allowed ramping per hour to 600 MW/h for all HVDC links, in accordance with Nord Pool restrictions on the day-ahead market, which the TSOs impose to reduce risks of comprimising security of supply [35]. Scaling to a time-resolution of 5 minutes per time-step gives $\overline{R}_{i,j}^{hvdc}$=50 MW.

$$-\overline{R}_{i,j}^{hvdc} \leq P_{i,j,t} - P_{i,j,t-1} \leq \overline{R}_{i,j}^{hvdc}, \qquad \forall \quad i,j \in Lines^{hvdc}, t \in T > T_{start} \tag{3.10}$$

Voltage angle at reference bus is constrained by equation 3.11:

$$\delta_{i_{ref},t} = 0, \qquad \forall \quad t \in T \tag{3.11}$$

3.2.3 Product Specific Constraints

In this Section the equations that constrain how long a bid must be active, bid delivery profiles and delivery volumes are presented.

Equation 3.12 express that activated mFRR in time-step t must be between a maximum and minimum value, $\overline{y_b}$ and $\underline{y_b}$ respectively. Similar constraints for aFRR bids are presented in 3.13. Maximum activation volume of all bids is specified in the bid lists presented in Section 3.3.4, while minimum activation volume is 5 MW for both mFRR and aFRR bids. Equations 3.12 and 3.13 also set binary commitment variables $u_{b,t}$ and $q_{b,t}$ for mFRR and aFRR respectively, which are non-zero if bid b is delivering energy in time-step t.

$$\underline{y_b} \cdot u_{b,t} \leq y_{b,t} \leq \overline{y_b} \cdot u_{b,t}, \qquad \forall b \in (B_b, B_u), t \in T \tag{3.12}$$

$$\underline{x_b} \cdot q_{b,t} \leq x_{b,t} \leq \overline{x_b} \cdot q_{b,t}, \qquad \forall \quad b \in (B_b, B_u), t \in T \tag{3.13}$$

Equations 3.14 and 3.15 state that total net FCR activation must not exceed a maximum volume, $\overline{z}$. Maximum FCR capacity is set to $\overline{z}$=2500 MW, corresponding to a full volume FCR activation for a steady-state frequency deviation of $\pm$ 0.5 Hz for frequency bias factor λ=5000 MW/Hz, in accordance with [15, page 8]. Large FCR capacity and low FCR pricing may lead to balancing by frequency deviations, and is further discussed in Section 4.2.1.

$$\sum_{i \in Buses} z_{i,t}^{\uparrow} \leq \overline{z}, \qquad \forall \quad t \in T \tag{3.14}$$

$$\sum_{i \in Buses} z_{i,t}^{\downarrow} \leq \overline{z}, \qquad \forall \quad t \in T \tag{3.15}$$

Constraints in equation 3.16 set binary bid initiation variable, $v_{b,t}$. This is a variable for mFRR bids that is positive if bid b is starting its delivery period in time-step t, meaning that the bid was not active in time-step $t-1$. Note that the delivery period begins after the preparation and ramping period is completed.

$$\begin{aligned} v_{b,t} &\geq u_{b,t} - u_{b,t-1}, \qquad \forall \quad b \in (B_u, B_d), \quad t \in T > T_{start} \\ v_{b,t} &\leq u_{b,t}, \qquad \forall \quad b \in (B_u, B_d), \quad t \in T > T_{start} \end{aligned} \tag{3.16}$$

MFRR bids are specified with a minimum duration of delivery period $\underline{DP_b}$ for which the activated volume from bid b is to remain constant. This is formulated by equations 3.17 to 3.20. These constraints are only formulated for mFRR bids due to the assumption of no time-coupling of aFRR bids. Similar constraints for minimum duration period were formulated in [28], however the constraints have been expanded to account for bids with different minimum duration requirements.

Constraint in equation 3.17 forbids new activations before minimum duration period has passed by constraining the initiation variable $v_{b,t}$ for a duration equal to the minimum delivery period. Equation 3.18 sets activated volume to correct volume as given by set-point variable $y^S_{b,t}$. Equation 3.19 is only formulated for bids that have a minimum duration of 1 time-step (5 minutes). This means that activated volume is constrained by the set-point variable $y^S_{b,t}$ for only 1 time-step. Equation 3.20 states that activated volume from bid b $y_{b,t}$ is constrained by the set-point variable for a duration equal to the minimum duration period, i.e. the bids must follow a flat profile the entire minimum duration profile after the FAT is completed. When minimum duration is over, the bids are allowed to change output without going through another FAT. This is a simplification that is not necessarily physically possible and may lead to unrealistic profitability of Standard Products with short minimum duration period, further discussed in Section 4.2.5.

$$v_{b,t} \leq 1 - \sum_{q=t-\underline{DP_b}+1}^{q=t-1} v_{q,t}, \qquad \forall \quad b \in (B_u, B_d), \quad t \in T \geq T_{start} - 1 + \underline{DP_b} \tag{3.17}$$

$$y_{b,t} \geq \overline{y_b} \cdot y^S_{b,q}, \qquad \forall \quad b \in (B_u, B_d), \quad q \in \{t - \underline{DP_b} + 1, t\}, \quad t \in T \tag{3.18}$$

$$y_{b,t} \leq \overline{y_b} \cdot (y^S_{b,t} + u_{b,t-1}), \qquad \forall \quad b \in (B_u^{\underline{DP_b}=1}, B_d^{\underline{DP_b}=1)}, \quad t > T_{start} \tag{3.19}$$

$$y_{b,t} \leq \overline{y} \cdot \sum_{q=t-\underline{DP_b}+1}^{t} y^S_{b,q}, \qquad \forall \quad b \in (B_u^{\underline{DP_b}>1}, B_d^{\underline{DP_b}>1)}, \quad t \geq T_{start} + \underline{DP_b} + 1 \tag{3.20}$$

Equation 3.21 is formulated to forbid activations exceeding maximum duration of delivery specified in Standard Product specifications. A maximum duration of 6 time-steps equalling 30 minutes is used for all products.

$$\sum_{q=t-\overline{DP_b}}^{q=t} u_{b,q} \leq \overline{DP_b}, \qquad \forall \quad b \in (B_u, B_d), \quad t > T_{start} + \overline{DP_b} \tag{3.21}$$

3.2.4 Constraints on Full Activation Time and Ramping Profiles

In this Section the equations that ensure ramping profiles as depicted in Figure 3.4 are presented. Different constraints are formulated for bids that have a 5 minute FAT and 15 minutes FAT. For readability, the constraints for each FAT is presented separately.

Constraints for 15 minutes FAT

The following equations ensure that ramping power $y^R_{b,t}$ of bid b 5 minutes before start of delivery period is equal to 2/3 of delivery volume, and that ramping power 10 minutes before start of delivery period is 1/3 of the delivery volume, according to left ramping profile in Figure 3.4. Equation 3.22 states that a new delivery period is started when set-point variable $y^S_{b,t}$ takes non-zero values. Equation 3.23 states that in order to begin a new delivery period, either a ramping period must have been completed or the new delivery period is a continuation of a former delivery period (the bid is already active, and no new ramping period is required). Equations 3.24-3.25 says that the ramping power $y^R_{b,t}$ is set as a share of the activated volume at the beginning of the delivery period, unless the bid is already active. Equation 3.26 ensures that total ramping power in the ramping period equals the delivery set-point in the beginning of the delivery period. Equation 3.27 ensures a preparation period 15 minutes before start of delivery period. If a bid b has a positive bid initiation value 15 minutes ahead, $v_{b,t+3} = 1$, then the ramping power in time-step t is constrained to a zero value, $y^R_{b,t} \leq 0$. Finally, equations 3.28-3.29 states that no ramping power can be delivered if the bid has started its delivery period.

$$y^S_{b,t} \leq v_{b,t}, \qquad \forall b \in (B_u, B_d), t \in T \tag{3.22}$$

$$v_{b,t} \leq y_{b,t-2} + y^R_{b,t-2}, \qquad \forall b \in (B_u, B_d), t > (T_{start} + 2) \tag{3.23}$$

$$y^R_{b,t} \geq \frac{2}{3}\overline{y_b}(y^S_{b,t+1} - u_{b,t}), \qquad \forall b \in (B_u, B_d), t < T_{end} \tag{3.24}$$

$$y^R_{b,t} \geq \frac{1}{3}\overline{y_b}(y^S_{b,t+2} - u_{b,t}), \qquad \forall b \in (B_u, B_d), t < T_{end} - 1 \tag{3.25}$$

$$y^R_{b,t} \leq \overline{y_b}(\frac{2}{3}y^S_{b,t+1} + \frac{1}{3}y^S_{b,t+2}), \qquad \forall b \in (B_u, B_d), t < T_{end} - 1 \tag{3.26}$$

$$y^R_{b,t} \leq \overline{y_b}(1 - v_{b,t+3}), \qquad \forall b \in (B_u, B_d), t < T_{end} - 2 \tag{3.27}$$

$$y^R_{b,t} \leq \overline{y_b}(1 - u_{b,t-1}), \qquad \forall b \in (B_u, B_d), t > T_{start} \tag{3.28}$$

$$y^R_{b,t} \leq \overline{y_b}(1 - u_{b,t}), \qquad \forall b \in (B_u, B_d), t \in T \tag{3.29}$$

Ramping Constraints for 5 minutes FAT

A shorter FAT of 5 minutes has been formulated for the P5 product. The ramping profile of a P5 product is depicted rightmost in Figure **??** and shows that the FAT only consist of a single time-step

where the ramping power $y^R_{b,t}$ is equal to half of the delivery set-point power. Equations 3.30, 3.34 and 3.35 are equal to equations 3.22, 3.28 and 3.29, and will therefore not be described again.

Equation 3.31 states that the bid is either at the beginning of a new delivery period or a continuation of a former delivery period. Equations 3.32-3.33 states, similary to the 15 minutes FAT, the relation between ramping power and set-point power. For a bid with 5 minutes FAT ramping power equals 50 % of the set-point power.

$$y^S_{b,t} \leq v_{b,t}, \qquad \forall b \in (B_u, B_d), t \in T \tag{3.30}$$

$$y_{b,t} \leq \overline{y_b} \cdot (y^S_{b,t} + u_{b,t-1}), \qquad \forall b \in (B_u, B_d), t > T_{start} \tag{3.31}$$

$$y^R_{b,t} \geq \frac{1}{2}\overline{y_b}(y^S_{b,t+1} - u_{b,t}), \qquad \forall b \in (B_u, B_d), t < T_{end} \tag{3.32}$$

$$y^R_{b,t} \leq \overline{y_b}(\frac{1}{2}y^S_{b,t+1}), \qquad \forall b \in (B_u, B_d), t < T_{end} - 1 \tag{3.33}$$

$$y^R_{b,t} \leq \overline{y_b}(1 - u_{b,t-1}), \qquad \forall b \in (B_u, B_d), t > T_{start} \tag{3.34}$$

$$y^R_{b,t} \leq \overline{y_b}(1 - u_{b,t}), \qquad \forall b \in (B_u, B_d), t \in T \tag{3.35}$$

3.2.5 Setting Cost for Load/Generation Shedding

The load/generation shedding functionality is the last resort for model to achieve feasibility and has therefore been modelled with a large fictional price. Equations 3.36-3.39 are formulated to give correct penalty cost according to the piecewise-linear cost curve for load shedding/production tripping as depicted in Figure 3.5 on page 36. The variable $dev^{o,1}_{i,t}$ has a penalty cost of p_1=10.000 €/MWh for disconnecting a volume below 1 MW, while $dev^{o,2}_{i,t}$ has a cost of p_2=100.000 €/MWh for larger disconnected volumes. The indices o and u specifies the direction of the shedding, while the indices 1 and 2 specifies the cost piece in the piecewise-linear cost curve; $dev^{o,1}_{i,t} > 0$ if $0 < dev_{i,t} < 1$, hence representing the generation shedding, while $dev^{u,1}_{i,t}$ >0 if $-1 < dev_{i,t} < 0$, hence representing load shedding. In the case of larger volumes of load/generation shedding; $dev^{o,2}_{i,t} > 0$ if $dev_{i,t} > 1$, and $dev^{u,2}_{i,t} > 0$ if $dev_{i,t} < -1$. Load and generation shedding share same cost.

$$dev^{o,1}_{i,t} \leq 1, \qquad \forall i \in Buses, t \in Time \tag{3.36}$$

$$dev^{o,1}_{i,t} + dev^{o,2}_{i,t} \geq dev_{i,t}, \qquad \forall i \in Buses, t \in Time \tag{3.37}$$

$$dev^{u,1}_{i,t} \leq 1, \qquad \forall i \in Buses, t \in Time \tag{3.38}$$

$$dev^{u,1}_{i,t} + dev^{u,2}_{i,t} \geq -dev_{i,t}, \qquad \forall i \in Buses, t \in Time \tag{3.39}$$

3.2.6 Calculating System Frequency Deviation Estimate

As previously described, an activation of FCR will result in a deviation in frequency from the nominal value of 50 Hz in the Nordic synchronous grid. This effect is ensured by equations 3.40-3.42.

Equation 3.40 states that system frequency in time-step t is the sum of the inherited system frequency and product of net FCR activation and frequency bias factor λ. A net activation of upward FCR will result in a negative frequency deviation, while net downward FCR activation lead to a positive deviation. This sign convention is based on the energy balance in equation 3.5, where an energy deficiency requires activation of upward FCR $z^{\uparrow}_{i,t}$, and an activation of upward FCR will therefore reduce system frequency.

Equations 3.41-3.42 ensures that activated FCR remain active as long as there is a frequency deviation in the system.

$$f_t^{sys} = f_{t-1}^{sys} - \lambda \sum_{i \in Buses} (z^{\uparrow}_{i,t} - z^{\downarrow}_{i,t}), \qquad \forall t \in T \tag{3.40}$$

$$\sum_{i \in Buses} z^{\uparrow} \geq \lambda (f_n - f_t^{sys}), \qquad \forall t \in T \tag{3.41}$$

$$\sum_{i \in Buses} z^{\downarrow} \geq \lambda (-f_n + f_t^{sys}), \qquad \forall t \in T \tag{3.42}$$

3.2.7 Non-Negativity and Binary Requirements

Equation 3.43 summarizes the binary and non-negativity constraints for model decision variables.

$$\begin{aligned}
y^{\uparrow}_{b,t}, y^{\downarrow}_{b,t}, y^{R,\uparrow}_{b,t}, y^{R,\downarrow}_{b,t}, x^{\uparrow}_{b,t}, x^{\downarrow}_{b,t}, y^{S}_{b,t} \geq 0 \quad & \forall \quad b \in (B_u, B_d), \quad t \in T \\
z^{\uparrow}_{i,t}, z^{\downarrow}_{i,t} \geq 0 \quad & \forall \quad i \in Buses, \quad t \in T \\
\delta_{i,t}, dev_{i,t}, P_{i,j,t}, f_t^{sys} \in \Re \quad & \forall \quad i,j \in Buses, \quad t \in T \\
dev^{o,k}_{i,t}, dev^{u,k}_{i,t} \geq 0 \quad & \forall \quad i \in Buses, \quad t \in Time, \quad k \in K \\
u_{b,t}, v_{b,t} \in \{0,1\} \quad & \forall \quad b \in (B_u, B_d), \quad t \in Time
\end{aligned} \tag{3.43}$$

3.3 Data Inputs: Imbalances, Network Representation and Balancing Market Data

3.3.1 Historical Area Imbalance Data

The imbalances input to optimisation problem are historical imbalances that occurred in January, 2017, obtained from Statnett data. These are defined per area. Balancing operation is simulated between January 3. 05:00 and January 4. 05:00, and area imbalances in this period are presented in Figure 3.10.

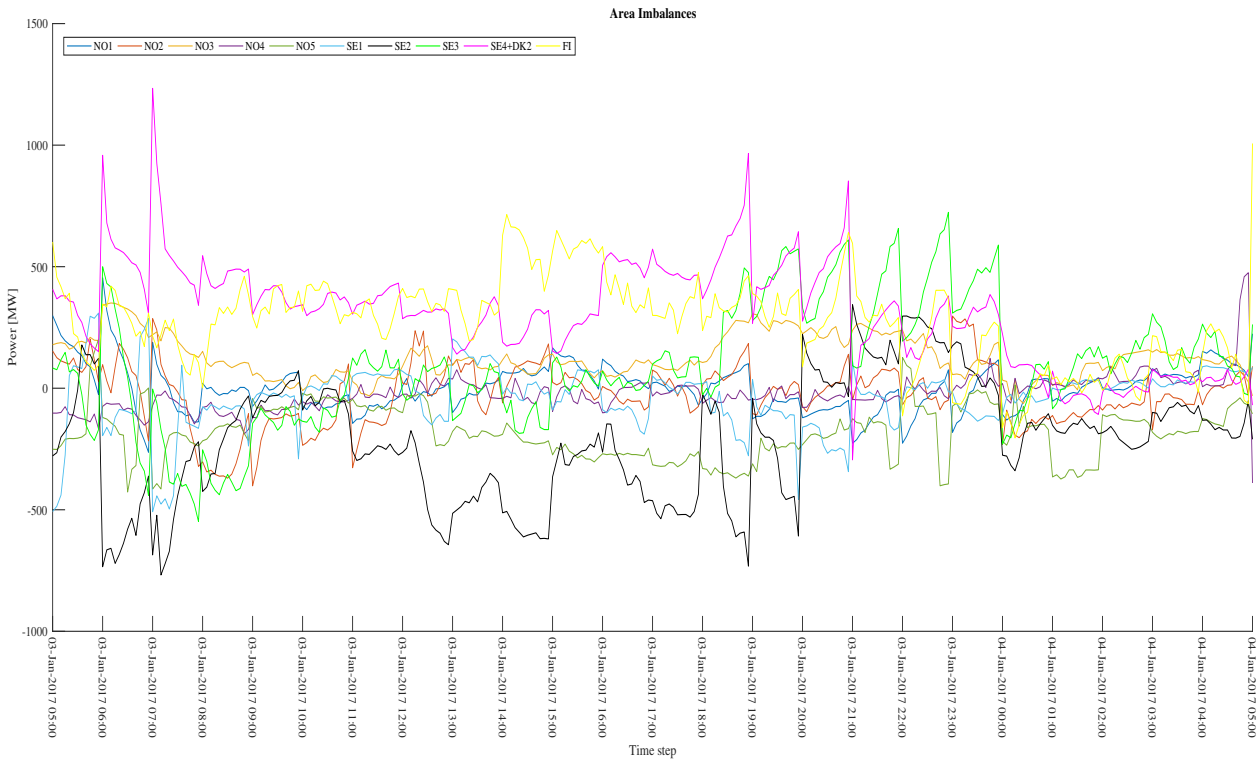

Figure 3.10: Area imbalances.

It is observed that areas SE4 and DK2 contribute to large positive imbalances with a peak of about 1500 MW in the morning of January 6. The imbalance in FI remains positive almost entire period. Area imbalances in SE2 and SE3 are often counteracting the positive imbalance in areas SE4 and DK2, except in the evening of January 3. This leads to peak net system imbalance on January 3. around 21:00 as depicted in Figure 3.12. The imbalances in Norway are small compared to the other Nordic countries, except in the morning on January 2. where a negative imbalance of about 400 MW is observed in NO2. Large structural imbalance occur in Southern Sweden and Finland in early morning and evening, lasting until midnight.

3.3.2 Geographical Distribution of Imbalances

The data set defines imbalances at area level, and therefore needs to be distributed to all buses within each area in a reasonable manner, such that the sum of all bus imbalances equal the area imbalance, although the imbalances at the buses within the area may differ. To ensure that the distribution of imbalances within each area represent possible distributions, the imbalances are distributed using the standard deviation in historical load distributions in day-ahead clearing. A correlation between the load and imbalance is thereby assumed. This results in a distribution where buses with largest loads have imbalance volume uncertainty, as load deviation is a typical source of imbalance.

The bus load distributions for 2015 are part of the data files in [47]. Using load distributions from 2015 to map 2017 imbalances is a source of error due to the lack of later load data. However, it is the distribution of loads that is of interest, and one may argument that the load distribution re-

mains fairly unchanged over two years, assuming little new industry, significant urban development or depopulation occurred ins these two years.

Load distributions are defined at hourly intervals, and the imbalance is therefore distributed within each area with a variance that is updated at hourly intervals. The bus imbalances are randomly selected from a normal distribution with a mean equal to the area imbalance divided by number of buses in area, and standard deviation of 5% of the bus load. Equation 3.44 states the method of distributing the bus imbalances, where f(μ,σ) is the normal probability function. The area average imbalance is calculated by dividing area total imbalance $w_{a,t}$ by number of buses in area N_a, and the standard deviation is 5 % of the load at bus i, $L_{i,t}$.

$$w_{i,t} = f(\frac{w_{a,t}}{N_a}, 0.05 \cdot L_{i,t}) \qquad \forall \quad i \in Buses, t \in T \tag{3.44}$$

Inclusion of production technology in the geographical imbalance mapping procedure, giving buses with intermittent production possibly larger imbalances, would be interesting to more accurately map the imbalances.

To ensure that sum of all bus imbalances match area imbalances, a corrective algorithm depicted in Figure 3.11 was formulated. The purpose of this algorithm is to shift the bus imbalance distributions within an area such that net imbalance of that area is equal to the area imbalance in the data set provided by supervisor. An error of $\epsilon = 1$ has been used, and the algorithm will therefore correct the imbalance distribution until the net area imbalance deviates from the Statnett data with less than 1 MW.

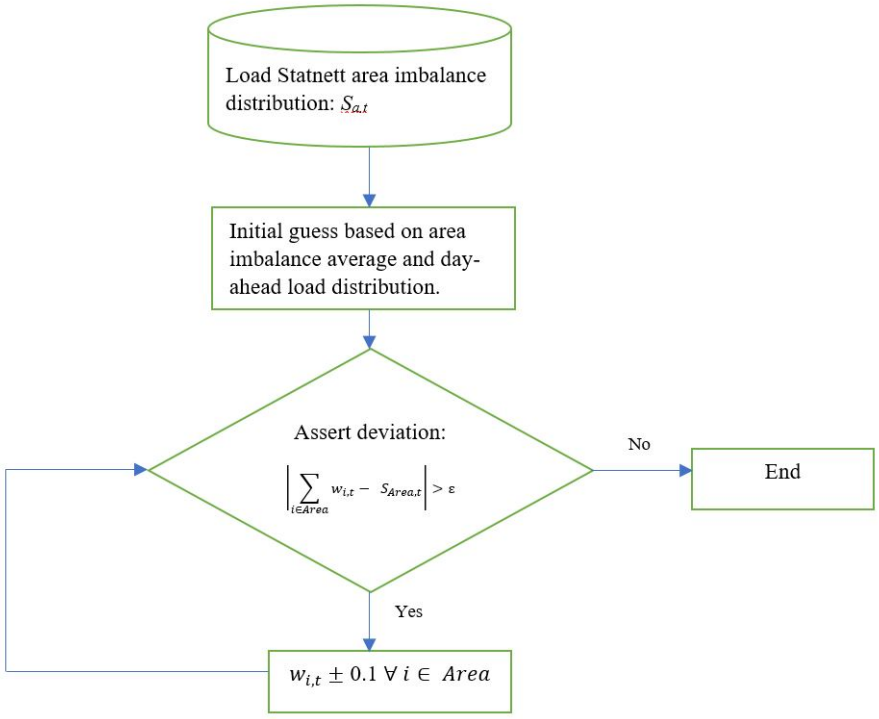

Figure 3.11: Imbalance mapping algorithm

Resulting net system imbalance is depicted in Figure 3.12. The largest imbalance of approximately 1900 MW occurs in the evening of January 3. This is mainly due to increased positive imbalances in SE4 in combination with reduced negative imbalance in SE2. The peak in SE4 in the morning January 6. depicted in Figure 3.10 is cancelled out by negative imbalances in SE2, resulting in a lower net imbalance in Figure 3.12.

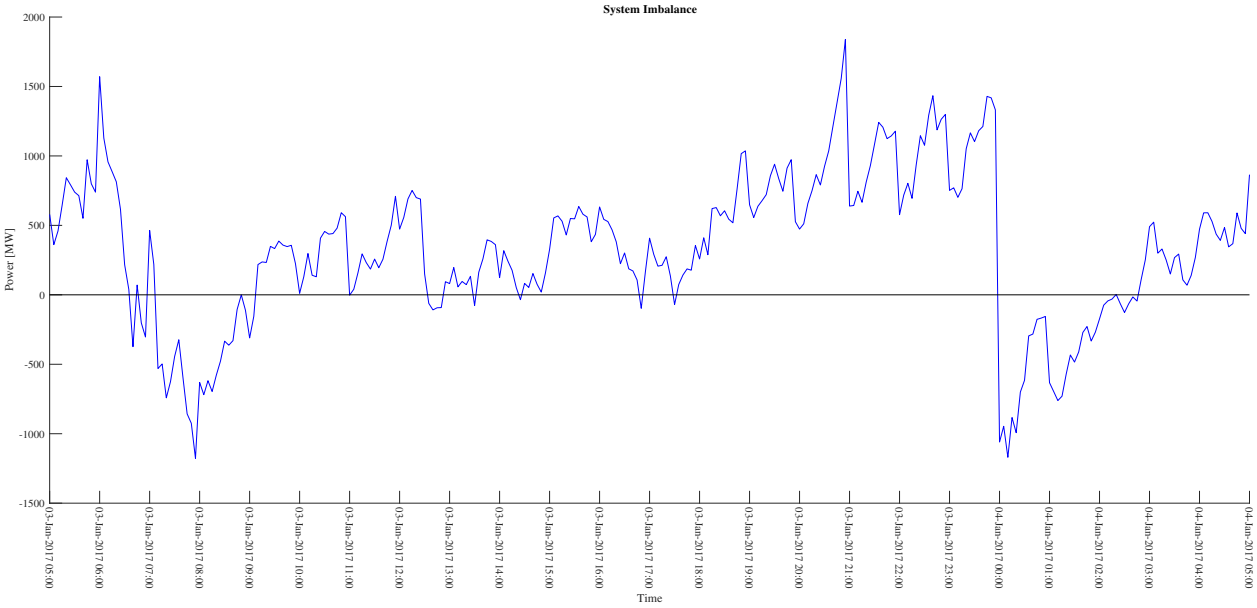

Figure 3.12: System imbalance between January 3. 05:00 and January 4. 05:00 used in model.

3.3.3 Network Representation

In this project a representation of the Nordic synchronous system is used to put balancing operations into a physical context. A Nordic 44-bus model has been used. The model is first presented in [48], and the raw and processed data files corresponding to the model are available as an open data set and documented in [47].

The network is available as PSS/E or RAW files which are converted to a MATPOWER case struct by using conversion functions described in [52, page 92].

The network consist of 44 buses and 79 lines, where 8 of the lines are HVDC-cables. The network is depicted in figure 3.13.

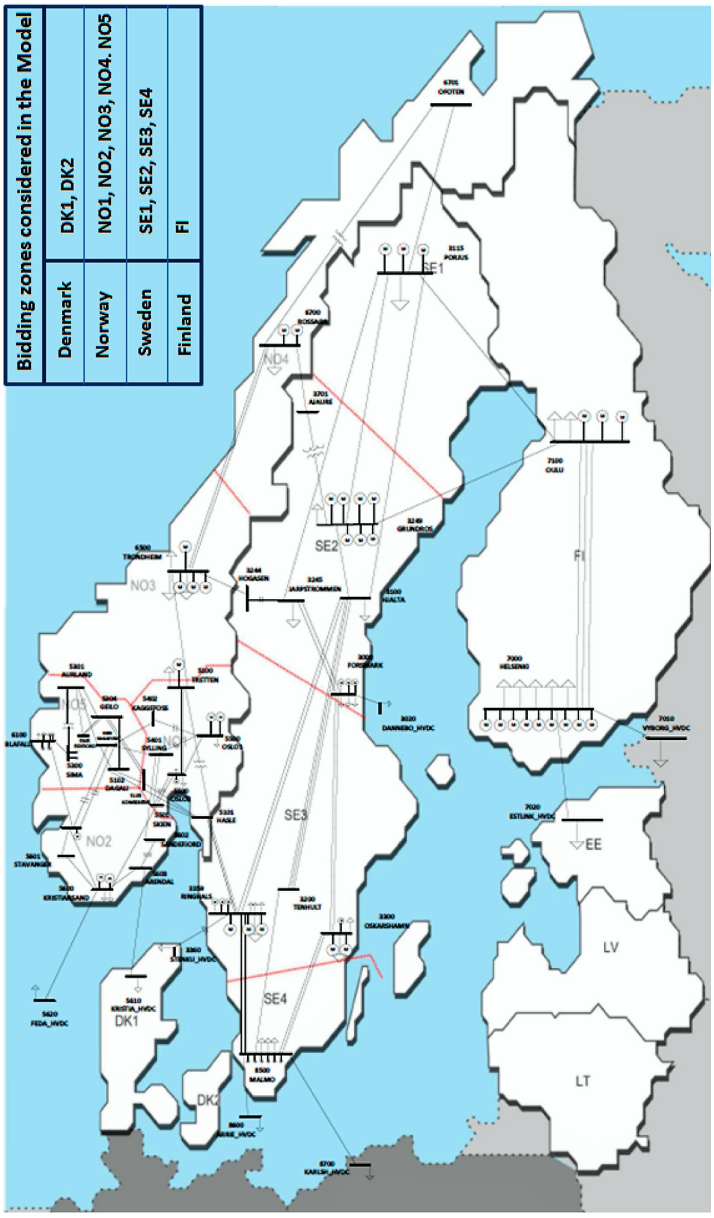

Figure 3.13: 44-bus network used in project, from [47].

One important modification was made to the network structure that makes the used network deviate from the network in Figure 3.13. In the actual Nordic grid, Fenno-Skan between zone SE3 and FI plays an important role in transferring balancing energy to Finland. However, the HVDC link from SE3 in Figure 3.13 does not connect Sweden and Finland and it has therefore been replaced by a HVDC link between Forsmark bus and Helsinki.

3.3.4 Balancing Activation Market Data

[38] describes a proposal for Standard Products to be used on integrated balancing markets. Based

on that proposal and Statnett data of price lists on RK, fictional, common Nordic bid lists for upward and downward energy balancing bids presented in Table 3.4 and 3.5, respectively, are developed. The mFRR bid portfolio consist of 20 bids in each direction distributed on 4 Standard Products. The Standard products are defined by minimum duration, maximum duration, volume and FAT. The Standard Products used in this project were presented on page 22, but are revisited in Table 3.2. The divisibility row specifies if partial activation of the bid volume is allowed. Whether partial mFRR bid activation is allowed is specified by BSP. The maximum capacity of the bid would be a significant rationale behind mFRR activations if all mFRR bids were indivisible. All balancing bids are set divisible to prevent that effect.

Product type	**P1**	**P2**	**P3**	**P5**
Preparation period	5 minutes			0 minutes
Ramping period	10 minutes			5 minutes
Full Activation Time	15 minutes			5 minutes
Minimum volume	5 MW			
Maximum volume	9999 MW			
Minimum duration of delivery period	5 minutes	10 minutes	15 minutes	5 minutes
Maximum duration of delivery period	30 minutes	30 minutes	30 minutes	30 minutes
Divisible	Defined by BSP			

Table 3.2: Specifications for mFRR Standard Products used in model.

The bid lists on balancing energy are based on the list used in [27] and distributed to resemble real life tendencies of flexible hydro power in Norway and northern Sweden, while less flexible thermal power plants are located in Finland and Southern Sweden. This leads to lower prices on bids located in Norway and northern Sweden, while bids in southern Sweden and Finland are characterized by higher prices, as bid prices reflect marginal cost of production. A spot price of 30 €/MWh is assumed constant throughout. Thus, differing area prices due to bottlenecks have not be modelled. The merit order curve for mFRR bids is presented in Figure 3.14. Table 3.3 summarizes total regulating capacities in the activation market. A total upward and downward mFRR volume of respectively 1688 MW and 1769 MW is bid in the balancing market. FCR and aFRR capacity of $\overline{z}$=2500 MW and $\overline{x}_b$=300 MW accompanies mFRR capacity.

	Capacity [MW]
$\text{mFRR}^{\uparrow}$	1688
$\text{mFRR}^{\downarrow}$	1769
$\text{aFRR}^{\uparrow}$	300
$\text{aFRR}^{\downarrow}$	300
FCR	2500

Table 3.3: Regulating capacities in model [MW].

Bid number	Location	Area	Max volume [MW]	Price [€/MWh]	Divisible	Product Type
1	Trondheim	NO3	81	37	Yes	P2
2	Aurland	NO5	64	39	Yes	P5
3	Arendal	NO2	63	34	Yes	P5
4	Sima	NO5	84	35	Yes	P5
5	Kristiansand	NO2	48	40	Yes	P3
6	Blåfalli	NO2	71	34	Yes	P5
7	Malmø	SE4	72	49	Yes	P3
8	Ringhals	SE3	55	52	Yes	P3
9	Grundfors	SE2	53	51	Yes	P2
10	Porjus	SE1	29	38	Yes	P5
11	Rossaga	NO4	36	45	Yes	P1
12	Tretten	NO1	67	42	Yes	P2
13	Skien	NO1	64	46	Yes	P1
14	Geilo	NO5	103	34	Yes	P5
15	Oulu	FI	44	51	Yes	P3
16	Forsmark	SE3	42	44	Yes	P3
17	Oslo 1	NO1	39	41	Yes	P1
18	Oslo 2	NO1	30	39	Yes	P2
19	Dagali	NO5	94	36	Yes	P5
20	Helsinki	FI	85	53	Yes	P3
21	Forsmark	SE3	90	40	Yes	P3
22	Porjus	SE1	50	36	Yes	P2
23	Sandefjord	NO2	42	39	Yes	P5
24	Sima	NO5	63	35	Yes	P5
25	Kristiansand	NO2	30	31	Yes	P3
26	Blåfalli	NO2	78	37	Yes	P5
27	Malmø	SE4	42	40	Yes	P3
28	Ringhals	SE3	16	38	Yes	P3
29	Grundfors	SE2	28	46	Yes	P3
30	Arendal	NO2	25	51	Yes	P1

Table 3.4: Common Nordic mFRR fictional bid list for upward regulation.

Bid number	Location	Area	Max volume [MW]	Price [€/MWh]	Divisible	Product Type
1	Rossaga	NO4	54	25	Yes	P1
2	Porjus	SE1	43	21	Yes	P1
3	Grundfors	SE2	38	15	Yes	P2
4	Helsinki	FI	110	19	Yes	P3
5	Trondheim	NO3	93	26	Yes	P2
6	Tretten	NO1	66	28	Yes	P1
7	Malmø	SE4	34	10	Yes	P3
8	Oscarshavn	SE3	43	7	Yes	P3
9	Blåfalli	NO5	57	9	Yes	P5
10	Stavanger	NO2	76	13	Yes	P2
11	Oulo	FI	33	20	Yes	P3
12	Hogasen	SE2	13	15	Yes	P3
13	Ringhals	SE3	31	17	Yes	P1
14	Kristiansand	NO2	66	14	Yes	P5
15	Dagali	NO5	68	24	Yes	P5
16	Geilo	NO5	69	24	Yes	P5
17	Sylling	NO1	57	23	Yes	P1
18	Skien	NO1	63	22	Yes	P2
19	Oslo 1	NO1	51	18	Yes	P2
20	Oslo 2	NO1	77	19	Yes	P2
21	Forsmark	SE3	66	20	Yes	P3
22	Trondheim	NO3	57	23	Yes	P2
23	Aurland	NO5	90	21	Yes	P5
24	Sima	NO5	81	25	Yes	P5
25	Kristiansand	NO2	44	20	Yes	P3
26	Blåfalli	NO2	39	26	Yes	P5
27	Malmø	SE4	50	11	Yes	P3
28	Ringhals	SE3	22	8	Yes	P3
29	Grundfors	SE2	80	7	Yes	P2
30	Arendal	NO2	50	26	Yes	P5

Table 3.5: Common Nordic mFRR fictional bid list for downward regulation.

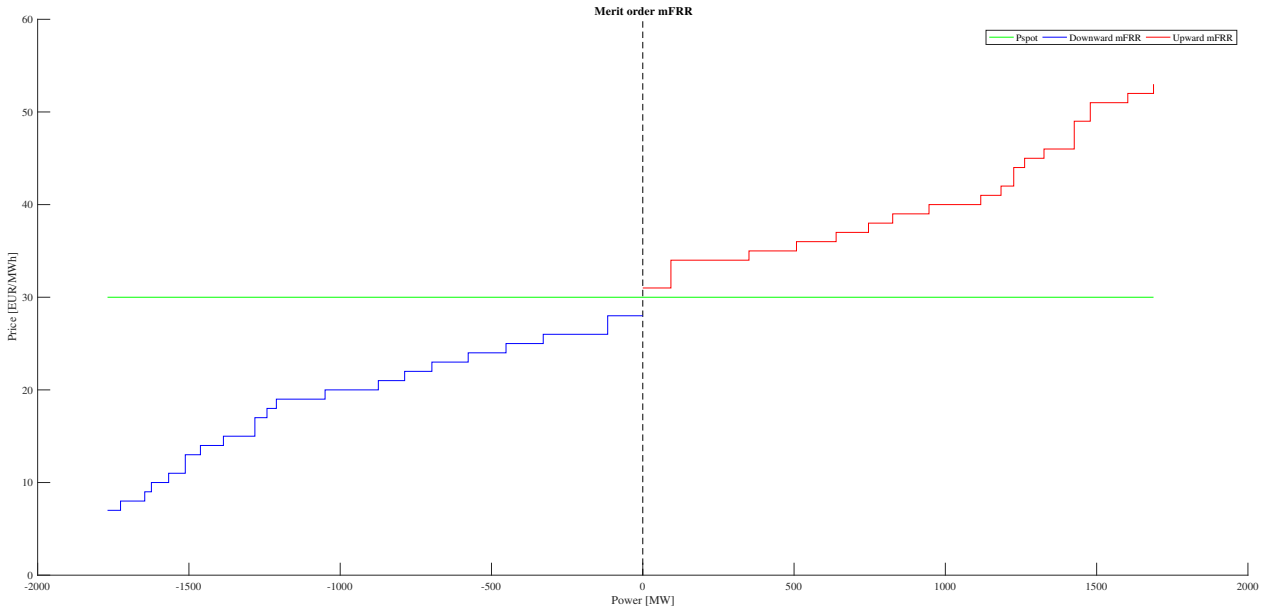

Figure 3.14: Merit order curve of mFRR bids.

Bid number	Location	Max volume [MW]	Price [€/MWh]
1	Kristiansand	20	55
2	Arendal	20	55
3	Oslo 2	20	55
4	Geilo	25	55
5	Trondheim	15	55
6	Rossaga	20	55
7	Porjus	35	55
8	Grundfors	25	55
9	Ringhals	50	55
10	Malmø	50	55
11	Helsinki	20	55

Table 3.6: aFRR bid list for upward regulation

Bid number	Location	Max volume [MW]	Price [€/MWh]
1	Kristiansand	20	55
2	Arendal	20	55
3	Oslo 2	20	55
4	Geilo	25	55
5	Trondheim	15	55
6	Rossaga	20	55
7	Porjus	35	55
8	Grundfors	25	55
9	Ringhals	50	55
10	Malmø	50	55
11	Helsinki	20	55

Table 3.7: AFRR bid list for downward regulation.

3.4 Description of Scenarios

In total 5 different scenarios are investigated. All scenarios are analyzed for same imbalance defined in Section 3.3.1, and the scenarios are more thoroughly described in the following subsections.

Scenario	Cross-border Capacity	Bid List Modification	Forecast Accuracy
Reference	NTC	Original	$k = 5$
Low Integration	0	Original	$k = 5$
No P5	NTC	P5 $\rightarrow$ P1	$k = 5$
Bad Forecast	NTC	Original	$k = 30$
High Flexibility	NTC	$\underline{DP}_b$=1 $\quad \forall \quad b \in (B_u, B_d)$	$k = 5$

Table 3.8: Overview of scenarios developed in project.

Reference Scenario

The second column in Table 3.8 states that in the Reference scenario, all cross-border capacities will be set as the margin between the Nord Pool NTCs and day-ahead clearing, without further modifications, as presented in Section 3.1.6. In the third column, "Original" means that mFRR and aFRR bid lists are unchanged from bid lists presented on pages 56 to 59. The scaling error parameter in the imbalance forecast, k, is specified in the rightmost column. All scenarios except the Bad Forecast scenario are simulated with factor $k = 5$, which means that a forecast for 9 time-steps ahead (45 minutes), will be drawn from a distribution with a standard deviation at every bus of $kt = 45$ MW.

Low Integration Scenario

Low Integration Scenario is developed formulated to study the effect on balancing cost if the Nordic countries did not cooperate in balancing operation. All lines that cross country boundaries between

Norway, Sweden and Finland are made unavailable for balancing purposes. Available transfer corridors for balancing energy exchange in Low Integration scenario is depicted in Figure 3.15. The opportunity cost of balancing market integration and balancing energy exchange, with consequences for other synchronous systems, will be investigated. All other parameters are equal to their value in the Reference scenario.

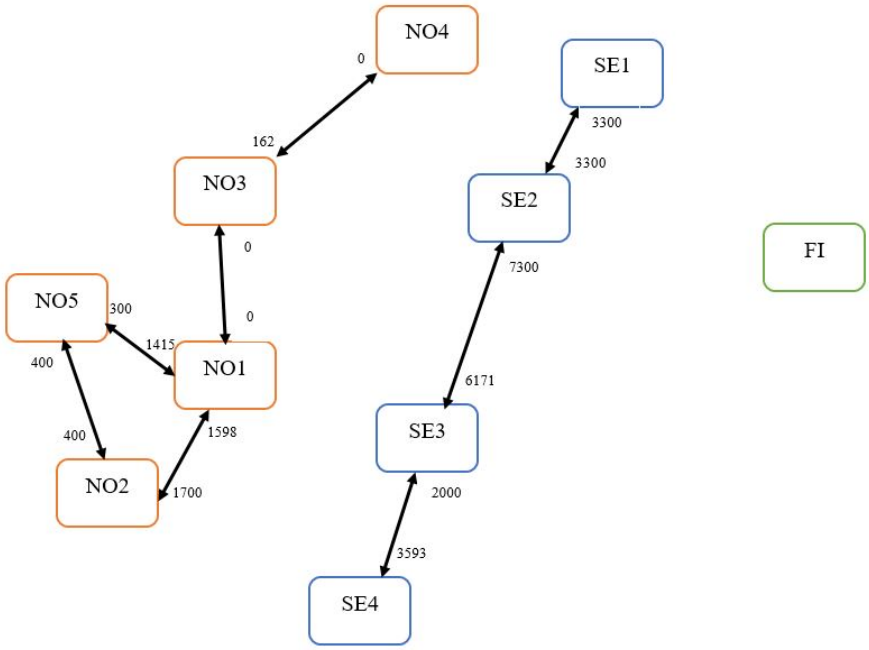

Figure 3.15: Example of transfer capacities (NTCs) in model on January 2 from 00:00 to 01:00 in Low Integration scenario.

No P5 Scenario

The proposed optimisation model may be used to investigate effect of Standard Product definitions on balancing cost, and the effect of eliminating the P5 product will be studied in No P5 scenario. All mFRR P5 bids in the original bid lists are replaced by P1 bids. The P1 bids have longer FAT of 15 minutes but equal minimum duration period of 5 minutes as P5 bids. Eliminating the P5 product represent increased mFRR response time and reduced mFRR product flexibility, and are interesting parameters in energy balancing which effect ought to be analyzed. The bid price and volume remains constant, giving the mFRR bid lists in Tables 3.9 and 3.10.

Bid number	Location	Area	Max volume [MW]	Price [€/MWh]	Divisible	Product Type
1	Trondheim	NO3	81	37	Yes	P2
2	Aurland	NO5	64	39	Yes	P1
3	Arendal	NO2	63	34	Yes	P1
4	Sima	NO5	84	35	Yes	P1
5	Kristiansand	NO2	48	40	Yes	P3
6	Blåfalli	NO2	71	34	Yes	P1
7	Malmø	SE4	72	49	Yes	P3
8	Ringhals	SE3	55	52	Yes	P3
9	Grundfors	SE2	53	51	Yes	P2
10	Porjus	SE1	29	38	Yes	P1
11	Rossaga	NO4	36	45	Yes	P1
12	Tretten	NO1	67	42	Yes	P2
13	Skien	NO1	64	46	Yes	P1
14	Geilo	NO5	103	34	Yes	P1
15	Oulu	FI	44	51	Yes	P3
16	Forsmark	SE3	42	44	Yes	P3
17	Oslo 1	NO1	39	41	Yes	P1
18	Oslo 2	NO1	30	39	Yes	P2
19	Dagali	NO5	94	36	Yes	P1
20	Helsinki	FI	85	53	Yes	P3
21	Forsmark	SE3	90	40	Yes	P3
22	Porjus	SE1	50	36	Yes	P2
23	Sandefjord	NO2	42	39	Yes	P1
24	Sima	NO5	63	35	Yes	P1
25	Kristiansand	NO2	30	31	Yes	P3
26	Blåfalli	NO2	78	37	Yes	P1
27	Malmø	SE4	42	40	Yes	P3
28	Ringhals	SE3	16	38	Yes	P3
29	Grundfors	SE2	28	46	Yes	P3
30	Arendal	NO2	25	51	Yes	P1

Table 3.9: Modified mFRR fictional bid list for upward regulation used in No P5 scenario

Bid number	Location	Area	Max volume [MW]	Price [€/MWh]	Divisible	Product Type
1	Rossaga	NO4	54	25	Yes	P1
2	Porjus	SE1	43	21	Yes	P1
3	Grundfors	SE2	38	15	Yes	P2
4	Helsinki	FI	110	19	Yes	P3
5	Trondheim	NO3	93	26	Yes	P2
6	Tretten	NO1	66	28	Yes	P1
7	Malmø	SE4	34	10	Yes	P3
8	Oscarshavn	SE3	43	7	Yes	P3
9	Blåfalli	NO5	57	9	Yes	P1
10	Stavanger	NO2	76	13	Yes	P2
11	Oulo	FI	33	20	Yes	P3
12	Hogasen	SE2	13	15	Yes	P3
13	Ringhals	SE3	31	17	Yes	P1
14	Kristiansand	NO2	66	14	Yes	P1
15	Dagali	NO5	68	24	Yes	P1
16	Geilo	NO5	69	24	Yes	P1
17	Sylling	NO1	57	23	Yes	P1
18	Skien	NO1	63	22	Yes	P2
19	Oslo 1	NO1	51	18	Yes	P2
20	Oslo 2	NO1	77	19	Yes	P2
21	Forsmark	SE3	66	20	Yes	P3
22	Trondheim	NO3	57	23	Yes	P2
23	Aurland	NO5	90	21	Yes	P1
24	Sima	NO5	81	25	Yes	P1
25	Kristiansand	NO2	44	20	Yes	P3
26	Blåfalli	NO2	39	26	Yes	P1
27	Malmø	SE4	50	11	Yes	P3
28	Ringhals	SE3	22	8	Yes	P3
29	Grundfors	SE2	80	7	Yes	P2
30	Arendal	NO2	50	26	Yes	P1

Table 3.10: Modified mFRR fictional bid list for downward regulation used in No P5 Scenario

Bad Forecast

It can be expected that the accuracy of the imbalance forecast will affect the activation schedules and balancing cost. Large forecasting deviations will require re-optimisation of prior activation schedules to account for imbalance forecasting errors. Bad Forecast scenario is developed to study how a large deviation in the imbalance forecast affects model behaviour and specifically mFRR product activation and balancing cost.

Bad Forecast scenario is developed by increasing the forecast scaling error factor to k=30. This means that bus imbalance forecasts for t time-steps ahead will be drawn from a distribution with a

standard deviation of kt MW, possibly creating large deviations in the imbalance forecast on system level. For instance, a imbalance forecast deviation from actual imbalance 9 time-steps ahead of time may amount to $kt = 30 \cdot 9 = 270$ MW.

High Flexibility Scenario

To study the effect of time-coupling of mFRR decisions on balancing cost, the minimum duration of all mFRR bids is set to 5 minutes in High Flexibility scenario. Bids may therefore be deactivated or changed to a new power level after a single time-step, increasing the mFRR flexibility. No change is made for the maximum duration period or other parameters.

Previous study on balancing energy in [27] concluded that producer flexibility was an important parameter in reducing social cost of balancing. High Flexibility scenario is formulated to study the effect of increased flexibility on balancing cost and model behaviour when also a physical network is considered.

Chapter 4

Results and Discussion

4.1 Introduction

In this Chapter, the results from operating the balancing activation optimisation function for 24 hours between January 3. 05:00 and January 4. 05:00 are presented. These hours have been selected because they contain the largest total system imbalance in the first week of January 2017 and allow for presentation of entire range of model functions. Results from each scenario will be presented and commented in the same Chapter to improve readability of the report.

The Chapter begins with a discussion of assumptions that have been made and how most important simplifications affect results. Results from each scenario are presented afterwards and subsequently compared. A sensitivity analysis that studies the effect of increased FCR price and cross-border transmission capacity follows, before improvements and future work close the Chapter.

4.2 Most Important Modelling Simplifications and Assumptions

4.2.1 Assumptions in FCR modelling

In modelling the primary control there have been made simplifications to pricing and geographical distribution of reserves as well as frequency response via the frequency bias factor λ. The formulation of primary control is not meant to represent real primary control, that would require a higher time resolution to encapture transient effects, plus a non-linear bias factor.

Entire FCR Capacity Available at Every Bus

The assumption that entire FCR capacity is available at every bus is a simplification due to the lack of data in real-life FCR distribution. Droop settings are reported to TSO, but the actual FCR capacity and its physical distribution, is not readily available. In reality only a small part of the Nordic FCR capacity would be available at each generator as the spinning reserve, i.e. the margin between power rating and actual load. Having a large FCR capacity available at every bus suggest that a significantly larger amount of FCR may be activated at every bus compared to real-life operation.

This distances the model from reality and allow unrealistic possibilities for FCR balancing. Following this argument, some of the solutions presented in this work would in reality possibly require shedding as the energy deviation after balancing by mFRR and aFRR is too large to be handled by FCR alone.

Determining Fictional FCR Price

Determining price of FCR may be indirectly interpreted as setting the model incentive to maintain nominal frequency. In reality, FCR capacity is offered by producers in the capacity market and settled with marginal pricing ex-post [44]. Thus, an energy priced FCR is a modelling measure which in effect equivalents a penalty cost for frequency deviation. A low FCR price would lead to frequency quality being sacrificed for reduced cost of balancing mFRR or aFRR, and the FCR price will in this regard represent social cost of reduced frequency quality.

The FCR price is determined by incremental increase until a satisfactory frequency quality is achieved, c.f. Section 3.1.2, based on specific balancing market and imbalance data. This implies that the FCR price that is found, and thus resulting in satisfactory frequency deviations for one scenario, may not give a satisfactory frequency quality in a different scenario, in which different imbalances may occur or a different bid list may be inputted. However, using the same FCR price of C^{fcr}=40 €/MWh in all scenarios enables a comparison of the scenarios' effect on frequency quality, as the financial incentive to maintain nominal frequency is equal in all scenarios. In the sensitivity analysis in Section 4.5.1 it is analyzed how an increased FCR price affects activation behavior and shows a significant increase in aFRR activations upon FCR price increase.

Frequency Bias Factor and Frequency Deviation Estimate

The frequency bias factor, λ, is a measure of how much FCR that is activated for a given frequency deviation, and the total bias factor in the Nordic system is the aggregate of all generator droop settings in the system, c.f. Section 2.3.1. In this formulation it is assumed that all FCR reserve is available at all frequencies. This is a simplification when considering that the Nordic system uses two different FCR reserves for normal (FCR-N) and disturbance (FCR-D) operation. Since FCR-D and FCR-N operate in different frequency ranges the frequency bias is non-linear with frequency deviation, as depicted in Figure 4.1 [49, page 299] from Norway, which shows that the frequency bias is lower outside the FCR-N band of $\pm$ 0.1 Hz. A frequency bias of λ=5000 MW/Hz for the Nordic system is therefore the average of the frequency bias over the frequency deviation range $\pm$ 0.5 Hz.

In addition, it should be noted that the load is assumed frequency independent. Frequency dependency of demand is smaller than for production and may thus be assumed negligible without affecting the frequency response to a large extent.

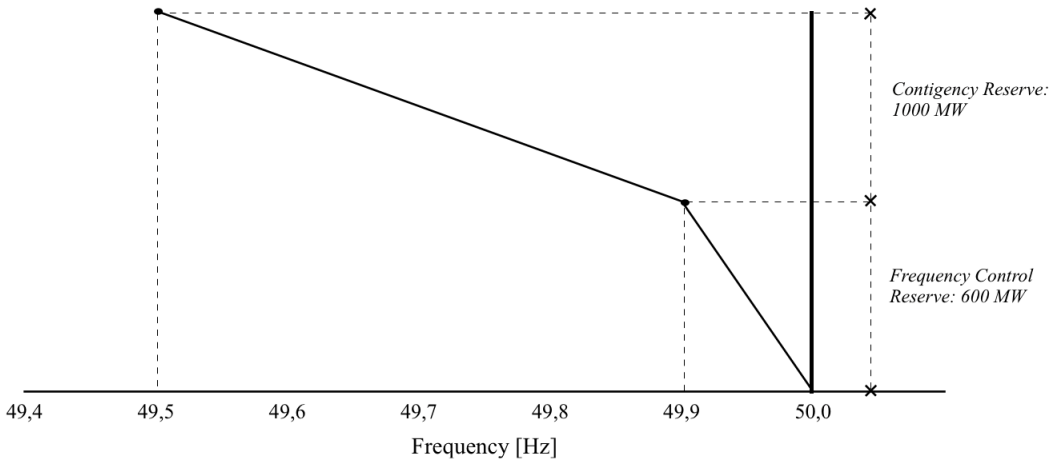

Figure 4.1: Non-linearity of frequency response, from [49, page 299].

4.2.2 Assumptions in aFRR modelling

The aFRR has been modelled as an expensive and fast-ramping reserve with a total capacity of 300 MW distributed in the Nordic system. The price of aFRR is set to a fixed price of 55 €/MWh for all aFRR bids and it is assumed that the entire aFRR volume can be ramped within 5 minutes. The aFRR price does not represent any actual aFRR price, but is a modelling measure to prevent that system security is compromised by the exhaustion of aFRR capacity. It is thereby assumed that aFRR is more expensive to activate than mFRR in the Nordic system. A common Nordic aFRR market is currently under development, and relevant historical aFRR activation data is therefore not available, and the future activation cost of aFRR in comparison to mFRR is uncertain. The main implication of the assumptions in the aFRR modelling is that aFRR will not be activated unless the total mFRR capacity is exhausted, or if the aFRR flexibility due to its high ramping capability is required.

As explained in Section 2.3.2, Nordic aFRR is automatically activated based on a frequency signal [9, page 13]. Setting a price of aFRR implies that the model will compare the cost of aFRR with other balancing measures when creating balancing schedules. This behaviour distances the model from real-life operation since aFRR activation is not planned ahead of time, but is automatically activated in real-time based on a Nordic frequency signal. Such a behaviour could be modelled by a constraint that activates aFRR if there is a frequency deviation in the system. On the other hand, that would be equivalent to an increased fictional FCR cost, and more mFRR would be activated to prevent frequency deviations.

4.2.3 DC simplifications

In a DC OPF the assumptions of flat voltage profile, small voltage angles and negligible resistance are used to linearise AC load flow equations, allowing them to be used in a linear dispatch optimi-

sation problem. The computation of DC equations are easier for the solver and a solution can be found faster. However, it may be expected that the optimal dispatch will be different in an AC load flow when considering transmission losses and reactive power. Still, transmission losses would have an increasing effect with reducing voltage level, and since the high voltage transmission system has been modelled in this project, the transmission losses could be assumed low even with AC equations.

In [46], the installment of power flow controlling equipment such as the phase-shifting transformer, HVDC cables and FACTS, motivates a re-validation of DC load flow result accuracy. In that paper, a comparison of AC and DC load flow results on a IEEE 30 bus system is done to assess the validity and precision of the DC load flow simplifications. MATPOWER is used for the actual load flow computations. Previous work in [37] concludes that DC load flow does not introduce significant active power estimation error when the ratio between line reactance and resistance is greater than 4, $\frac{X}{R} > 4$. The mean ratio between line reactance and resistance in the network used in this project is 14.89 and the median is 12.80. However, the minimum ratio is 1.31. This implies that for this line, the negligible line resistance assumption may not be valid. There are 6 lines with ratio $\frac{X}{R} < 4$, the other 73 lines have $\frac{X}{R} \geq 4$. Considering this result, the negligible line resistance assumption is valid.

4.2.4 Algorithm Performance and Convergence Gaps

Since the model formulation consist of a binary unit commitment problem and linear economic dispatch problem, the problem blockiness has an effect on the best solution that may be obtained. Dual simplex algorithm in XPRESS software solves the optimisation problem by first relaxing the binary constraints and then use a "Branch and Bound" method to search the relaxed solutions for integer solutions. The method can be further studied in [4, page 21]. The difference between the best integer and relaxed solution is referred to as the relative MIP gap, as presented in equation 4.1.

$$MIP_{rel} = \frac{|(\text{Best solution} - \text{Best bound})|}{\text{Best bound}} \tag{4.1}$$

In XPRESS it is possible to set the lowest acceptable relative MIP gap and to avoid long run times the minimum relative MIP gap is set to 5 %. This means that any integer solution with a MIP gap below 5 % will exit the optimisation algorithm and be output. In addition, a maximum computation time of 60 seconds is set for each simulation. If no solution within MIP gap margin of 5 % is found before 60 seconds, the optimisation algorithm will accept the solution and move on. It is therefore assumed that the solution converges to a reasonable small MIP gap within 60 seconds, which may not always be the case. Table 4.1 presents the maximum and average MIP gap and run times in each scenario. A MIP gap above 5 % implies that the solver was unable to find activation schedule below this margin within 60 seconds. The table shows that a reasonable small MIP gap is found within 60 seconds for all scenarios except the High Flexibility with a maximum MIP gap of 20.6 %. The activation schedules in the High Flexibility scenario have the greatest mean gaps and run-times, indicating that cheaper solutions could have been found if the solver was given more time. Bad Forecast scenario has the lowest mean MIP-gap of 2.6 % and is the only scenario where a reasonable MIP gap could be achieved within 60 seconds for all schedules. Figure 4.2 depicts the MIP gap in each scenario in the upper figure and run times in the bottom figure.

Scenario	Max MIP gap [%]	Mean MIP gap [%]	Max run-time [s]	Mean run-time [s]
Reference	5.3	3.6	60	8.7
Low Integration	7.6	3.4	60	5.33
No P5	6.9	3.5	60	12.3
Bad Forecast	5.0	2.6	29.8	5.9
High Flexibility	20.6	4.7	60	19.41

Table 4.1: Max MIP gap, mean MIP gap and mean run time in each scenario

A likely reason for longer run-times in High Flexibility scenario is that the number of sunk decisions is reduced when the minimum duration of all bids is shortened to 5 minutes. When activating an mFRR bid with 15 minutes minimum duration, the decision variable for this bid is sunk in the subsequent 2 optimisations. This reduces the feasible solution area for the solver and leads to shortened run-time. When all mFRR bids have 5 minute minimum duration, the solver can change the mFRR bid output in each time-step (while not violating the maximum duration constraint), which requires a larger computational effort and also contributes to longer run-time in High Flexibility scenario.

A possible explanation for the short run-times and small MIP gaps in the Bad Forecast scenario is the fact that the imbalance forecast at each bus is drawn from a normal probability distribution with high standard deviation. The high standard deviation at every bus may smoothen large shifts in the imbalance forecast. The model will think that it has made well-fitting mFRR activations, but may not be able to re-optimise the decisions when the actual imbalance turned out to be deviating from the forecast due to the time-coupling of mFRR bids. The increased balancing by FCR and aFRR in this scenario decrease the run-times as these reserves are not coupled in time and have in general fewer constraints to consider.

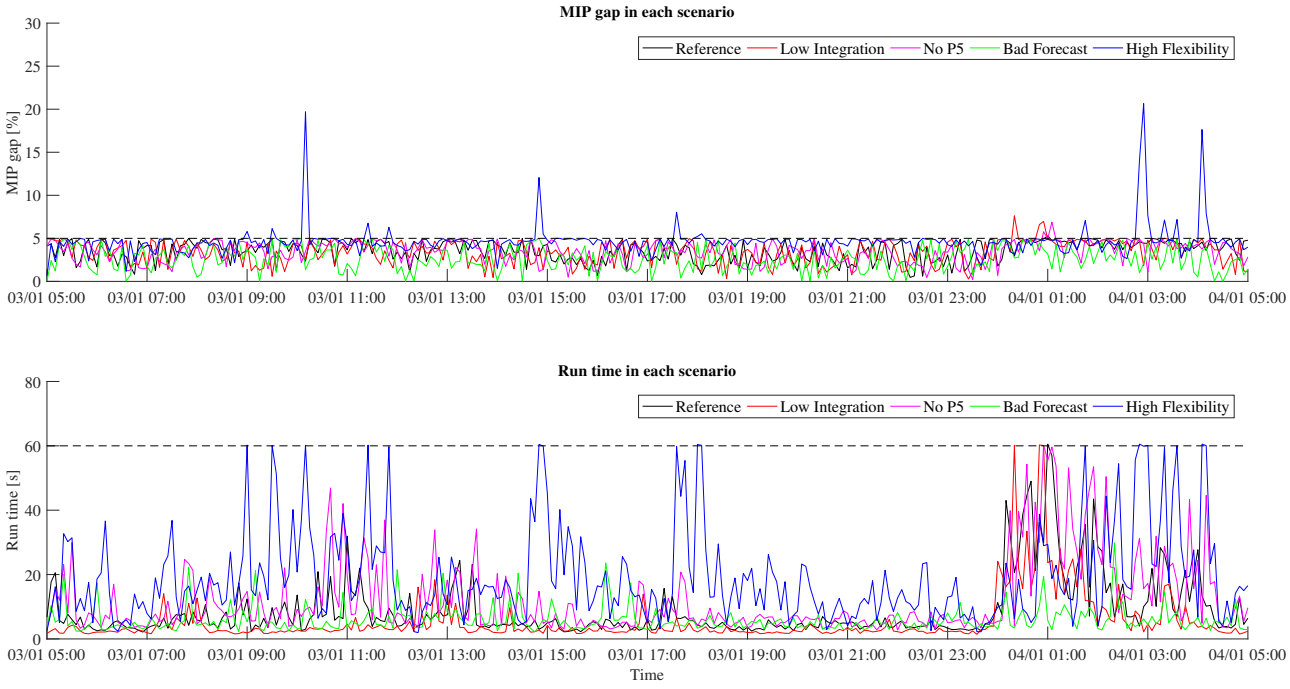

Figure 4.2: MIP gaps and run time in each scenario.

4.2.5 Change of mFRR Bid Power Output Without New Full Activation Time (FAT)

As presented in Section 3.1.3, mFRR bids are constrained to follow a ramping profile after activation. Bids must follow a flat profile the entire minimum duration profile after FAT is completed which means that when the minimum duration is over, the bids are allowed to change output without going through another FAT. This is depicted in Figure 4.3 for an mFRR bid with 15 minute FAT and 10 minute minimum duration, $\underline{DP}_{b,t} = 2$. The bid is activated in $t = 1$ and the delivered energy during ramping is marked with blue. Although the bid was ramped to a delivery set point of 40 MW, the power level is allowed to be changed to 10 MW after the minimum duration period without a new FAT.

Even though mFRR is delivered from generators in operation it may be reasonable to assume that a bid requires preparation and ramping time when the change in bid output is large. The producer flexibility formulated in this project may therefore be somewhat unrealistic. Constraining the allowed change of bid output after FAT to a share of bid capacity would reduce the mFRR flexibility and increase the balancing cost, especially for the High Flexibility scenario in which intra-delivery change of output is the root cause for reduced balancing cost.

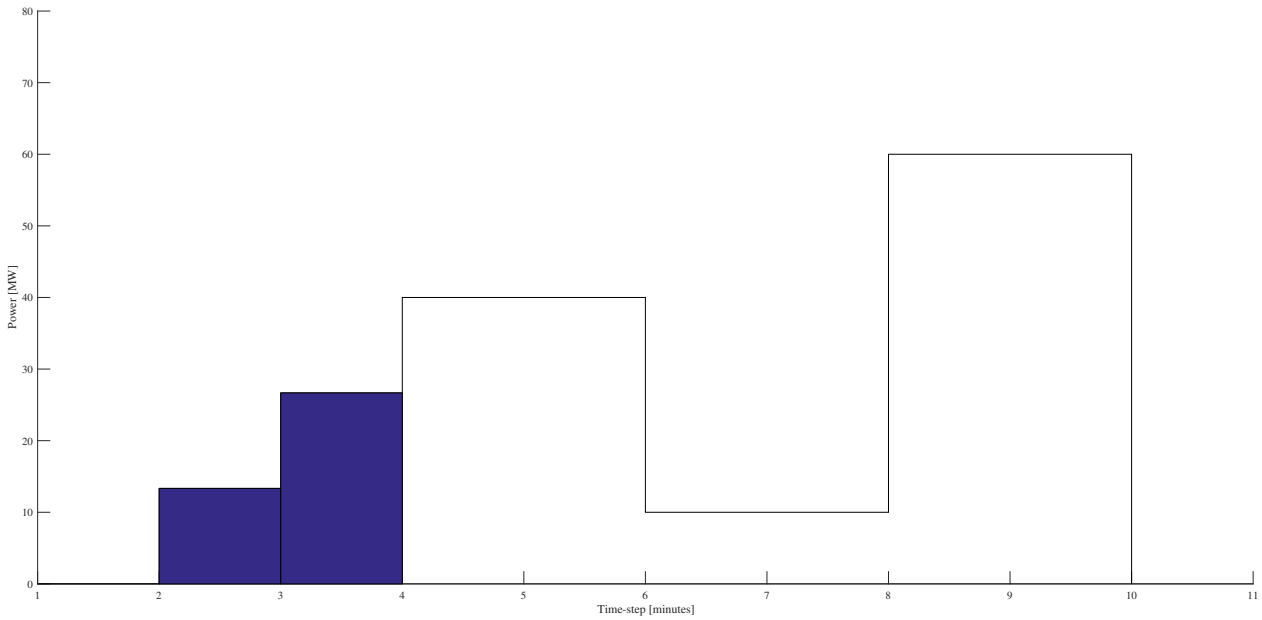

Figure 4.3: A possible mFRR bid delivery profile when FAT is 15 minutes and minimum duration period is 10 minutes. Ramping energy is marked with blue.

4.2.6 Ramping Constraints on HVDC Links

There are formulated constraints on how much the power flow may change on HVDC links in accordance with [35], and change of HVDC-flow may not exceed 600 MW/h. An HVDC ramping constraint of 50 MW per time-step has been used in this project, which equals the hourly HVDC ramping restriction averaged over 12 time-steps per hour when the time resolution is 5 minutes. This is a simplification because the flow may change more rapidly in real-life, although below limit of 600 MW/h. The simplified constraint on HVDC ramping may effect the result when the negative imbalance in SE3 plumits around midnight on January 4., as the flow on Fenno-Skan is reversed from export to import into SE3. If Fenno-Skan flow was allowed to change more rapidly, possibly a larger amount of FI imbalance could be netted with the Swedish imbalance, affecting total balancing cost.

4.3 Presentation and Discussion of Results From Each Scenario

4.3.1 Results from Reference Scenario

Figure 4.4 presents the sum of all bus imbalances as the net system imbalance together with FCR, aFRR and mFRR activations in the top graph. Activation of FCR is presented by the dashed line and aggregate FCR power equals the difference between the system imbalance and net aFRR and mFRR power. The bottom graph in Figure 4.4 depicts modelled frequency in the Nordic system. A peaking frequency deviation of about + 0.3 Hz is observed at midnight.

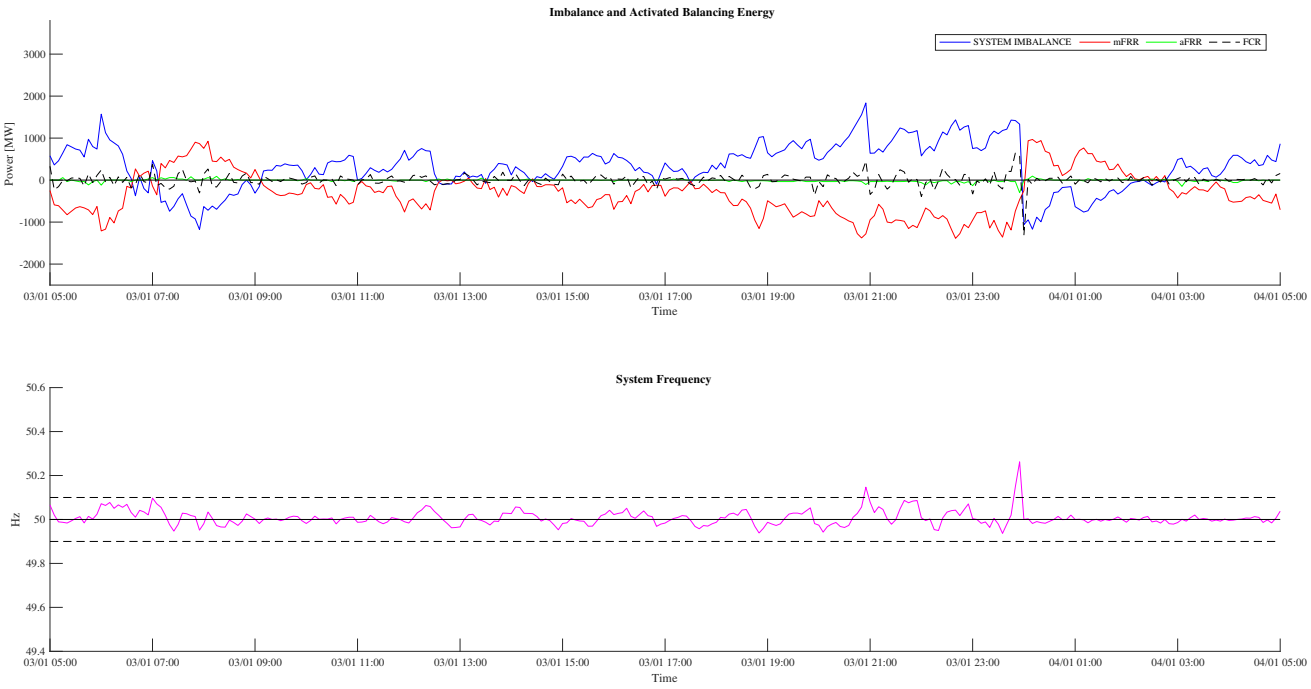

Figure 4.4: Activation schedules and system frequency in Reference scenario between January 3. 05:00 and January 4. 05:00.

Balancing activations oppose system imbalance at most occasions, except during fast shift in imbalance direction at midnight January 4. To explain the mFRR activations at that hour shift, the minimum duration specification of mFRR must be taken into consideration. If no such constraint was formulated, downward regulating mFRR could be remain active longer. Because of the minimum duration of mFRR bids, downward mFRR bids are deactivated before the imbalance shift to prevent continued downward activations after midnight, when the imbalance drops to large negative values. In addition, the upward bids have to go through a preparation and ramping period before they can deliver their full capacity, delaying the response of upward mFRR after midnight. The model is therefore unable to switch off downward mFRR and activate upward mFRR fast enough to prevent a large frequency deviation in bottom graph in Figure 4.4. When minimum duration period of all bids is 5 minutes as studied in High Flexibility scenario is Section 4.3.5, the large frequency deviation at midnight is prevented. The large system frequency is an indirect consequence of the assumptions of FCR price since a higher price of FCR would lead to more aFRR activations between 23:00 and 01:00 to reduce frequency deviations. In the sensitivity analysis of the FCR price parameter C^{fcr} in Section 4.5.1 it is shown that the peak frequency deviation around midnight is reduced when C^{fcr} is set to 60 €/MWh.

Table 4.2 is divided in separate columns showing activated balancing energy and cost. All values in the leftmost columns have unit GWh, while the values in rightmost columns have unit 1000 €. The values are calculated for balancing operation between January 3. 05:00 and January 4. 05:00. The left column shows that 20.37 GWh of mFRR is activated with a cost of 410 680 €.

aFRR is least activated with a total volume of 0.4235 GWh while 10.40 GWh of FCR is delivered. In real-life balancing, the aFRR would automatically follow the FCR since aFRR activation is based on a frequency signal. The low aFRR volume in this scenario is therefore somewhat unrealistic. Although, it should be noted that the figures are absolute values and that upward and downward FCR may be activated simultaneously without leading to a system frequency deviation. With an aFRR price higher than FCR price, the mFRR is used to relieve FCR, while in reality this is the function of aFRR. A zero price of aFRR would ensure that aFRR contributes in relieving FCR and lead to results that more closely resemble real-life operations, which would be equivalent to a dead band around nominal frequency where no cost for frequency deviation was incurred on the solution, which is also discussed in [27]. The activated energy of FCR may be interpreted as frequency quality and cost of FCR activations as reduced social welfare from frequency deviations.

	Energy [GWh]			Cost [1000 €]		
	FCR	aFRR	mFRR	FCR	aFRR	mFRR
Total by reserve	10.40	0.4235	20.37	416.11	23.30	410.68
Sum	31.12			850.08		

Table 4.2: Volume and cost results from Reference scenario for analysis period January 3. 05:00 to January 4. 05:00.

The bar graph in Figure 4.5 presents the activation duration of each upward and downward bid. The number on the top of the bar is the bid number. The blue graph in the background is the merit order and the bids are located based on their price. Consequently, the rightmost upward bid 20 is the most expensive upward bid for the model to activate, while bid 8 is the least economical for downward regulation when only considering the bid price. The color of the bar specify in which bidding area in the Nordic region the bid is located. The aggregate activation time of upward regulating bids is lower than downward regulation duration since the net system imbalance volume is positive most of the time.

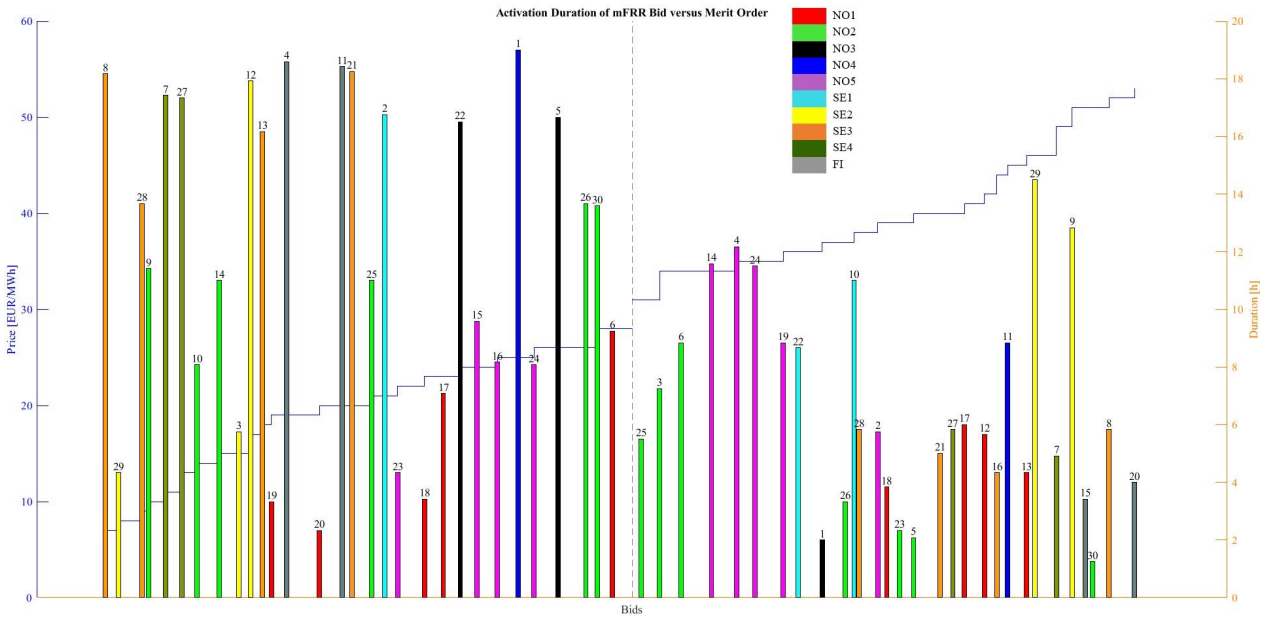

Figure 4.5: Total activated duration of each mFRR bid and their location in the merit order in Reference scenario between January 3. 05:00 and January 4. 05:00.

The distribution in Figure 4.5 show that it is not necessarily the activation of the cheapest upward regulating or most expensive downward regulating mFRR bids that lead to the lowest balancing costs. Several bids are skipped in price order and the possibility of skipping bids by marking them unavailable in operational hour is also possible for TSO in real-life balancing. Figure 4.5 shows that mFRR bids are skipped in both regulating directions. Downward bid 8, with a price of 7 €/MWh is active for about 18.5 hours, and expensive upward bids 29 and 9 are active about 15 and 13 hours, respectively. Downward bid 1, which is a P1 product located in Rossaga in NO4, is the most active downward regulating bid, with a total active duration of 19 hours. A possible explanation of large activation of this bid, in addition to its short minimum duration and price, is a bottleneck between NO3 and NO1 after day-ahead. Nord Pool flow of 100 MW from NO3 to NO1 equals the NTC on this border in most hours, thus preventing the exchange of balancing energy between NO3 and NO1 and effectively splitting Norway in two. NO3 has a positive imbalance most of the day that must be balanced by resources in NO3 or NO4, or be exported to Sweden. The Swedish bids both in SE1 and SE2 are more expensive than the bids in NO3 and NO4, and the large activation of downward regulation in NO3 and NO4 is therefore observed.

The downward bids located in NO1 are the least activated bids. As the largest upward imbalances occur in Southern Sweden the power is imported into NO1 in Hasle corridor when possible, and thus forwarded to cheaper downward bids in NO2. It is also noticed that downward NO2 bids 9, 10 and 14 are more active than considerably more economical NO1 bids. This can be explained by the difference in product characteristics. The downward NO2 bids 9 and 14 are P5 products, while NO1 bid 19, 20 and 18 are P2 bids with a longer ramping and minimum duration period. The bottleneck between NO1 and NO3 after day-ahead may also explain the low activation of downward NO1 bids, since large downward regulation would increase the power flow from NO3 to NO1. This is likely the cause of low activation of P1 bid 6 located in Tretten, NO1, on the border to NO3.

The activation of mFRR as presented in Figure 4.5 is therefore a consequence of network capacities and transfer corridors and the preferable characteristics of bids with short minimum duration and price.

For upward regulation, the expensive upward bid 29 is most activated with about 15 hours followed by bid 9. Both bid 29 and 9 are located in SE2. Bid 29 is a P3 product, while bid 9 is a P2 product. A larger activation of the P3 product compared to the P2 product implies that the value of increased flexibility in the P2 product is lower than the price difference between the bids, which may be explained by a non-fluctuating negative SE2 imbalance. If the SE2 imbalance was shifting between positive and negative values more often, the possibility of quickly deactivating the upward bid would possibly cause a favoring of the more flexible bid 9.

4.3.2 Results from Low Integration Scenario

The frequency quality deteriorates compared to the Reference scenario without possibility of balancing energy exchange between countries in Low Integration scenario. This is depicted in Figure 4.6, showing a peaking frequency deviation in the evening, January 3. This is a consequence of simultaneously large positive structural imbalances in SE2, SE3, SE4+DK2 and FI, and reduced exchange possibilities between countries increase the FCR activations and resulting frequency deviations. There is also observed an increase in aFRR activations compared to Reference as the local mFRR capacity is exchausted in Sweden and Finland, and aFRR is activated to prevent larger frequency deviations and generation shedding.

Figure 4.6: Activation schedules and system frequency in Low Integration scenario between January 3. 05:00 and January 4. 05:00.

The activation volume of FCR increases with 5.36 GWh in the Low Integration scenario, compared to the Reference, as presented in Table 4.3. The increased balancing by FCR is the most significant contributor to the increased balancing cost in this scenario. The activated mFRR balancing energy is reduced with 1.26 GWh because less of the positive imbalance is exported from Southern Sweden to be balanced by downward bids in NO5 and NO2. In other words, eliminating the possibility of mFRR exchange leads to more balancing by local, less economical resources. This result confirms the motivation for the integration of European balancing markets and the exchange of balancing energy in increased usage efficiency of balancing resources.

	Energy [GWh]			Cost [1000 €]		
	FCR	aFRR	mFRR	FCR	aFRR	mFRR
Total by reserve	+5.36	+0.80	-1.26	+214.39	+13.98	-21.76
Sum	+4.90			+236.62		

Table 4.3: Change in volume and cost results from Reference scenario in Low Integration scenario.

Comparing each mFRR activation duration in Figure 4.7 shows that downward bid 11 in Helsinki is most active for downward regulation while bid 14 is most active for upward regulation. Comparing with the Reference it is observed a similar frequent activation of downward regulation by

bid 26 and 30 in NO2, which underlines the importance of these flexible P5 products in balancing Southern Norway when there is a bottleneck between NO3 and NO1.

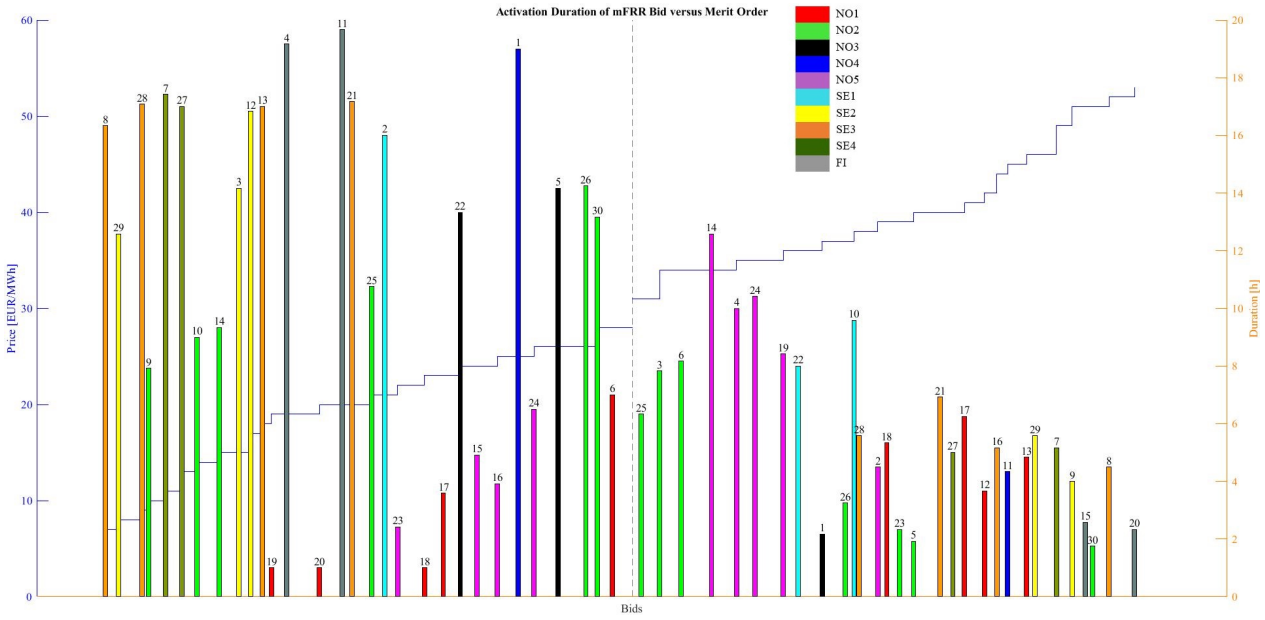

Figure 4.7: Total activated energy from each mFRR bid and the bids location in the merit order for Low Integration scenario.

Since no imbalance power is exported from Sweden into NO3, less energy is activated in NO3 in comparison to the Reference. Most of the positive NO3 imbalance is balanced by the P1 downward bid 1 in NO4. Since the NO3 downward bids 22 and 5 are both P2 products, this observation is in line with previous observations of favoritism of bids with short minimum duration.

4.3.3 Results from No P5 Scenario

No P5 scenario has a similar system frequency as the Reference, with a peak of about 50.3 Hz around midnight, January 3, depicted in Figure 4.8.

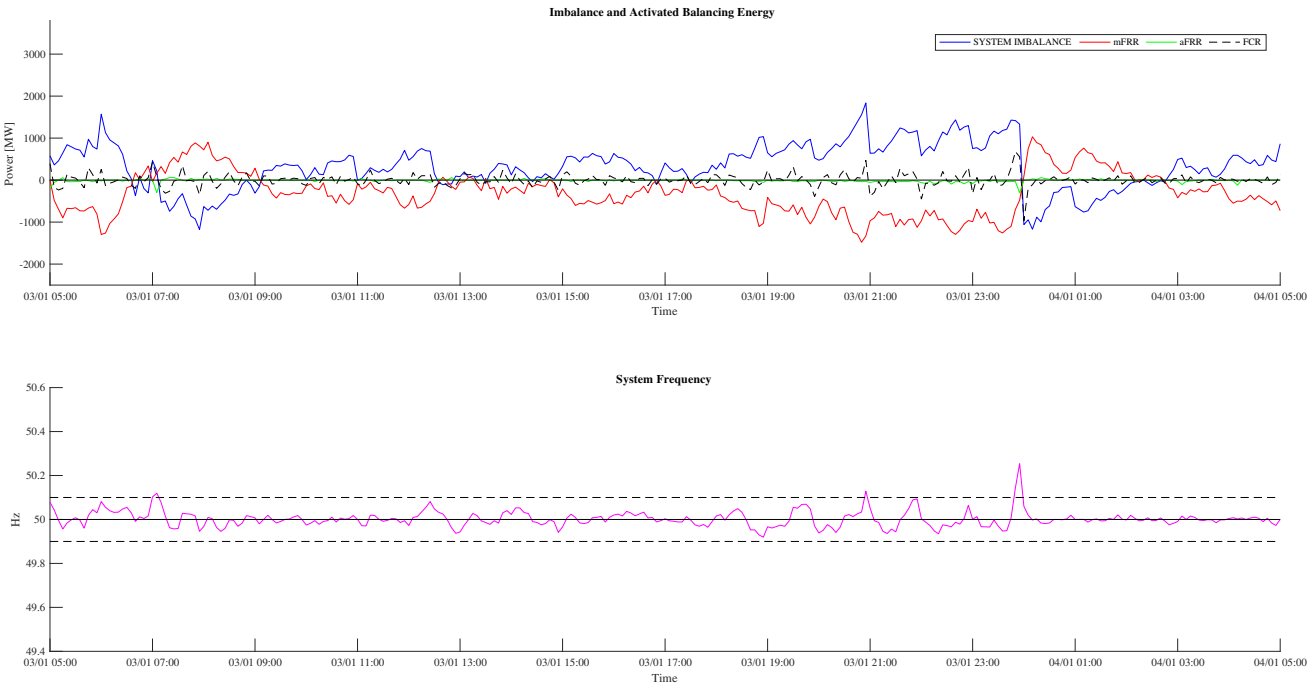

Figure 4.8: Activation schedules and system frequency in No P5 scenario between January 3. 05:00 and January 4. 05:00.

Table 4.4 shows an increase in activation from FCR and mFRR of 0.22 GWh and 0. 73 GWh, contributing to the cost increase of 26 650 €from Reference. The activated aFRR volume is equal to the volume in the Reference. The results show the opportunity costs of ramping time. As the number of bids with long FAT increases more mFRR is required to balance the system and the frequency quality is reduced. A plausible reason for the increased mFRR activation is that other mFRR bids are activated to counter the effect of delivered energy during ramping. Having fast-ramping mFRR available means that mFRR volume can be withheld until the imbalance actually occurs. The increased mFRR volume could also be explained by increased ramping power. It may therefore be concluded that the contribution of fast ramping hydro power increase frequency quality if the resources are activated optimally, although this is dependent on the penalty cost of frequency deviation. No load/generation shedding is activated.

	Energy [GWh]			Cost [1000 €]		
	FCR	aFRR	mFRR	FCR	aFRR	mFRR
Total by reserve	+0.22	+0	+0.73	+8.63	+0	+18.11
Sum	+0.94			+26.65		

Table 4.4: Change in volume and cost results from Reference scenario in No P5 scenario.

MFRR activations in Figure 4.9 resemble the result in Reference scenario to a large extent, but

with a slight increase in activations from the P5 products that are changed to P1 products because of increased ramping power.

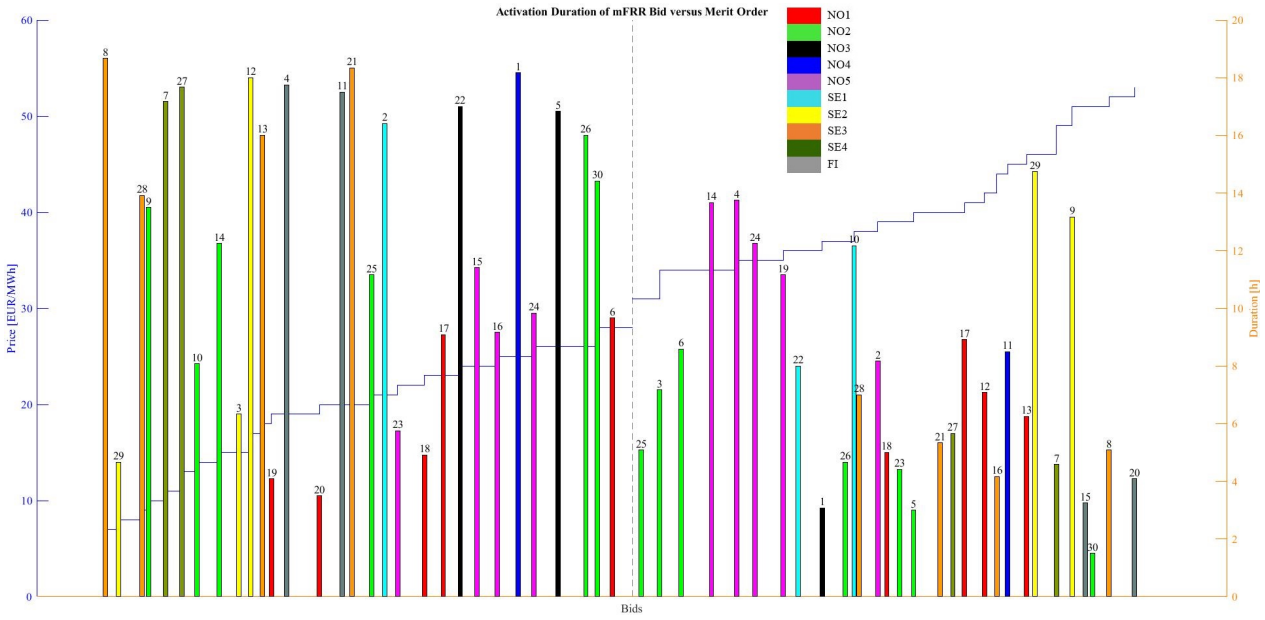

Figure 4.9: Total activated energy from each mFRR bid and the bids location in the merit order for No P5 scenario.

4.3.4 Results from Bad Forecast Scenario

The system frequency obtained in the Bad Forecast scenario share characteristics with the Reference, and the peak frequency deviation occurs around midnight, January 3. However, a generation shedding of about 17 MW occurs around 20:30 on January 3, c.f. Figure 4.10. This demonstrates that the deviation in the imbalance forecast was so large that the model could not re-optimize activation schedules to maintain energy balance when the imbalance actually occurred. A deterministic formulation will therefore require more accurate imbalance forecast to avoid shedding.

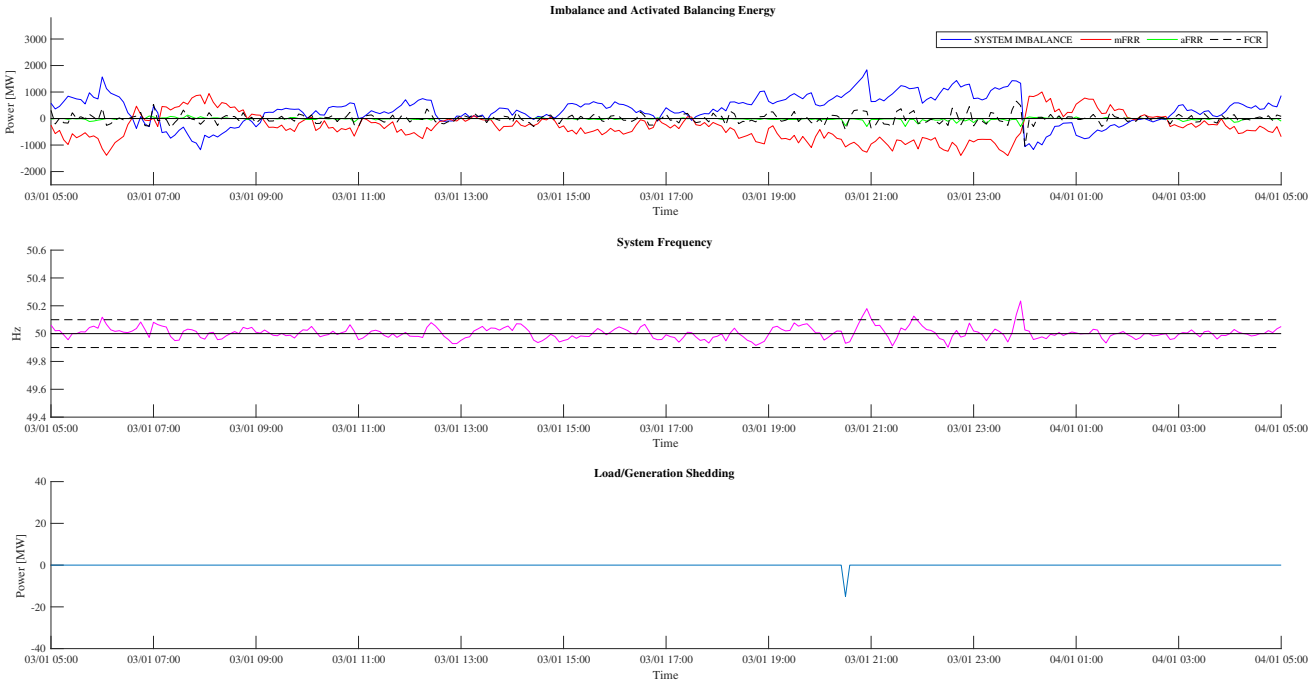

Figure 4.10: Activation schedules and system frequency in Bad Forecast scenario between January 3. 05:00 and January 4. 05:00.

Table 4.5 presents the increase in activated FCR, aFRR and mFRR volume of 1.77 GWh, 0.20 GWh and 4.02 GWh compared to the Reference. The increased mFRR volume is explained by the time- coupling of bids through ramping and minimum duration constraints, so that additional mFRR must be activated to counter the earlier activated mFRR when the imbalance forecast is corrected closer to real-time, leading to increased volume of mFRR. AFRR energy also increases because fast-ramping and flexible resources are necessary for effective re-optimisation.

	Energy [GWh]			Cost [1000 €]		
	FCR	aFRR	mFRR	FCR	aFRR	mFRR
Total by reserve	+1.77	+0.20	+4.02	+70.63	+10.80	+108.40
Sum	+5.99			+189.82		

Table 4.5: Change in volume and cost results from Reference scenario in Bad Forecast scenario

	Energy [MWh]	Cost [1000 €]
Load Shedding	0	0
Generation Shedding	0.0125	12.5
Sum	0.0125	12.5

Table 4.6: Activated load/generation shedding in Bad Forecast scenario.

Figure 4.11 show that more mFRR is activated both upward and downwards than in Reference to counter the effect of activations based on a less-accurate imbalance forecast.

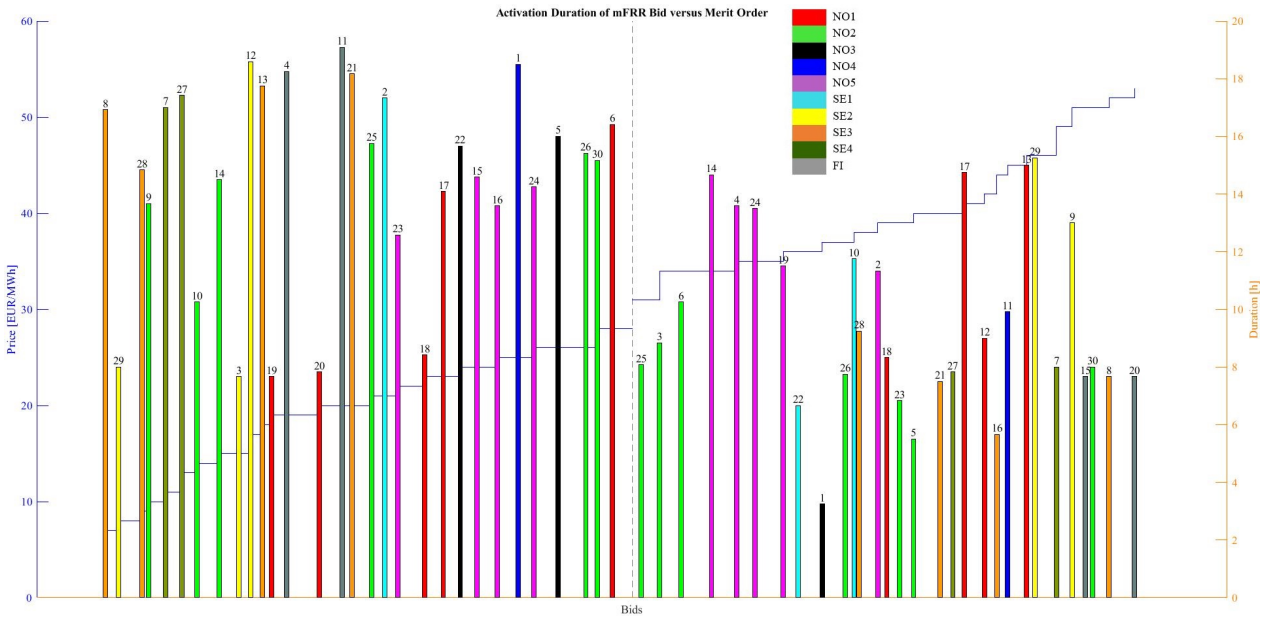

Figure 4.11: Total activated energy from each mFRR bid and the bids location in the merit order for Bad Forecast scenario.

4.3.5 Results from High Flexibility Scenario

When comparing the frequency in the High Flexibility scenario with the Reference, it is observed a reduced amount of time outside the frequency deviation band of $\pm$ 0.1 Hz. Especially during the imbalance shift at midnight, January 3., the frequency quality improvement is significant. A maximum frequency deviation of approximately +0.11 Hz is observed at peak imbalance 21:00.

A short minimum duration improves the ability of closely matching mFRR bids and imbalance at each bus and the model can re-optimise activations at shorter notice. As previously discussed in Section 4.2.5, the unconstrained change of bid output during delivery without having to go through another FAT is an important cause for the profitability of bids with short minimum duration. If the change in output was constrained by e.g. 30 % of the bid capacity, the cost savings in this scenario could be expected to decrease.

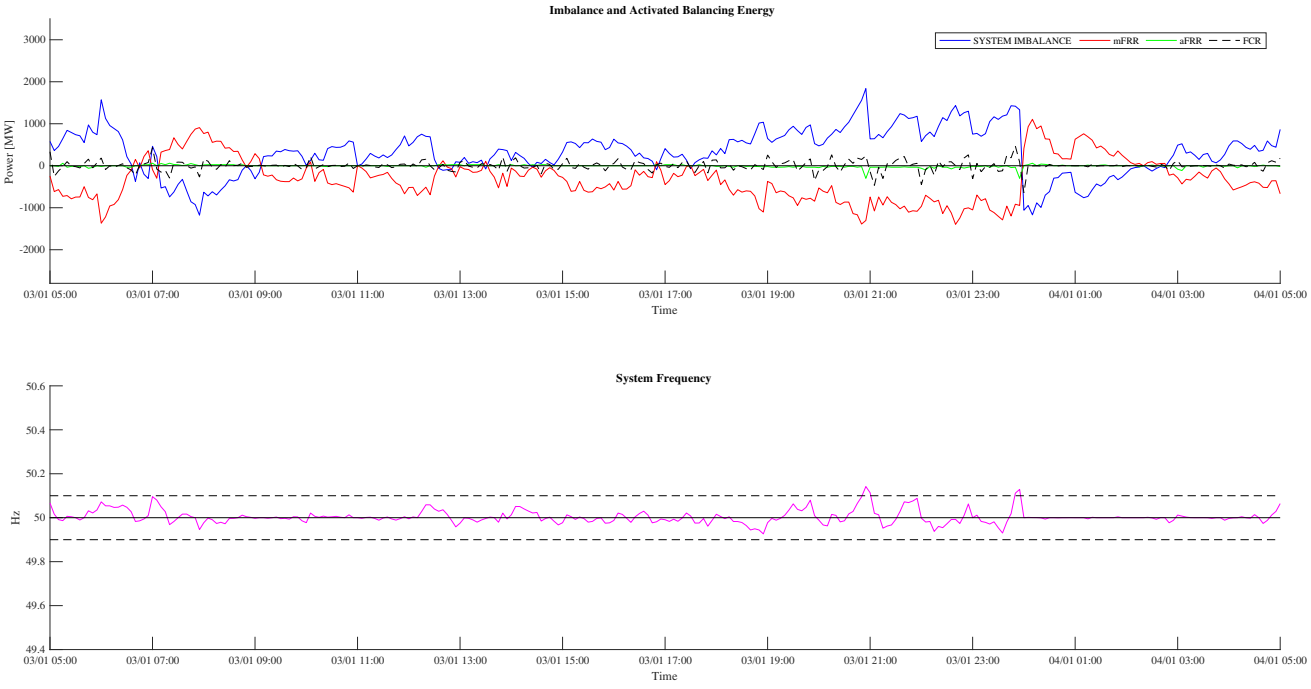

Figure 4.12: Activation schedules and system frequency in High Flexibility scenario between January 3. 05:00 and January 4. 05:00.

The improved frequency quality is presented by reduced FCR volume of 1.88 GWh in Table 4.7. No load/generation shedding is activated. 1.61 GWh less energy is used to balance the system, with an increase in social welfare of 74 100 €, compared to the Reference. It is observed that the amount of balancing energy delivered from mFRR increases from the Reference by 0.21 GWh. This is a consequence of the high FCR price compared to mFRR bid price, which means that the model rather activates an expensive but flexible mFRR bid for a short duration instead of accepting a frequency deviation when that is possible.

	Energy [GWh]			Cost [1000 €]		
	FCR	aFRR	mFRR	FCR	aFRR	mFRR
Total by reserve	-1.88	-0.02	+0.21	-75.23	-1.20	+2.33
Sum	-1.61			-74.10		

Table 4.7: Changes in volume and cost results from Reference scenario in High Flexibility scenario.

Figure 4.13 depicts a particular increase in activation from downward mFRR in NO3 compared to the Reference scenario. Downward bid 1 is a P1 product, while downward bids 22 and 5 are P2 products. The differences between bids 1 and 5 is therefore price, volume, location and minimum duration. In the Reference scenario, a short minimum duration of the P1 bid 1 led to transfer of positive NO3 imbalances to NO4 to be balanced by bid 1, even though bid 5 is more economical. When the minimum duration of both bids are set to 5 minutes more of the positive imbalance in NO3 is balanced locally by downward 5. An example of the opposite effect can also be observed in upward bids 29 and 9. Bid 9 is a P2 product with 10 minute minimum duration, while bid 29 is a P3 product with 15 minute minimum duration. Both bids are located in the same bus in SE2, Grundfors. Comparing with the Reference scenario shows an increased activation from expensive bid 9 in High Flexibility scenario, a non-intuitive result from the above discussion. However, the increased flexibility of bid 9 enables it to replace more expensive aFRR and FCR activations.

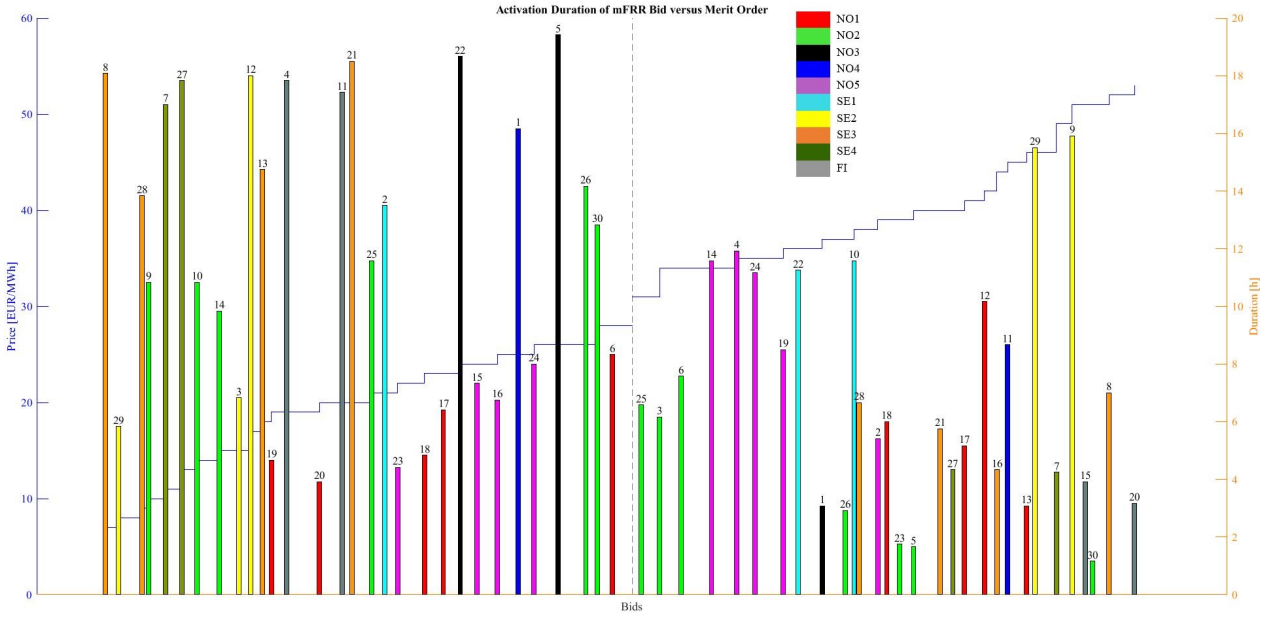

Figure 4.13: Total activated energy from each mFRR bid and the bids location in the merit order for High Flexibility scenario.

4.4 Comparison of Scenarios

Table 4.8 presents balancing cost in all scenarios in the left column and cost from load/generation shedding in the right column. The balancing cost column is the sum of FCR, aFRR and mFRR activation cost. Low Integration scenario has the highest balancing cost of 1 087 mill. €. Load/-generation shedding is only activated in the Bad Forecast scenario with a cost of 12 000 €. High Flexibility scenario has the lowest balancing cost of 776 000 €.

Scenario	Balancing Cost [1000 €]	Load/Generation Shedding Cost [1000 €]
Reference	850	0
Low Integration	1087	0
No P5	877	0
Bad Forecast	1040	12.50
High Flexibility	776	0

Table 4.8: Cost from activation and load/generation shedding in each scenario in [1000 €].

Table 4.9 presents the netted energy in each scenario and netted energy as share of total imbalance energy. Netted volume is calculated as the share of total imbalance volume that is not balanced by FCR, aFRR, mFRR or shedding, as netting occurs when imbalance at a bus is cancelled by an opposite imbalance at another bus. The netting power is presented in Figure 4.14 as the difference between imbalance power and sum of FCR, aFRR and mFRR (the example is from the Reference scenario). A negative imbalance netting observed around midnight means that activated balancing power exceeds imbalance power, caused by large amounts of counter-activations when ramping of upward regulation begins around midnight, c.f. Section 4.3.1.

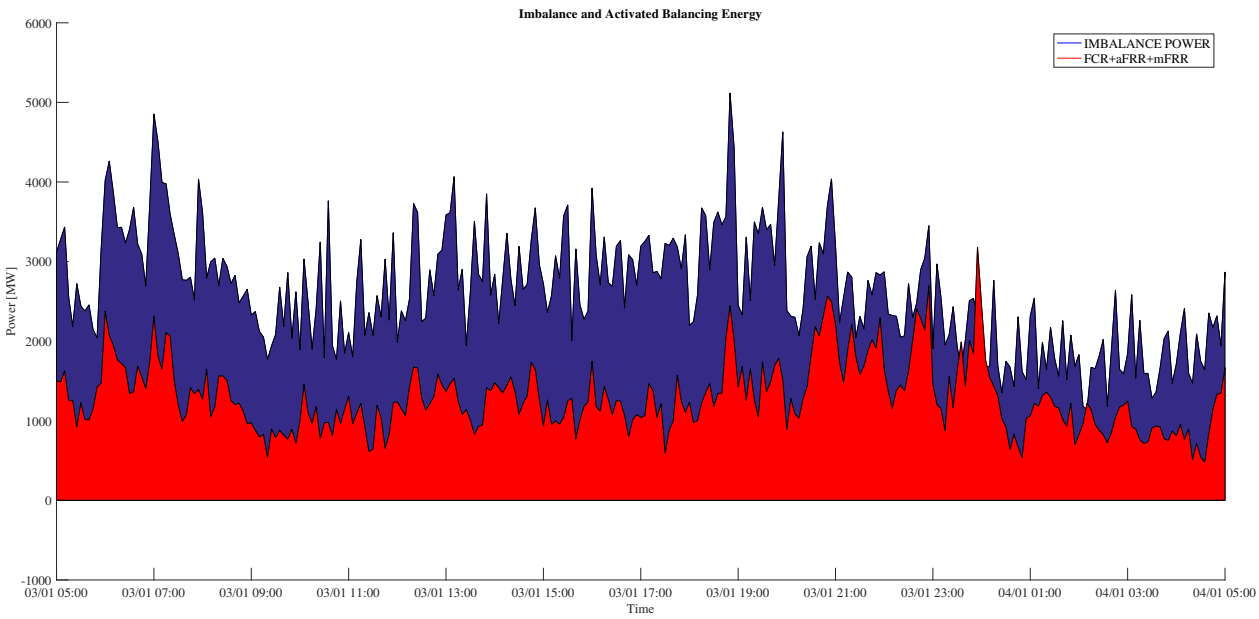

Figure 4.14: Imbalance netting as the difference between imbalance power and activated balancing power (example from Reference scenario).

The results in Table 4.9 show a netting of about half the total imbalance energy and a maximum share of 53.6 % netted volume in the High Flexibility scenario. The Low Integration and Bad Forecast scenarios have less imbalance netting of 43.2 % and 41.5 %, respectively, and these scenarios are also associated with the greatest balancing costs. This result demonstrates the correlation between imbalance netting and total balancing activation cost. As more imbalance is handled by cancelling of opposing imbalances, less balancing energy is activated. Imbalance netting is a root cause of increased balancing cost in the Low Integration scenario together with increased cost from activation of aFRR since local mFRR capacities are exhausted.

Scenario	Netted Imbalance Volume [GWh]	Share of Total Imbalance Volume
Reference	32.39	50.9 %
Low Integration	27.49	43.2 %
No P5	31.45	49.5 %
Bad Forecast	26.41	41.5 %
High Flexibility	34.10	53.6 %

Table 4.9: Netted imbalance volume in each scenario [GWh] and share of total imbalance volume.

Table 4.10 present the activation of each mFRR product as a share of the total activated mFRR energy. There is made no distinction in the activation direction. In the row for No P5 scenario, the share of P5 activation represents the activation of the bids that are P5 bids in the other scenarios, but are changed to P1 bids in the No P5 scenario. The result from the No P5 scenario show that bids that are changed from P5 to P1 products are not lot less activated even though the FAT is lengthened to 15 minutes. This is due to the fact that all the P5 bids that are converted to P1 bids

will still have a minimum duration period of 5 minutes. When comparing bids that are located in the same bus but with different minimum duration, it is observed that the bids with the shortest minimum duration are most activated, meaning that the converted P5 products are still preferable compared to bids with longer minimum duration. Note that the figures in Table 4.10 include energy delivered during ramping and this means that a considerate amount of the calculated energy is ramping energy, which is twice as much for a 15 minute FAT product compared to a 5 minute FAT product with the same delivery set-point.

Largest share of energy is delivered from P3 products in all scenarios except in Bad Forecast scenario, in which flexibility of P5 product is necessary for re-optimisation. Large share of P3 activation may be explained by the fact that most upward and downward P3 bids are located in large imbalance areas SE3, SE4 and FI and must be activated to prevent activation by more expensive FCR and aFRR. When exchange of balancing energy is constrained by NTCs it may also be assumed that P3 activations are done to prevent violation of NTCs to neighbouring areas. Sensitivity analysis with increased transmission capacity in Section 4.5.2 demonstrate this effect.

Scenario	P1	P2	P3	P5	Sum mFRR [GWh]
Reference	11.0%	18.9%	37.0%	33.1%	20.37
Low Integration	11.0%	18.8%	37.5%	32.7%	19.11
No P5	12.0%	19.9%	34.7%	(33.4%)	21.10
Bad Forecast	12.8%	20.6%	32.8%	33.8%	24.39
High Flexibility	10.3%	22.7%	35.8%	31.3%	20.58

Table 4.10: Activated mFRR volume by product as share of total mFRR activation.

Table 4.11 presents the activation duration in hours for each mFRR Standard Product type for downward regulation. Total activation duration is the sum of durations of all bids of a given product, which explains durations longer than 24 hours. The P3 product is most active in all scenarios due to discussion in previous paragraph. The fast-ramping P5 product is the second most active product in all scenarios. The value of bid flexibility is demonstrated by the difference between P1 and P2 activation duration. Since the P1 product has 5 minutes shorter minimum duration than the P2 product, it is favoured in all scenarios. In the High Flexibility scenario in which all bids have equal minimum duration period of 5 minutes, the P2 products are more activated because of the the price bias. A bottleneck between NO1 and NO3 was presented as a possible explanation for low P2 activation in Reference scenario. This is particularly true for downward bid 6 located in Tretten in NO1, which is connected to Trondheim in NO3. It is true that most of the increased activation from P2 products in the High Flexibility scenario come from bids in other areas than NO1, but it is also observed an increased activation of P2 products in NO1 in that scenario. The increased activation of P2 products located in NO1 in the High Flexibility scenario therefore refutes the argument of NO1-NO3 bottleneck being the sole cause of low P2 product activations, although it is part of the explanation.

Scenario	P1	P2	P3	P5
Reference	68.25	60.42	139.75	90.83
Low Integration	62.58	66.25	140.67	73.17
No P5	69.33	65.42	139.0	(103.5)
Bad Forecast	84.08	81.50	140.25	129.50
High Flexibility	62.50	78.83	143.92	88.08

Table 4.11: Activation duration [h] of each mFRR product type for downward regulation.

4.5 Sensitivity Analysis

Changes in balancing behaviour when key parameters FCR price and transmission capacities across borders are presented and discussed in the following sections.

4.5.1 Increased FCR Price

In this section, all scenarios have been re-run with a FCR price C^{fcr}= 60 €/MWh to study the effect of FCR price on model behaviour. In such a case, the model will use all available measures to reduce frequency deviations over time since FCR price is higher than aFRR and mFRR price. Table 4.12 shows that FCR is replaced by aFRR and mFRR when the FCR price is increased in all scenarios except in Low Integration scenario, in which the mFRR activation volume decreases with 0.03 GWh. The FCR and aFRR activation volume was large also in the case with C^{fcr}=40 €/MWH in the Low Integration scenario because mFRR could not be exchanged to handle large structural imbalances in Southern Sweden, and any further increase in FCR price may therefore be assumed to not change total mFRR activation volume. Reference scenario has the largest increase in mFRR volume of 1.20 GWh. The change in aFRR and mFRR activation volume, Δ aFRR and Δ mFRR, indicates whether frequency quality has been sacrificed for social welfare in the case where the FCR price, C^{fcr}=40 €/MWh, is lower than aFRR and mFRR price. An increase in aFRR and mFRR activation volume for an increased FCR price implies that frequency quality could be improved on the expenditure of social welfare. This is the case in Reference scenario where 1.20 GWh more mFRR energy is activated for an FCR price increase of 20 €/MWh. No P5 has the largest increase in aFRR volume. Removing P5 products with short FAT increase the demand for fast-ramping and flexible balancing energy. Thus, when setting a higher price for FCR more of this demand will be supplied by aFRR.

Scenario	FCR [GWh]	aFRR [GWh]	mFRR [GWh]	Δ FCR [GWh]	Δ aFRR [GWh]	Δ mFRR [GWh]
Reference	9.70	1.02	21.52	-0.74	+0.60	+1.20
Low Int.	14.90	1.85	19.08	-0.90	+0.62	-0.03
No P5	9.77	1.12	21.43	-0.85	+0.70	+0.33
Bad F.	11.25	1.24	24.50	-0.92	+0.62	+0.11
High Flex.	8.01	0.97	21.40	-0.51	+0.56	+0.82

Table 4.12: Activation volume by reserve [GWh] for $C^{fcr} = 60$ €/MWh and change in activation volume when increasing FCR price from $C^{fcr} = 40$ €/MWh to $C^{fcr} = 60$ €/MWh.

4.5.2 Increased Transmission Capacity Between Market Areas

The shadow cost of transmission capacity between market areas has been investigated by increasing the transmission capacity of all lines to long term thermal capacity. These capacities are specified in data set in [47] but were modified to match NTCs in the purpose of this project. All scenarios have been re-run with previous balancing market data, imbalance and Standard Product definitions, but with long-term thermal capacity on each line. The flow resulting from day-ahead has been set

to zero, meaning that the total thermal capacity is available for imbalance netting and exchange of balancing energy.

Figure 4.15 depicts the activation duration of each mFRR bid when the transmission capacity of all lines that cross area boundaries are set to thermal value. This result show a significantly improved ability to follow the mFRR merit order. Share of netted imbalance increases to 76 % and the balancing cost is reduced to 233 813 €, representing a balancing cost reduction of 72.5 % from a situation where margin between NTCs and day-ahead flow determines exchange capacities. This implies that a significant amount of balancing activations in the previous scenarios are done to prevent violation of NTC transmission constraints.

In Figure 4.15 the value of bid flexibility is observed, as flexible downward bid 1 in NO4 balances NO3 imbalances instead of less flexible bid 5 in NO3. Similar effects are observed for cheap upward mFRR in NO2. Bid 25 is a P3 product, while bids 3 and 6 are P5 products. Figure 4.16 shows that nominal frequency is to a large extent maintained by mFRR activations alone since more imbalance power can be exchanged and cancelled with opposing imbalances in other areas.

These results are unrealistic because a significant amount of transmission capacity is used to facilitate day-ahead power trade, in addition to margins imposed by the N-1 criterion. Hence, full thermal capacity of lines is not available in normal operation. Reserving transmission capacity for balancing purposes was discussed in Section 2.4 and may lead to reduced overall outcome of the day-ahead market, although increase social welfare in balancing. A simultaneous optimisation of day-ahead clearing and transmission capacity reservation would be necessary to find the optimal cross-border capacity in both markets.

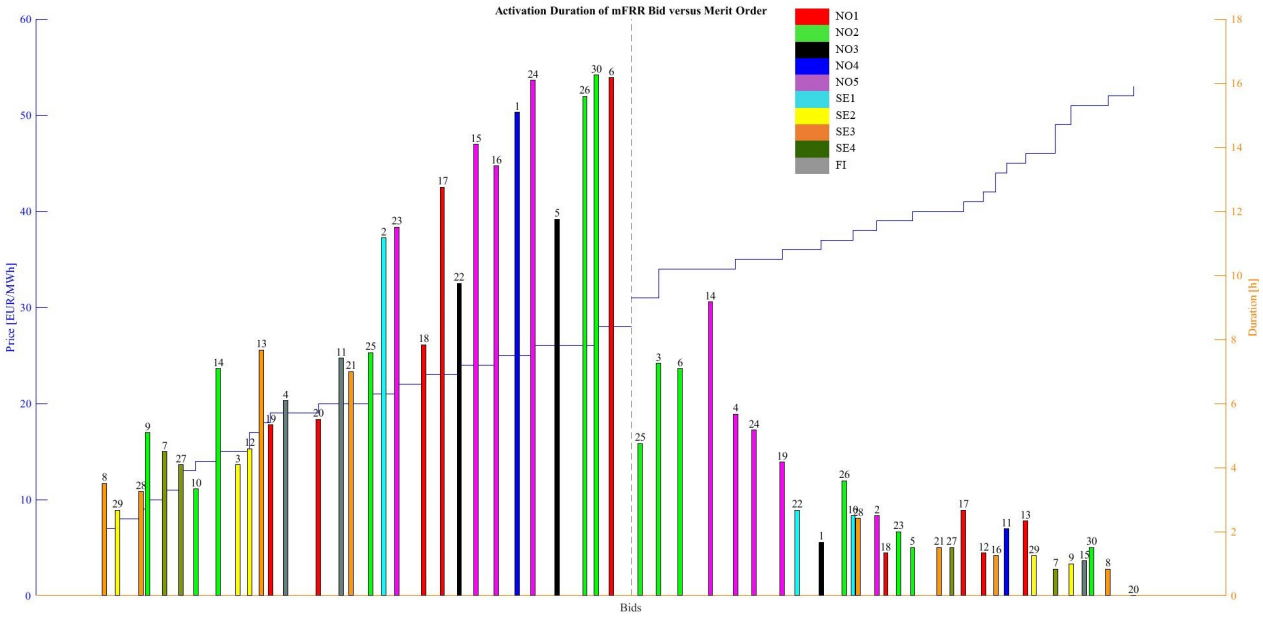

Figure 4.15: Activation duration of each bid versus merit order for thermal cross-border transmission capacity in Reference scenario.

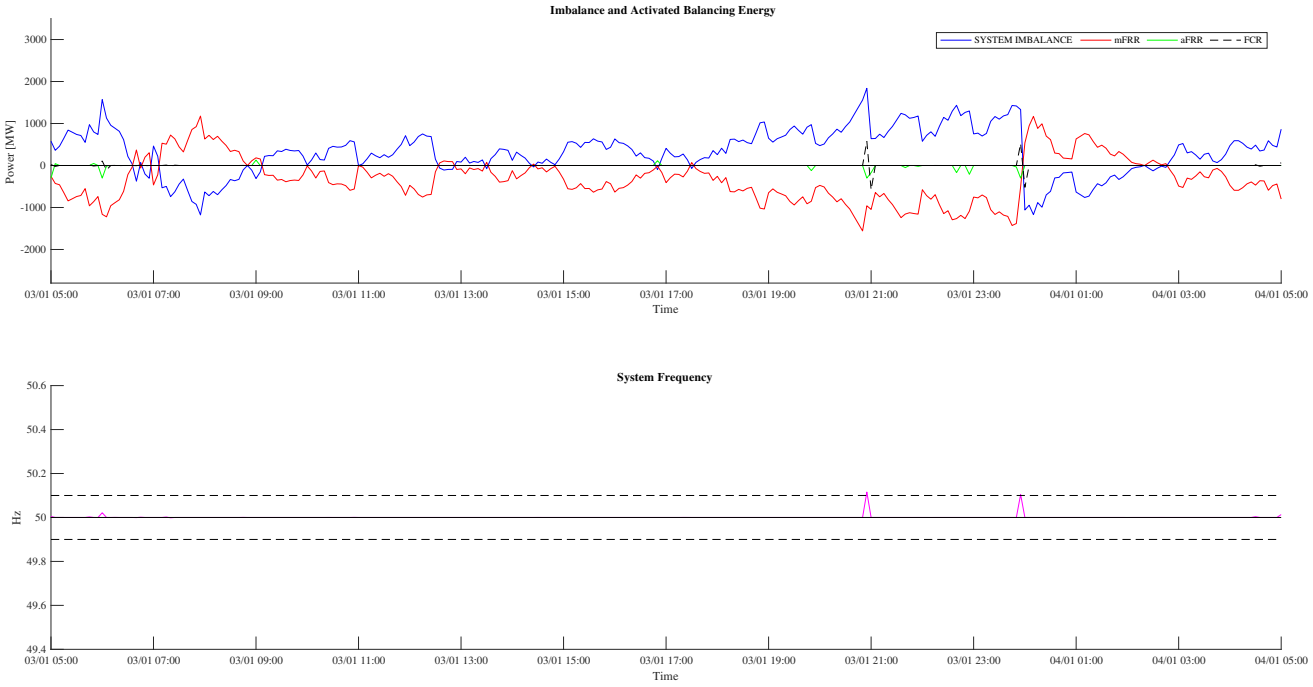

Figure 4.16: System imbalance, balancing activations and resulting frequency when cross-border capacities are set to thermal values.

4.6 Improvements and Further Work

Imbalance Forecast Generation Algorithm

The imbalance forecast input to the optimisation model is based on a fictional forecasting error scaling factor k. That means that knowledge of future imbalances is a prerequisite in the current formulation. Actual imbalances follows somewhat deterministic patterns, particularly the structural imbalances, and a imbalance forecast could be developed based on historical imbalance data. Bad Forecast scenario demonstrated the effect of low accuracy in the forecast. Artificial intelligence and machine learning could be used to recognize imbalance patterns, resulting in possibly more accurate forecasts. Although that is out of the scope of this project, it is an interesting possibility.

Constrain Number of TSO Instructions

The change of a mFRR bid output would in real-life operation imply an instruction from TSO to BSP. Hence, it is not reasonable to assume that there is no limit to how many times a bid output can be changed, and is an important cause for reduced balancing cost in High Flexibility scenario. In this scenario there was on average sent 15.6 and 6.2 instructions for downward and upward regulation respectively every 5 minutes. In the Reference scenario the average amount of instructions every 5 minutes were 14.8 upwards and 5 downwards, representing a considerable amount of

work for an operator. A soft constraint on the amount of instructions could have been formulated to give a cost optimal schedule with the fewest operations to adapt the model for real-life operation. Including such a constraint could be assumed to reduce the profitability of having flexible mFRR products since the increased social welfare in the High Flexibility scenario comes from the possibility of re-optimise activation schedules in every time-step.

Setting Cross-Border Transmission Capacities

The cross-border capacity has been set by distributing the NTC evenly on all lines crossing the border, implying that one line alone can not transfer total NTC power if there are more lines crossing the border. An improved formulation would constrain the net flow in both directions based on the sum of flows on all lines, leading to a single line possibly transferring the entire NTC. Such a formulation could give different results since the possible solutions for the model increase.

Multiple Formats of Energy Offers

In TERRE project [26, page 15] multiple formats of exchangeable energy offers are described. Temporal links have been formulated in this project but links in volume and bid offers could also be used in e.g. multi-part or exclusive bids.

Exchange of mFRR with Continental System

A possibility of mFRR energy exchange with the Continent over HVDC cables could be included by defining bids located on the buses on the non-Nordic side of HVDC cables. That would increase total mFRR capacity available, even though transfer of mFRR energy would adhere to the HVDC ramping constraints, but this was out of the scope of a Nordic AOF development.

Chapter 5

Conclusion

In this thesis there is developed a deterministic optimisation model for activation of balancing energy in the Nordic synchronous system consisting of Norway, Sweden, Finland and Eastern Denmark. The model is a prototype for an Activation Optimisation Function that will compare Standardized manual balancing products with different location, capacity and price.

Fictional balancing market activation data resembling a Nordic balancing market is developed. Historical imbalance data from Nordic bidding areas have been input together with an aggregate network representation of the Nordic transmission grid. Available transmission capacities for exchange of balancing energy between market areas are determined as margin between Nord Pool NTCs and power flows resulting from Nord Pool day-ahead clearing. Five scenarios were defined to analyze effects of Standard Product specifications and network effects on modelling behaviour and cost of energy balancing.

A simplified representation of primary and secondary control has been formulated. Pricing of FCR indirectly sets penalty cost of frequency deviations and has been determined by the minimum price that gives a system frequency complying with Nordic frequency quality requirements.

Although balancing activations result from complex considerations of a large set of product- and network-specific constraints, a favor of bids with short minimum duration and Full Activation Time (FAT), i.e. P1 and P5 products, is observed. P3 products have longest activation duration because P3 products are located in areas with largest imbalances and are activated to prevent violation of NTCs with neighbouring areas and to maintain bus energy balance without use of more expensive resources. Balancing cost reduction in scenarios with increased mFRR product flexibility is dependent on FCR price level since flexible mFRR replace FCR.

Network constraints that reduce opportunities of imbalance netting by cancelling opposing imbalances lead to increased balancing cost. It is therefore observed highest balancing cost and low social welfare in Low Integration scenario in which no exchange of balancing energy between the Nordic countries occur. The case with increased transmission capacity between Nordic countries in the sensitivity analysis presents a significant increase in social welfare and cost-efficient usage of mFRR. Reservation of transmission capacity for balancing purposes on day-ahead will therefore lead to netting possibilities of imbalance energy in the operational phase, but transmission capacity reservation effect on day-ahead market outcome is not analyzed.

Unconstrained change in energy delivery from mFRR bids between delivery periods is a root cause of cost reduction in the scenario in which minimum duration of delivery period for mFRR is

shortened. More energy would be delivered from bids with longer minimum duration as the change of bid power level would imply deactivation and initialization of new preparation period.

Results demonstrate that fewer time-couplings of mFRR bids simplifies balancing by mFRR, and increase resource efficiency as less total balancing energy is activated in scenario with shortened minimum duration period. Flexible Standard Products with short FAT and minimum duration are encouraged and should be included for resource efficient balancing.

EU ambition of increased resource efficiency through integrated balancing markets is supported by the study of balancing energy activation with network constraints in this thesis. Increased social welfare through reduced balancing cost and resource usage is demonstrated when Nordic countries cooperate and exchange balancing energy. Optimal activation schedule deviates from price order when transmission security margins are taken into account, and TSO ability of activating independently from price order by skipping bids should be continued. Results demonstrate the profitability of product flexibility, which encourages participation of hydro power on balancing markets. Although work remains, the presented AOF prototype for the Nordic system shows promise as valuable decision support for TSO.

Appendix A

XPRESS Code

```
model "copy2.mos"
uses "mmxprs"; !gain access to the Xpress-Optimizer solver
uses "mmive";
uses "mmsystem";

!Enable Optimizer logs
setparam("XPRS_VERBOSE",true)
setparam("XPRS_MAXTIME",120)
setparam("XPRS_MIPRELSTOP",0.05)

!                                        Declare sets
declarations
hvdcLines:set of integer
nonHvdcLines: set of integer

nonhvdc_buses:set of integer
hvdc_buses:set of integer
end-declarations


!                                        Pre-declarations
declarations

Time: integer
Lines:integer
Buses:integer
refBus:integer
fupper:real
flower:real
p1:integer
p2:integer
Pspot:real
Ft:integer
nBidsUp:integer
nBidsDn:integer
MAXSTEP: integer
```

```
STEP: integer

nAFRRUp: integer
nAFRRDn: integer

Areas: integer

end-declarations

!                                          Pre-initializations

initializations from "matlab.mws:"
Time
refBus
Lines
Buses
fupper
flower
p1
p2
Pspot
Ft
nBidsUp
nBidsDn

MAXSTEP
STEP

nAFRRUp
nAFRRDn

Areas

end-initializations

!                                            Declarations
declarations


!                                             Ranges
BidUp=1..nBidsUp
BidDn=1..nBidsDn
Tstart=1
nTime= 1..Time
pastTime=-4..0
nLines=1..Lines
nBus=1..Buses
nAreas=1..Areas

AFRRUpR=1..nAFRRUp
AFRRDnR=1..nAFRRDn
```

```
!                                        Parameters

AFRRPRICEUP: array(AFRRUpR) of real
AFRRPRICEDN: array(AFRRDnR) of real

AFRRCAPUP: array(AFRRUpR) of real
AFRRCAPDN: array(AFRRDnR) of real

AFRRUpToBus: array(AFRRUpR, nBus) of integer
AFRRDnToBus: array(AFRRDnR, nBus) of integer

UpBidsToArea: array(nAreas,BidUp) of integer
DnBidsToArea: array(nAreas,BidDn)of integer

hasBeenActUp: array(BidUp) of  integer
hasBeenActDn: array(BidDn) of integer

LbUp: array(BidUp) of integer
LbDn: array(BidDn) of integer

L: array(BidUp,1..2) of integer
Ldn: array(BidDn, 1..2) of integer

isDivisibleUp:array(BidUp) of integer
isDivisibleDn: array(BidDn) of integer

baseflow:array(nLines,nTime) of real

linecapNeg: array(nLines,nTime) of real
linecapPos: array(nLines,nTime) of real

lineMatrix: array(nBus,nLines) of real
UpBidsToBus: array(BidUp,nBus) of real
DnBidsToBus: array(BidDn,nBus) of real
susceptance: array(nLines) of real

isHVDC:array(nLines) of integer

MAXHVDCRAMPUP: real
MAXHVDCRAMPDN: real

MAXUPRAMP: array(BidUp) of real
MAXDNRAMP: array(BidDn) of real

BIDPRICEUP: array (BidUp) of real
BIDPRICEDN: array (BidDn) of real
BIDCAPUP: array (BidUp) of real
BIDCAPDN: array(BidDn) of real
BIDMIN: integer
DPMINUP: array(BidUp) of integer
DPMINDN: array(BidDn) of integer
DPMAXUP: array(BidUp) of integer
```

```
DPMAXDN: array(BidDn) of integer

IMBALANCE: array(nBus,nTime) of real

S1UP: array(BidUp) of range
S2UP: array(BidUp) of range
S1DN: array(BidDn) of range
S2DN: array(BidDn) of range
SUMRANGE1: range
SUMRANGE2: range
AFRRPRICE: integer

FCRprice:real

FATUP: array(BidUp) of real
FATDN: array(BidDn) of real

!                                        Constraints

TotalCost: linctr
EnBal: array(nTime) of linctr
BidCapUp: array(BidUp,nTime) of linctr
BidCapUpMin: array(BidUp,nTime) of linctr
BidCapDn:array(BidDn,nTime) of linctr
BidCapDnMin: array(BidDn,nTime) of linctr
TimeMin1Up: array(BidUp,nTime) of linctr
TimeMin1Dn: array(BidDn,nTime) of linctr
TimeMin2Up: array(BidUp,nTime) of linctr
TimeMin2Dn: array(BidDn,nTime) of linctr
TimeMaxUp:array (BidUp) of linctr
TimeMaxDn:array (BidDn) of linctr
rampCtr: array(BidUp,nTime) of linctr
Transmission1: array(nLines,nTime) of linctr
Transmission2: array(nLines,nTime) of linctr
Transmission3: array(nLines,nTime) of linctr



!                                        Decision vars.


AFRRUp: array(AFRRUpR,nTime) of mpvar
AFRRDn: array(AFRRDnR, nTime) of mpvar

AFRRIsRunningUp: array(AFRRUpR,nTime) of mpvar
AFRRIsRunningDn: array(AFRRDnR, nTime) of mpvar

areaPriceUp: array(nAreas, nTime) of mpvar
areaPriceDn:array(nAreas, nTime) of mpvar


mFRRUp: array (BidUp,-6..Time) of mpvar
```

```
mFRRDn: array (BidDn,-6..Time) of mpvar
lineFlow: array(nLines,0..Time) of mpvar
isRunningUp: array (BidUp,-6..Time) of mpvar
isRunningDn: array (BidDn,-6..Time) of mpvar
bidActUp:array(BidUp,-6..Time) of mpvar
bidActDn:array(BidDn,-6..Time) of mpvar
angle: array(nBus,nTime) of mpvar

deviation: array(nBus,nTime) of mpvar
delivered: array(nBus, nTime) of mpvar

frequency:array(nBus, nTime) of mpvar
devUp1: array(nBus,nTime) of mpvar
devUp2:   array(nBus,nTime) of mpvar
devDn1:   array(nBus,nTime) of mpvar
devDn2:   array(nBus,nTime) of mpvar

rampPowerUp:array(BidUp, -6..Time) of mpvar
rampPowerDn:array(BidDn, -6..Time) of mpvar

isRampingDn:array(BidDn, -6..Time) of mpvar

setPointUp:array(BidUp, -6..Time) of mpvar
setPointDn: array(BidDn, -6..Time) of mpvar

sysfrequency: array(nTime) of mpvar

FCRUp: array(nBus, nTime) of mpvar
FCRDn: array(nBus, nTime) of mpvar



!                                        Post-processing variables
solUp: array(BidUp,nTime) of real
objValue: real
SolDn:array(BidDn,nTime) of real
LineFlow:array(nLines,nTime) of real
Angle: array(nBus, nTime) of real
NACT: real
TOTUP: real
TOTDN: real
IMBUP: real
IMBDN: real
Freq: array(nBus,nTime) of real
soldevDn1:array(nBus,nTime) of real
soldevDn2:array(nBus,nTime) of real
soldevUp1:array(nBus,nTime) of real
soldevUp2:array(nBus,nTime) of real

solAFRRUP: array(AFRRUpR,nTime) of real
solAFRRDN: array(AFRRDnR, nTime) of real
solIsRampingDn: array(BidDn, nTime) of real
```

```
solRampPowerUp:array(BidUp,nTime) of real
solRampPowerDn: array(BidDn,nTime) of real

solSetPointUp:array(BidUp,nTime) of real
solSetPointDn:array(BidDn,nTime) of real
solsysfrequency: array(nTime) of real

solFCRUp: array(nBus, nTime) of real
solFCRDn:array(nBus,nTime) of real

soldeviation: array(nBus,nTime) of real

mipObjVal: real
bestBound: real
gap: real

solfatup: array(BidUp) of real



!History parameters

postMFRRUp: array(BidUp, 1..MAXSTEP+15) of real
postIsRunningUp: array(BidUp, 1..MAXSTEP+15) of integer
postBidActUp: array(BidUp, 1..MAXSTEP+15) of integer
postMFRRDn: array(BidDn, 1..MAXSTEP+15) of real
postIsRunningDn: array(BidDn, 1..MAXSTEP+15) of integer
postBidActDn: array(BidDn, 1..MAXSTEP+15) of integer

postLineFlow:array(nLines,1..MAXSTEP+15) of real
postBaseFlow:array(nLines, 1..MAXSTEP+15) of real


postRampPowerUp:array(BidUp, 1..MAXSTEP+15) of real
postRampPowerDn: array(BidDn, 1..MAXSTEP+15) of real

postSetPointUp: array(BidUp, 1..MAXSTEP+15) of real
postSetPointDn: array(BidDn, 1..MAXSTEP+15) of real

postSysfrequency: array(1..MAXSTEP+15) of real

end-declarations

                                        !Initialize parameters from Matlab
initializations from "matlab.mws:"
                                        !Network data
lineMatrix
baseflow
linecapPos
linecapNeg
UpBidsToBus
```

```
DnBidsToBus
IMBALANCE
susceptance

isHVDC
MAXHVDCRAMPUP
MAXHVDCRAMPDN
                                        !Regulating market data
BIDPRICEUP
BIDPRICEDN
BIDCAPUP
BIDCAPDN
DPMINUP
DPMINDN
DPMAXUP
DPMAXDN
MAXUPRAMP
MAXDNRAMP
BIDMIN

isDivisibleUp
isDivisibleDn

FATUP
FATDN
                                        !AFRR
AFRRPRICEUP
AFRRPRICEDN
AFRRCAPUP
AFRRCAPDN
AFRRUpToBus
AFRRDnToBus
UpBidsToArea
DnBidsToArea
!!

                                        !History
postMFRRUp
postIsRunningUp
postBidActUp
postMFRRDn
postIsRunningDn
postBidActDn
postRampPowerUp
postRampPowerDn
postSetPointUp
postSetPointDn
postSysfrequency
postLineFlow

FCRprice
```

```
hvdcLines
nonHvdcLines
hvdc_buses
nonhvdc_buses


end-initializations

                                        !Dec. variables specifications

forall(i in nLines, t in nTime)do
lineFlow(i,t) is_free
end-do

forall(n in nBus, t in nTime)do
angle(n,t) is_free
deviation(n,t) is_free
end-do

forall(b in BidUp, t in -6..Time)do
isRunningUp(b,t) is_binary
bidActUp(b,t) is_binary
end-do

forall(b in BidDn, t in -6..Time) do
isRunningDn(b,t) is_binary
bidActDn(b,t) is_binary
end-do

forall(a in AFRRUpR, t in nTime)
AFRRIsRunningUp(a,t) is_binary


forall(a in AFRRDnR, t in nTime)
AFRRIsRunningDn(a,t) is_binary

                                              ! Objective function

TotalCost :=

(5/60)*( sum (t in nTime, b in BidUp)(mFRRUp(b,t)*BIDPRICEUP(b))+
sum(t in nTime, b in BidDn)(mFRRDn(b,t)*(Pspot-BIDPRICEDN(b))) )+
sum(t in nTime, a in AFRRUpR)(AFRRUp(a,t)*AFRRPRICEUP(a)) +
sum(t in nTime, a in AFRRDnR)(AFRRDn(a,t)*(AFRRPRICEDN(a))) +
sum(t in nTime, b in nBus)(FCRprice*FCRUp(b,t)+FCRprice*FCRDn(b,t))+
sum(t in nTime)(p1*sum(b in nBus)devUp1(b,t)+p2*sum(b in nBus)devUp2(b,t)+
                p1*sum(b in nBus)devDn1(b,t)+p2*sum(b in nBus)devDn2(b,t))


                                              ! Frequency deviations and penalty costs
```

```
forall(t in nTime|t>1)
sysfrequency(t)=sysfrequency(t-1)-(1/7000)*sum(b in nBus)(FCRUp(b,t)-FCRDn(b,t))

sysfrequency(1)=postSysfrequency(1)-(1/7000)*sum(b in nBus)(FCRUp(b,1)-FCRDn(b,1))

forall(t in nTime)do
sum(b in nBus)FCRUp(b,t)>=5000*(50-sysfrequency(t))
sum(b in nBus)FCRDn(b,t)>=5000*(sysfrequency(t)-50)
end-do

!Cost of nodal energy balance deviation (=cost of load shedding/regulation)
forall(b in nBus,t in nTime) do
devUp1(b,t)<=1
devUp1(b,t)+devUp2(b,t)>=deviation(b,t)
devDn1(b,t)<=1
devDn1(b,t)+devDn2(b,t)>=-deviation(b,t)
end-do

                                        !Network constraints and nodal balance

forall(l in nLines) do
lineFlow(l,0)=postLineFlow(l,1);
end-do

!Line flow at AC-lines
forall(i in nonHvdcLines, t in nTime) do
lineFlow(i,t)=-(sum(n in nBus)(lineMatrix(n,i)*angle(n,t)))*susceptance(i)
!Line capacities
lineFlow(i,t)+baseflow(i,t) <=linecapPos(i,t)
lineFlow(i,t)+baseflow(i,t) >=- linecapNeg(i,t)
end-do

!Capacity and ramping at HVDC-lines
forall( l in hvdcLines, t in nTime) do
lineFlow(l,t)+baseflow(l,t)<=linecapPos(l,t)
lineFlow(l,t)+baseflow(l,t)>=-linecapNeg(l,t)

lineFlow(l,t)-lineFlow(l,t-1)<=MAXHVDCRAMPUP
lineFlow(l,t)-lineFlow(l,t-1)>=-MAXHVDCRAMPDN
end-do
                                        !Nodal energy balance

                                        !Non-hvdc-buses

forall(b in nonhvdc_buses, t in nTime) do
sum(i in nLines)(lineMatrix(b,i)*lineFlow(i,t)) +
sum(n in BidUp)(UpBidsToBus(n,b)*(mFRRUp(n,t)+rampPowerUp(n,t)))-
sum(n in BidDn)(DnBidsToBus(n,b)*(mFRRDn(n,t)+rampPowerDn(n,t)))+
sum(n in AFRRUpR)(AFRRUpToBus(n,b)*AFRRUp(n,t))-
sum(n in AFRRDnR)(AFRRDnToBus(n,b)*AFRRDn(n,t))+
IMBALANCE(b,t)+FCRUp(b,t)-FCRDn(b,t)=deviation(b,t)
end-do
```

```
                                        !HVDC-buses

forall(b in hvdc_buses, t in nTime) do
sum(i in nLines)(lineMatrix(b,i)*lineFlow(i,t)) +
sum(n in BidUp)(UpBidsToBus(n,b)*(mFRRUp(n,t)+rampPowerUp(n,t)))-
sum(n in BidDn)(DnBidsToBus(n,b)*(mFRRDn(n,t)+rampPowerDn(n,t)))+IMBALANCE(b,t)=0
end-do

                                        !Angle at ref.bus

forall(t in nTime)do
angle(refBus,t)=0
end-do

                                        !FCR-capacity

forall(t in nTime)do
sum(b in nBus) (FCRUp(b,t))<=2500
sum(b in nBus) (FCRDn(b,t))<=2500
end-do

                                        !FCR at buses not in nordic sync.
forall(t in nTime)
sum(b in hvdc_buses)(FCRUp(b,t)+FCRDn(b,t))=0

                                        ! Product-specific constraints

                                        !Initialize from history-files
forall(b in BidUp,t in -6..0) do
       mFRRUp(b,t)=postMFRRUp(b,1-t)
       isRunningUp(b,t)=postIsRunningUp(b,1-t)
       bidActUp(b,t)=postBidActUp(b,1-t)
       rampPowerUp(b,t)=postRampPowerUp(b,1-t)
       setPointUp(b,t)=postSetPointUp(b,1-t)
end-do
forall(b in BidDn, t in -6..0)do
        mFRRDn(b,t)=postMFRRDn(b,1-t)
        isRunningDn(b,t)=postIsRunningDn(b,1-t)
         bidActDn(b,t)=postBidActDn(b,1-t)
        rampPowerDn(b,t)=postRampPowerDn(b,1-t)
         setPointDn(b,t)=postSetPointDn(b,1-t)
end-do

if (STEP=1) then
        forall(b in BidUp)
         if (FATUP(b)=3) then
           rampPowerUp(b,1)=0
         end-if
        forall(b in BidDn)
         if(FATDN(b)=3) then
           rampPowerDn(b,1)=0
```

```
        end-if
end-if


                                        !Capacity constraints

forall (t in nTime, b in BidUp) do
    if (isDivisibleUp(b)=1) then
      BidCapUp(b,t):= mFRRUp(b,t) <= isRunningUp(b,t)*BIDCAPUP(b)
    else
        mFRRUp(b,t)=isRunningUp(b,t)*BIDCAPUP(b)
    end-if
mFRRUp(b,t) >= isRunningUp(b,t)*BIDMIN
end-do

forall(t in nTime, b in BidDn) do
    if (isDivisibleDn(b)=1) then
        BidCapDn(b,t):=mFRRDn(b,t)<=isRunningDn(b,t)*BIDCAPDN(b)
    else
        mFRRDn(b,t)=isRunningDn(b,t)*BIDCAPDN(b)
   end-if
mFRRDn(b,t) >= isRunningDn(b,t)*BIDMIN
end-do

forall(t in nTime, b in AFRRUpR) do
AFRRUp(b,t)<=AFRRCAPUP(b)*AFRRIsRunningUp(b,t)
AFRRUp(b,t)>=AFRRIsRunningUp(b,t)*5
end-do

forall(t in nTime, b in AFRRDnR) do
AFRRDn(b,t)<=AFRRCAPDN(b)*AFRRIsRunningDn(b,t)
AFRRDn(b,t)>=AFRRIsRunningDn(b,t)*5
end-do

                                        !Setting the bid initiation variable

forall (t in nTime,b in BidUp) do
bidActUp(b,t)>=isRunningUp(b,t)-isRunningUp(b,t-1)
end-do

forall(t in nTime, b in BidUp)do
(bidActUp(b,t)<=isRunningUp(b,t))
end-do

forall (t in nTime,b in BidDn) do
bidActDn(b,t)>=isRunningDn(b,t)-isRunningDn(b,t-1)
end-do

forall(t in nTime, b in BidDn)do
(bidActDn(b,t)<=isRunningDn(b,t))
end-do
```

```
                                        !Minimum delivery period

!Downward regulation
forall(b in BidDn) do
  if(DPMINDN(b)=1) then ! 5 min. products
      forall(t in -6..Time)
          mFRRDn(b,t)>=BIDCAPDN(b)*(setPointDn(b,t))
  else                  !Other products
      forall(t in -6+DPMINDN(b)-1..Time) do
           bidActDn(b,t)<=1-sum(q in t-DPMINDN(b)+1..t-1)bidActDn(b,q)
         forall(k in t-DPMINDN(b)+1..t)
           mFRRDn(b,t)>=BIDCAPDN(b)*setPointDn(b,k)
      end-do
  end-if
end-do

!Upward regulation
forall(b in BidUp) do
  if(DPMINUP(b)=1) then ! 5 min. products
      forall(t in -6..Time)
          mFRRUp(b,t)>=BIDCAPUP(b)*(setPointUp(b,t))
  else                  !Other products
      forall(t in -6+DPMINUP(b)-1..Time) do
           bidActUp(b,t)<=1-sum(q in t-DPMINUP(b)+1..t-1)bidActUp(b,q)
         forall(k in t-DPMINUP(b)+1..t)
           mFRRUp(b,t)>=BIDCAPUP(b)*setPointUp(b,k)
      end-do
  end-if
 end-do

!Maximum duration
forall(b in BidUp, t in -6+DPMAXUP(b)..Time)
    sum(q in t-DPMAXUP(b)..t)isRunningUp(b,q)<=DPMAXUP(b)

forall(b in BidDn, t in -6+DPMAXDN(b)..Time)
    sum(q in t-DPMAXDN(b)..t)isRunningDn(b,q)<= DPMAXDN(b)

                                        ! Ramping constraints

                                        ! 15 min. FAT

forall(b in BidDn,t in nTime) do
     if(FATDN(b)=3)then
         setPointDn(b,t)<=bidActDn(b,t)

         bidActDn(b,t)<=mFRRDn(b,t-2)+rampPowerDn(b,t-2)
     end-if
end-do

!Ensure activated volume matches ramping set-point
forall(b in BidDn) do
   if(FATDN(b)=3) then
```

```
        if (DPMINDN(b)=1) then !5 min products
            forall(t in -5..Time)
          mFRRDn(b,t)<=BIDCAPDN(b)*(setPointDn(b,t)+isRunningDn(b,t-1))

    else !Other products
          forall (t in -6+DPMINDN(b)-1..Time)
          mFRRDn(b,t)<=BIDCAPDN(b)*(sum(q in t-DPMINDN(b)+1..t)setPointDn(b,q))
    end-if
   end-if
end-do

forall(b in BidDn, t in -6..Time-2) do
    if(FATDN(b)=3) then
      rampPowerDn(b,t)>=(2/3)*BIDCAPDN(b)*(setPointDn(b,t+1)-isRunningDn(b,t))
      rampPowerDn(b,t)>=(1/3)*BIDCAPDN(b)*(setPointDn(b,t+2)-isRunningDn(b,t))
      rampPowerDn(b,t)<=BIDCAPDN(b)*((2/3)*setPointDn(b,t+1)+(1/3)*setPointDn(b,t+2))
    end-if
end-do

!0 ramp-power 15 min. before start of delivery period
forall(b in BidDn, t in -6..Time-3)
    if(FATDN(b)=3) then
      rampPowerDn(b,t)<=BIDCAPDN(b)*(1-bidActDn(b,t+3))
    end-if

!No ramping power during mFRR-delivery
forall(b in BidDn, t in -5..Time) do
   if (FATDN(b)=3) then
    rampPowerDn(b,t)<=BIDCAPDN(b)*(1-isRunningDn(b,t-1))
  end-if
end-do

forall(b in BidDn, t in -6..Time)do
   if(FATDN(b)=3)then
    rampPowerDn(b,t)<=BIDCAPDN(b)*(1-isRunningDn(b,t))
   end-if
end-do
                                        !5 min. FAT


 forall(b in BidDn, t in -6..Time)do
   if(FATDN(b)=1) then
      setPointDn(b,t)<=bidActDn(b,t)
   end-if
 end-do

 !Ensure activated volume matches ramping set-point
 forall(b in BidDn)do
  if(FATDN(b)=1) then
        if (DPMINDN(b)=1) then !5 min products
            forall(t in -5..Time)
          mFRRDn(b,t)<=BIDCAPDN(b)*(setPointDn(b,t)+isRunningDn(b,t-1))
```

```
    else !Other products
          forall (t in -6+DPMINDN(b)-1..Time)
          mFRRDn(b,t)<=BIDCAPDN(b)*(sum(q in t-DPMINDN(b)+1..t)setPointDn(b,q))
    end-if
 end-if
 end-do

 forall(b in BidDn, t in -6..Time-2) do
    if(FATDN(b)=1) then
      rampPowerDn(b,t)>=(1/2)*BIDCAPDN(b)*(setPointDn(b,t+1)-isRunningDn(b,t))
      rampPowerDn(b,t)<=BIDCAPDN(b)*((1/2)*setPointDn(b,t+1))
    end-if
end-do

!No ramping power during mFRR-delivery
forall(b in BidDn, t in -5..Time) do
   if (FATDN(b)=1) then
    rampPowerDn(b,t)<=BIDCAPDN(b)*(1-isRunningDn(b,t-1))
  end-if
end-do

forall(b in BidDn, t in -6..Time)do
   if(FATDN(b)=1)then
    rampPowerDn(b,t)<=BIDCAPDN(b)*(1-isRunningDn(b,t))
   end-if
end-do

                                        ! 15 min. FAT

forall(b in BidUp,t in nTime) do
   if (FATUP(b)=3)then
   setPointUp(b,t)<=bidActUp(b,t)

   bidActUp(b,t)<=mFRRUp(b,t-2)+rampPowerUp(b,t-2)
   end-if
end-do

!Ensure activated volume matches ramping set-point
forall(b in BidUp) do
  if (FATUP(b)=3) then
        if (DPMINUP(b)=1) then !5 min products
            forall(t in -5..Time)
          mFRRUp(b,t)<=BIDCAPUP(b)*(setPointUp(b,t)+isRunningUp(b,t-1))

    else !Other products
          forall (t in -6+DPMINUP(b)-1..Time)
          mFRRUp(b,t)<=BIDCAPUP(b)*(sum(q in t-DPMINUP(b)+1..t)setPointUp(b,q))
    end-if
  end-if
end-do
```

```
forall(b in BidUp, t in -6..Time-2) do
  if(FATUP(b)=3) then
   rampPowerUp(b,t)>=(2/3)*BIDCAPUP(b)*(setPointUp(b,t+1)-isRunningUp(b,t))
   rampPowerUp(b,t)>=(1/3)*BIDCAPUP(b)*(setPointUp(b,t+2)-isRunningUp(b,t))

   rampPowerUp(b,t)<=BIDCAPUP(b)*((2/3)*setPointUp(b,t+1)+(1/3)*setPointUp(b,t+2))
  end-if
end-do

!0 ramp-power 15 min. before start of delivery period
forall(b in BidUp, t in -6..Time-3)do
 if(FATUP(b)=3)then
   rampPowerUp(b,t)<=BIDCAPUP(b)*(1-bidActUp(b,t+3))
 end-if
end-do

!No ramping power during mFRR-delivery
forall(b in BidUp, t in -5..Time)do
 if(FATUP(b)=3)then
  rampPowerUp(b,t)<=BIDCAPUP(b)*(1-isRunningUp(b,t-1))
 end-if
end-do

forall(b in BidUp, t in -6..Time)do
 if(FATUP(b)=3)then
  rampPowerUp(b,t)<=BIDCAPUP(b)*(1-isRunningUp(b,t))
 end-if
end-do
                                        ! 5 min. FAT

 forall(b in BidUp, t in -6..Time)do
   if(FATUP(b)=1) then
      setPointUp(b,t)<=bidActUp(b,t)
   end-if
 end-do

 !Ensure activated volume matches ramping set-point
 forall(b in BidUp)do
  if(FATUP(b)=1) then
        if (DPMINUP(b)=1) then !5 min products
            forall(t in -5..Time)
          mFRRUp(b,t)<=BIDCAPUP(b)*(setPointUp(b,t)+isRunningUp(b,t-1))

    else !Other products
          forall (t in -6+DPMINUP(b)-1..Time)
          mFRRUp(b,t)<=BIDCAPUP(b)*(sum(q in t-DPMINUP(b)+1..t)setPointUp(b,q))
    end-if
 end-if
 end-do

 forall(b in BidUp, t in -6..Time-2) do
    if(FATUP(b)=1) then
```

```
      rampPowerUp(b,t)>=(1/2)*BIDCAPUP(b)*(setPointUp(b,t+1)-isRunningUp(b,t))
      rampPowerUp(b,t)<=BIDCAPUP(b)*((1/2)*setPointUp(b,t+1))
    end-if
end-do

!No ramping power during mFRR-delivery
forall(b in BidUp, t in -5..Time) do
   if (FATUP(b)=1) then
    rampPowerUp(b,t)<=BIDCAPUP(b)*(1-isRunningUp(b,t-1))
  end-if
end-do

forall(b in BidUp, t in -6..Time)do
   if(FATUP(b)=1)then
    rampPowerUp(b,t)<=BIDCAPUP(b)*(1-isRunningUp(b,t))
   end-if
end-do


minimize(TotalCost)

                                          !Post-processing!

forall(b in BidUp)
solfatup(b):=FATUP(b)

mipObjVal:= getparam("XPRS_MIPOBJVAL")

bestBound := getparam("XPRS_BESTBOUND")

gap := abs(100*(mipObjVal - bestBound)/(mipObjVal+0.000001))


forall(t in nTime, b in BidUp) do
   solUp(b,t):=getsol(mFRRUp(b,t))
   solisRunningUp(b,t):=getsol(isRunningUp(b,t))
   solbidActUp(b,t):=getsol(bidActUp(b,t))


   solRampPowerUp(b,t):=getsol(rampPowerUp(b,t))
   solSetPointUp(b,t):=getsol(setPointUp(b,t))
end-do

forall(t in nTime, b in BidDn) do
   solDn(b,t):=getsol(mFRRDn(b,t))
   solisRunningDn(b,t):=getsol(isRunningDn(b,t))
   solbidActDn(b,t):=getsol(bidActDn(b,t))

   solRampPowerDn(b,t):=getsol(rampPowerDn(b,t))
   solSetPointDn(b,t):=getsol(setPointDn(b,t))
   solIsRampingDn(b,t):=getsol(isRampingDn(b,t))
end-do
```

```
forall(t in nTime, a in AFRRUpR) do
   solAFRRUP(a,t):=getsol(AFRRUp(a,t))
end-do

forall(t in nTime, a in AFRRDnR) do
   solAFRRDN(a,t):=getsol(AFRRDn(a,t))
end-do

forall(i in nLines, t in nTime) do
   LineFlow(i,t) := getsol(lineFlow(i,t))
end-do

forall(n in nBus, t in nTime)do
    Angle(n,t):=getsol(angle(n,t))
    Deviation(n,t) :=getsol(deviation(n,t))
    Freq(n,t):=getsol(frequency(n,t))

    soldevDn1(n,t):=getsol(devDn1(n,t))
    soldevDn2(n,t):=getsol(devDn2(n,t))
    soldevUp1(n,t):=getsol(devUp1(n,t))
    soldevUp2(n,t):=getsol(devUp2(n,t))

    solFCRUp(n,t):=getsol(FCRUp(n,t))
    solFCRDn(n,t):=getsol(FCRDn(n,t))

    soldeviation(n,t):=getsol(deviation(n,t))

end-do


objValue:=getobjval

forall( t in nTime)
solsysfrequency(t):=getsol(sysfrequency(t))

initializations to "matlab.mws:"
        solfatup as "solfatup"
        objValue as "TotalCost"
        NACT as "nActivations"
        solbidActUp as "bidActUp"
        solbidActDn as "bidActDn"
        solisRunningUp as "isRunningUp"
        solisRunningDn as "isRunningDn"
        hasBeenActUp as "hasBeenActUp"
        hasBeenActDn as "hasBeenActDn"
        LbUp as "LbUp"
        LbDn as "LbDn"
        Freq as "frequency"
        solUp as "upActivation"
        solDn as "dnActivation"
        LineFlow as "LineFlows"
```

```
        soldevDn1 as "devDn1"
        soldevDn2 as "devDn2"
        soldevUp1 as "devUp1"
        soldevUp2 as "devUp2"
        Angle as "Angle"
        solAFRRUP as "AfrrUp"
        solAFRRDN as "AfrrDn"
        solRampPowerUp as "rampPowerUp"
        solRampPowerDn as "rampPowerDn"
        solSetPointUp as "setPointUp"
        solSetPointDn as "setPointDn"
        solIsRampingDn as "isRampingDn"
        soldeviation as "loadRegulation"
        solsysfrequency as "systemFrequency"
        solFCRUp as "FCRUp"
        solFCRDn as "FCRDn"
        gap as "MIPGAP"

end-initializations

end-model
```

Bibliography

[1] Tobias Aigner, Stefan Jaehnert, Gerard L Doorman, and Terje Gjengedal. "The effect of large-scale wind power on system balancing in Northern Europe". *IEEE Transactions on Sustainable Energy*, 3(4):751–759, 2012.

[2] J. Bialek, J. Bumby, and J. Machowski. *Power System Dynamics: Stability and Control*. John Wiley & Sons, LTD, West Sussex, PO19 8SQ, United Kingdom, second edition, 2008.

[3] Stephen J. Chapman. *Electric Machinery Fundamentals*. McGraw-Hill, fifth edition, 2012.

[4] Bob Daniel. "Xpress-optimizer reference manual". *Fair Isaac Corporation, Leamington Spa, Warwickshire, UK*, 2009.

[5] Gerard L. Doorman. "DC Power Flow in Power Markets". 2013. Lecture note in TET4185.

[6] Doorman, Gerard L and van der Veen, Reinier. "An analysis of design options for markets for cross-border balancing of electricity". *Utilities Policy*, 27:39–48, 2013.

[7] Fingrid Energinet.dk, Svenska Kraftnät and Statnett. "Methodology and concepts for the Nordic Flow Based Market Coupling Approach".

[8] Fingrid Energinet.dk, Svenska Kraftnät and Statnett. "Principle Approach for Assessing Nordic Welfare under Flow-based methodology".

[9] ENSTO-E. "ENTSO-E Continental Europe Operation Handbook; Policy P1: Load-Frequency Control and Performance". [Online] Available at: https://www.entsoe.eu/publications/system-operations-reports/operation-handbook/Pages/default.aspx.

[10] ENTSO-E. "System Operation Agreement appendices (English 2016 update)". [Online] Available at: https://www.entsoe.eu/publications/system-operations-reports/nordic/Pages/default.aspx.

[11] ENTSO-E. "AGREEMENT (Translation) regarding operation of the interconnected Nordic power system (System Operation Agreement)". [Online]Assessed at 28.04.2017, available at: https://www.entsoe.eu/publications/system-operations-reports/nordic/Pages/default.aspx, June 2006.

[12] ENTSO-E. "Position Paper On Cross-Border Balancing". July 2011.

[13] ENTSO-E. ”Network Code on Electricity Balancing”. August 2014.

[14] ENTSO-E. ”Supporting Document for the Network Code on Electricity Balancing” . August 2014.

[15] ENTSO-E. ”Nordic Balancing Philosophy”. June 2016.

[16] ENTSO-E. ”Principles for Determining the Transfer Capacities in the Nordic Power Market”. [Online]Assessed at 11.05.2017, available at: https://www.nordpoolspot.com/globalassets/download-center/tso/principles-for-determining-the-transfer-capacities.pdf, January 2017.

[17] Hossein Farahmand. ”integrated power system balancing in northern europe-models and case studies”. 2012.

[18] Hossein Farahmand and Gerard Doorman. ”Modelling of balancing market integration in the northern European continent”. *PSCC Stockholm, Sweden*, pages 21–25, 2011.

[19] Hossein Farahmand and Gerard L Doorman. ”Balancing market integration in the Northern European continent”. *Applied Energy*, 96:316–326, 2012.

[20] Hossein Farahmand, Seyed Mohammad Ali Hosseini, Gerard L Doorman, and Olav Bjarte Fosso. ”Flow based activation of reserves in the nordic power system”. In *Power and Energy Society General Meeting, 2010 IEEE*, pages 1–8. IEEE, 2010.

[21] FICO. Xpress matlab interface reference manual, release 7.7. [Online] Available at: https://www.msi-jp.com/xpress/learning/square/xpress_matlab_interface-2015.pdf.

[22] Agency for the Cooperation of Energy Regulators (ACER). ”Framework Guidelines on Capacity Allocation and Congestion Management for Electricity”. July 2011.

[23] Yonas Gebrekiros and Gerard Doorman. ”Optimal transmission capacity allocation for cross-border exchange of frequency restoration reserves (FRR)”. In *Power Systems Computation Conference (PSCC), 2014*, pages 1–7. IEEE, 2014.

[24] Yonas Gebrekiros, Gerard Doorman, Stefan Jaehnert, and Hossein Farahmand. ”Balancing Energy Market Integration Considering Grid Constraints”. In *PowerTech, 2015 IEEE Eindhoven*, pages 1–6. IEEE, 2015.

[25] Ove S Grande, Gerard Doorman, and BH Bakken. ”Exchange of balancing resources between the Nordic synchronous system and the Netherlands/Germany/Poland”. *SINTEF Energy Research, Project*, (12X535):02, 2008.

[26] TERRE Consultation Group. ”Public consultation document for the design of the TERRE”. March 2016.

[27] Martin André Håberg. ”standardprodukter for balansekraft”. Master’s thesis, NTNU, 2015.

[28] Martin Håberg and Gerard Doorman. "A Stochastic Mixed Integer Linear Programming Formulation for the Balancing Energy Activation Problem under Uncertainty" .

[29] Fangxing Li and Rui Bo. "DCOPF-based LMP simulation: algorithm, comparison with ACOPF, and sensitivity". *IEEE Transactions on Power Systems*, 22(4):1475–1485, 2007.

[30] Maas, GA and Bial, M and Fijalkowski, J. "Final report-system disturbance on 4 november 2006". *Union for the Coordination of Transmission of Electricity in Europe, Tech. Rep*, 2007.

[31] Jari Johannes Miettinen and Hannele Holttinen. "Characteristics of day-ahead wind power forecast errors in Nordic countries and benefits of aggregation". *Wind Energy*, pages n/a–n/a, 2016. WE-15-0321.R2.

[32] F. Milano, C. A. Canizares, and A. J. Conejo. "sensitivity-based security-constrained opf market clearing model". *IEEE Transactions on Power Systems*, 20(4):2051–2060, Nov 2005.

[33] Nordic Parties: Energinet.dk, Fingrid Oyj, Statnett SF, Svenska kraftnät. "Agreement on a Nordic Market for Frequency Restoration Reserves with automatic activation (aFRR)".

[34] Nordic Parties: Energinet.dk, Fingrid Oyj, Statnett SF, Svenska kraftnät. "Agreement on a Nordic Market for Frequency Restoration Reserves with automatic activation (aFRR): Appendix 2".

[35] Nordpool. "Ramping". [Online] Assessed at 12.05.2017, available at: http://www.nordpoolspot.com/TAS/Day-ahead-market-Elspot/Ramping/.

[36] Thomas J Overbye, Xu Cheng, and Yan Sun. "A comparison of the AC and DC power flow models for LMP calculations". In *System Sciences, 2004. Proceedings of the 37th Annual Hawaii International Conference on*, pages 9–pp. IEEE, 2004.

[37] Konrad Purchala, Leonardo Meeus, Daniel Van Dommelen, and Ronnie Belmans. "Usefulness of DC power flow for active power flow analysis". In *Power Engineering Society General Meeting, 2005. IEEE*, pages 454–459. IEEE, 2005.

[38] ENTSO-E Working Group Ancillary Services. "Proposal for standard products (draft)" .

[39] Nord Pool Spot. "Nord Pool Market Data". [Online]Assessed at 11.05.2017, available at: http://nordpoolspot.com/Market-data1/Elspot/Capacities1/Capacities/KEY/Norway/?view=table.

[40] Statnett. "Sekundærreserver (aFRR)". [Online] Assessed at 29.04.2017, available at: http://statnett.no/Kraftsystemet/Markedsinformasjon/sekundarreserver/.

[41] Statnett. "Systemvern". [Online] Assessed at 23.05.2017. Available at: http://www.statnett.no/Kraftsystemet/Systemansvaret/Systemtjenester/Systemvern/.

[42] Statnett. "Produksjonsglatting: Vilkår for deltakelse, håndtering og kompensasjon. Gjeldende fra 3. juni 2015". June 2015.

[43] Statnett. ”Vilkår for anmelding, håndtering av bud og prissetting i regulerkraftmarkedet (RKM)” . June 2016.

[44] Statnett. ”Vilkår for tilbud, aksept, rapportering og avregning i marked for FCR” . May 2016.

[45] R. A. C. van der Veen and R. A. Hakvoort. ”Balance responsibility and imbalance settlement in Northern Europe x2014; An evaluation”. In *2009 6th International Conference on the European Energy Market*, pages 1–6, May 2009.

[46] Dirk Van Hertem, Jody Verboomen, Konrad Purchala, Ronnie Belmans, and WL Kling. ”Usefulness of DC power flow for active power flow analysis with flow controlling devices”. In *AC and DC Power Transmission, 2006. ACDC 2006. The 8th IEE International Conference on*, pages 58–62. IET, 2006.

[47] L Vanfretti, SH Olsen, VS Narasimham Arava, G Laera, A Bidadfar, T Rabuzin, Sigurd H Jakobsen, J Lavenius, M Baudette, and FJ Gómez-López. ”An open data repository and a data processing software toolset of an equivalent Nordic grid model matched to historical electricity market data”. *Data in Brief*, 2017.

[48] Luigi Vanfretti, Tin Rabuzin, Maxime Baudette, and M Murad. ”itesla power systems library (ipsl): A modelica library for phasor time-domain simulations”. *SoftwareX*, 5:84–88, 2016.

[49] I. Wangensteen. *Power System Economics-the Nordic Electricity Market*. Fagbokforlaget, second edition, 2011.

[50] Daniel Waniek, C Rehtanz, and E Handschin. ”Flow-based evaluation of congestions in the electric power transmission system”. In *Energy market (EEM), 2010 7th international conference on the European*, pages 1–6. IEEE, 2010.

[51] ENTSO-E WGAS. ”Survey on Ancillary services procurement, Balancing market design 2016”. [Online]Assessed at 27.04.2017, available at: https://www.entsoe.eu/Documents/Publications/Market%20Committee%20publications/WGAS.pdf.

[52] Ray D. Zimmermann and Carlos E. Murillo-Sánchez. ”MATPOWER 6.0 User’s Manual”. [Online] Available at: http://www.pserc.cornell.edu/matpower/manual.pdf, December 1996.